NORTH-WEST UNIVERSITY
YUNIBESITI YA BOKONE-BOPHIRIMA
NOORDWES-UNIVERSITEIT
POTCHEFSTROOMKAMPUS

Gasification kinetics of blends of waste tyre and typical South African coals

C Gurai
B.Eng. (Chem. Eng.)

24711349

Dissertation submitted in fulfilment of the requirements for the degree *Magister* in Chemical Engineering at the Potchefstroom Campus of the North-West University

Supervisor:	Dr R Kaitano
Co-supervisor	Prof JR Bunt
Co-supervisor	Prof HWJP Neomagus

December 2014

Potchefstroom

NORTH-WEST UNIVERSITY
YUNIBESITI YA BOKONE-BOPHIRIMA
NOORDWES-UNIVERSITEIT

For the glory of God

Declaration

"I, Chaitamwari Gurai, hereby declare that the dissertation entitled:

Gasification kinetics of blends of used tyre and typical South African coals.

which I herewith submit to the North-West University in fulfilment of the requirements set for the degree Master of Engineering is my own original work and has not previously been submitted to any institution. If there was the need to quote, it was indicated and shown in a reference list."

Signed at Potchefstroom on this 11th day of December 2014.

.....

C. Gurai.

Acknowledgements

I would like to extend my heartfelt gratitude to the following people who assisted me in the work of this study and in my life during the period of this study:

- My Heavenly Father for love unfailing and so unconditional, guidance, wisdom, strength, peace that surpasses understanding, and unmerited favour.
- Dr. Rufaro Kaitano for academic guidance and personal support.
- Prof. John Bunt, Prof. Ray Everson and Prof. Hein Neomagus for their guidance and support.
- The Department of Science and Technology, National Research Foundation and the SARChI Coal Research Chair for financial support for this study.
- Mr. Gregory Okolo, Mr. Hennie Coetzee and Miss Mpho Rambuda for all the technical and academic assistance.
- Mr. Jan Kroeze and Mr. Adrian Brock for their technical assistance.
- My mum and dad and all my siblings for personal support.
- All friends and relatives who stood by me and supported me during the period of my study and in the difficult days leading to this period.

Abstract

With increasing energy demand globally and, in particular, in South Africa coupled with depletion of the earth's fossil energy resources and growing problem of disposal of non-biodegradable waste such as waste tyres, there is a need and effort globally to find alternative energy from waste material including waste tyres. One possible way of exploiting waste tyre for energy or chemicals recovery is through gasification for the production of syngas, and this is what was investigated in this study. The possibility of gasification of waste tyre blended with coal after pyrolysis was investigated and two Bituminous coals were selected for blending with the waste tyre in co-gasification. A sample of ground waste tyre / waste tire, WT, a high vitrinite coal from the Waterberg coalfield (GG coal) and a high inertinite coal from the Highveld coalfield (SF coal) were used in this investigation.

The waste tyre sample had the highest volatile matter content of 63.8%, followed by GG coal with 27% and SF coal with 23.8%. SF coal had the highest ash content of 21.6%, GG coal had 12.6% and waste tyre had the lowest of 6.6%. For the chars, SF char still had the highest ash of 24.8%, but WT char had higher ash, 14.7%, when compared to GG char with 13.9% ash. The vitrinite content in GG coal was 86.3%, whilst in SF coal it was 25% and SF coal had a higher inertinite content of 71% when compared to GG coal with 7.7%. SF char had the highest BET surface area of 126m^2/g, followed by GG char with 113m^2/g, and WT had the lowest value of 35.09m^2/g. The alkali indices of the SF, WT and GG chars were calculated to be 8.2, 4.2 and 1.7 respectively.

Coal samples were prepared by crushing and milling to particle sizes less than 75µm before charring in a packed bed balance reactor at temperatures up to 1000^{o}C.Waste tyre samples were charred at the same conditions before milling to < 75µm particle size. Coal and WT chars were blended in ratios of 75:25, 50:50 and 25:75 before gasification experimentation. Carbon dioxide gasification was conducted on the blends and the pure coal and WT chars in a Thermogravimetric analyser (TGA) at 900^{o}C, 925^{o}C, 950^{o}C and 975^{o}C and ambient pressure. 100% CO_2 was used at a flow rate of 2L/min.

Reactivity of the pure char samples was found to be in the order SF > GG > WT, and the relationship between the coal chars' reactivities could be explained by the high ash content of the SF char and low reactivity of the WT char corresponds to its low BET surface area. In

general, the coal/WT char mixtures were less reactive than the respective coal, but more reactive than the pure WT char, the only exception being the 75% GG char blend which was initially more reactive than the GG char, and reactivity decreased with increasing WT content. For all samples reactivity increased with increasing temperature.

The relationship between the reactivities of the GG char and its blends and that of the SF char and its blends was found to be affected by the amount of WT char added, especially at the lower temperatures 900ºC and 925ºC. SF coal is more reactive than GG coal, but at 900ºC and 925ºC, the reactivity of GG/WT blends improves in relation to the SF/WT blends with an increase in the ratio of WT in the blends, i.e. the 25% GG char blend is more reactive than the 25% SF char blend. The reactivity of the coal/WT blends was also checked against predicted conversion rates based on the conversion rates of the pure WT and coal samples. At 900ºC and 925ºC, the reactivities of the blends of both coal chars with WT char were found to be greater than the predicted conversion rates, and for the GG/WT blends the deviation increased with increasing WT ratios, while for the SF/WT blends the deviation increased with increasing SF ratios. These findings suggest the presence of synergism or enhancement between the coal chars and WT char in gasification reactions.

The random pore model (RPM) was used to model the gasification results and it was found to adequately describe the experimental data. Activation energies determined with the RPM were found to be 205.4kJ/mol, 189.9kJ/mol and 173.9kJ/mol for SF char, WT char and GG char respectively. The activation energies of the coal/WT blends were found to be lower than those of both the pure coal and the pure WT chars. For the GG/WT blends the activation energy decreased with increasing WT char ratio, while for the SF/WT blends the activation energy decreased with increasing SF char ratio.

The trends of the activation energies and conversion rates of the blends point to synergism or enhancement between the coal and WT chars in CO_2 gasification reactions, and in the GG/WT blends this enhancement is driven more by the WT char, while in SF/WT blends it is driven by SF chars. It is possible that enhancement of the reactions is caused by mineral matter catalysis of the gasification reactions. The ash contents and alkali indices of the pure samples follow the order SF > WT > GG.

Keywords: Waste tyre / waste tire, vitrinite-rich coal, inertinite-rich coal, carbon dioxide gasification, random pore model (RPM).

Table of Contents

List of Figures

List of Tables

Nomenclature

Symbol	Description	Units
E_a	Activation energy	kJ/mol
$f(X)$	Structural factor	m^{-1}
k_{so}	Pre-exponential factor	min^{-1}
k'_{so}	Lumped pre-exponential factor	min^{-1}
L_o	Total pore length per unit volume	$m \cdot m^{-3}$
m	Order of reaction with respect to CO_2 concentration	-
m_{ash}	Mass of ash	mg
m_0	Initial mass of char	mg
m_t	Mass of char at time, t	mg
r_s	Reaction rate	min^{-1}
R_s	Initial reactivity of the chars	min^{-1}
S	Slope of $\ln(t_f)$ against T^{-1} plot	K^{-1}
S_o	Initial surface area	$m^2 \cdot m^{-3}$
T	Temperature	^oC
t	Time	min
$t_{0.5}$	Time for fractional carbon conversion of 50%	min
$t_{0.9}$	Time for fractional carbon conversion of 90%	min
t_f	Time factor	min^{-1}
Greek Letters		
ε_o	Initial porosity of char samples	%
τ	Dimensionless time	-
$\tau_{0.9}$	Dimensionless time at 90% conversion	-
Ψ	Dimensionless structural parameter for char pores	-

Abbreviations

Acronym	Meaning
AFROX	African Oxygen Limited
ASA	Active surface area
ASTM	American Society for Testing and Materials
BET	Brunauer-Emmett-Teller Method
BR	Butadiene rubber
COx	Carbon oxides
CTC	Coal-to-chemicals
D-R	Dubinin-Radushkevich method
ESKOM	South African Electricity Supply Commission
ESS	Error sum of squares
IGCC	Integrated Gasification Combined Cycle
ISO	International Standards Organisation
NOx	Nitrogen oxides
RPM	Random pore model
SOx	Sulphur oxides
TSA	Total surface area
VM	Volumetric model
XRD	X-ray defraction
XRF	X-ray fluorescence

CHAPTER 1: GENERAL INTRODUCTION

1.1 Background and Motivation

The increase in economic activity worldwide has led to major challenges such as increased environmental pollution and depletion of the earth's resources such as energy resources among others. One major environmental problem linked to high economic activity is greenhouse gas emissions. These have been increasing world over and South Africa has been one of the significant players in the increase of such emissions. In 2009 South Africa was reported to be emitting 10.1 metric tons per capita of carbon dioxide, which is three times greater than China's emission at 5.8 metric tons per capita (World Bank, 2009). According to Du Plooy (Cited by Copans & Tyrer, 2008) South Africa's High carbon dioxide emissions can be attributed to its high energy and carbon intensive economic structure. The mining and the manufacturing/ industrial sectors consume half the national primary energy demand, while the residential sector accounts for only a sixth (Copans & Tyrer, 2008).

From various economic activities, there is also a worldwide problem of solid waste generation, used tyres being one of such products. Used tyres are non-biodegradable and contain about 1.43% hazardous waste, which can leach into the environment and is toxic to some living organisms (MWH New Zealand Ltd, 2004).

Energy production accounts for a large proportion of air pollution, hence there is a need for innovative ways of producing energy which releases fewer pollutants into the atmosphere without compromising the energy needs of the global economies, which are increasing and have been projected to continue increasing as shown in Figure 1 (U.S. EIA, 2011). While gasification of South African coals has been studied extensively, tyre gasification has not received much attention, but with the increasing tyre problem, it is worthwhile studying the use of waste tyres in clean energy technologies. Understanding the kinetics of the gasification reaction of waste tyres is important because it will give an insight to the feasibility and profitability of the technology. The mineral components of both coal and tyres are believed to have a catalytic effect on their gasification kinetics (Hattingh *et al*., 2011), therefore it is important to study the effect that components of both coal and tyre have on each other's reactivity if they are combined in co-gasification.

Co-gasification of tyres with coal is one innovative clean energy technology, it is a solution to the already existing tyre dumping problem, and gasification of tyres will help ease the burden on fossil fuels and will lead to a reduction of NOx emissions from coal. Talab *et al*. (2010) reported that the NO mass fraction at the outlet of their gasifier decreased by 17% when 5% of tyre was blended with coal, and by 52% for a 10% tyre-coal blend.

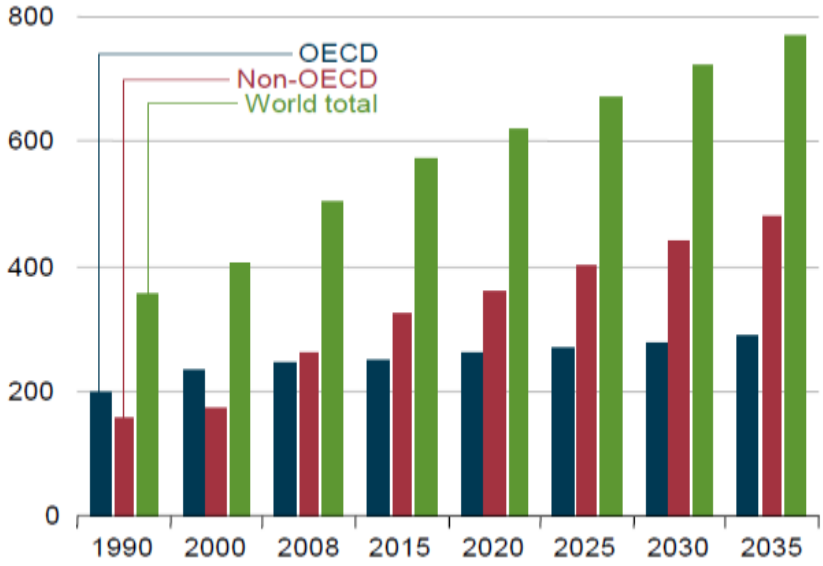

Figure 1.1: World energy consumption for 1990 to 2035 in Quadrillion Btu. (U.S. EIA, 2011)

1.1.1 Waste Tyre Problem

South Africa produces around 11-million scrap tyres every year and about 60 million waste tyres are already stockpiled in South Africa (Botes, 2012). Some of the tyres are often disposed of in landfills or open fields (Odendaal, 2012), but this is not sustainable because tyres consume a lot of landfill space (Wojtowicz & Serio, 1996). Disposal of tyres in open fields has environmental, health and safety hazards associated with it: i.e. (1) waste tyres occupy large tracts of land and this makes it unusable for any other purpose, (2) waste tyres can retain water and provide a breeding ground for mosquitoes, which can spread malaria and (3) the high flammability of tyres is also a serious challenge to the environment and human safety (Wojtowicz & Serio, 1996). Disposed tyres can catch fire and the fire is difficult to contain, due to the high amount of energy present in the rubber. The fire can also easily spread to other areas, posing a threat to humans and property. Waste tyres have also been dealt with by uncontrolled burning to recover scrap metal content (Odendaal, 2012). This releases highly polluting gases into the air.

In July 2012 The Government of South Africa's Department of Environmental Affairs came up with an initiative known as the Integrated Industry Waste Tyre Management Plan (IIWTMP), which is promoting re-use and recycling of waste tyres in South Africa. According to the plan, a fee of R2.30 per kilogram of tyre will be charged on all new tyres made or imported into South Africa. This will generate approximately R700 million annually, and 80% of the revenue will be invested directly into developing a sustainable tyre recycling industry, and to subsidise the collection of waste tyres and tyre recycling. The plan is aimed at ensuring that waste tyres do not end up being stockpiled or dumped at landfill sites, therefore minimising the negative environmental impacts of tyres and conserving resources (Botes, 2012).

Waste tyres contain some substances which are classified as hazardous wastes (United Kingdom, 2009), some of which are listed in Table 1. As tyres slowly decompose, they generate some oils and gases (Wojtowicz & Serio, 1996), which are also hazardous to the environment.

Table 1.1: Basel Convention hazardous waste constituents of waste tyres (UNEP, 2000)

Chemical Name	**Remarks**	**Content** (% weight)
Copper Compounds	Alloying constituent of the metallic reinforcing material (Steelcord)	Approx. 0.02 %
Zinc Compounds	Zinc Oxide, retained in the rubber matrix	Approx. 1 %
Acidic solutions or acids in solid form	Strearic acid, in solid form	Approx. 0.3 %
Organohalogen compounds other than substances in Annex of the Basel Convention	Halogen butyl rubber (tendency: decreasing)	Content of halogens max. 0.10 %

1.1.2 South African Coal

Coal is an abundant resource in South Africa and the coal reserves are estimated to be 53,8 billion short tonnes (Bell *et al.*, 2010). At the annual production rate of 279 million short tonnes per year (US Energy Information Administration, 2013), coal supply could be expected to last for nearly 200 years. However, with changes in coal usage patterns, prices and improved coal technology, the coal reserves may be available for much longer than estimated today.

Coal accounts for 65.9% of South Africa's primary energy needs and 93% of its electricity is generated from coal (Department of Energy, 2009). On the other hand, coal accounts for 30% of global primary energy needs and generates 42% of the world's electricity (World Coal Association, 2012). These figures reflect a high dependence of the South African economy on coal, and in terms of coal usage for electricity production it ranks number one in the world (World Coal Association, 2012).

South Africa produces a substantial amount of low grade and high-ash coal, characterised by low calorific value (< 25.5kJ·mol^{-1}) and high sulphur content (up to 1.67%). The lowest grade of this coal is discarded (Okolo, 2009; Kaitano, 2007). The inertinite-rich coal, produced in South Africa is used as power generation plant feedstock and some as a feed for syngas production by gasification.

However, coal usage has environmental challenges associated with it, such as the release of noxious gases into the atmosphere particularly NOx, SOx and COx.

As already demonstrated from literature, coal is an important source of energy for South Africa and worldwide. The shortcomings of coal, such as the environmental pollution directly associated with coal utilisation have been a motivating factor for research and development into cleaner ways of its utilisation.

1.1.3 Clean Energy Technology

Gasification is one of the leading clean coal technologies. Waste tyres are a rich source of carbon and can be gasified to produce syngas. The waste tyre can either be gasified in its pure form as pulverised particles or as chars after pyrolysis to recover gas and oil, which is the cleaner route. In both cases it can be gasified as is, or co-gasified with coal (Straka & Bucko, 2009, Talab *et al.*, 2010).

Gasification yields a product gas with a high calorific value, and the product gas is a potential resource for electrical energy production in gas turbines (Karatas *et al.*, 2012). The product gas can be used as a starting raw material in the synthesis of hydrocarbon liquid fuels and synthetic natural gas and other chemicals (Ondrey, 2011). Chemicals account for 45% of the products from syngas, and coal-to-chemicals (CTC) is showing the greatest growth in coal utilisation (Ondrey, 2011).

Tyres are rich in hydrocarbons, yet land filling of these materials is still practiced, causing potential risk to the ecosystem through gas emissions (especially CH_4) and ground water pollution due to leaching. Co-gasification provides a way of salvaging some value from the abundant waste tyres rather than having them lead to environmental problems. The use of waste tyre char in gasification can be seen as a form of "renewable energy" in the face of depletion of the earth's resources since tyre rubber comes from plants (Talab, 2010), but one which is cleaner than combustion of the waste tyres.

Co-gasification can be performed in existing coal gasifiers and this would minimize capital cost expenditure on infrastructure.

Char particles from tyre devolatilization are more porous than those resulting from coal (and hence more reactive), and this can offer some reactivity advantage in co-gasification (Talab *et al*. 2010). Talab *et al*. (2010) reported that the NO mass fraction at the outlet of their gasifier decreased by 17% when 5% of tyre was blended with coal, and by 52% for a 10% tyre-coal blend. The reduction of the NO mass fraction for coal and tyre co-gasification was due to the reduction of both thermal and fuel NOx (Talab *et al*., 2010).

Currently the regulations in South Africa do not promote the use of waste tyre in recovering their energy (South Africa, 2008). If this research can demonstrate that tyre and coal co-gasification can result in the utilisation of poor quality coals in a cleaner way, it can motivate a change of policy and attitude towards recovery of energy from waste tyres in this way.

1.2 Aims and Objectives of this Study

The overall aim of the study is to investigate (1) the carbon dioxide gasification kinetics of chars of two South African coals (a vitrinite-rich coal and an inertinite-rich coal), and waste tyre-derived chars separately and (2) the reactivity and kinetics of blends of the two respective coal chars with the waste tyre-derived char. The objectives being to:

1.0 Determine the extent to which blending of tyre char and coal chars affect their reactivity.
2.0 Determine the optimum mixing proportion of waste tyre char with each of the coal chars which will lead to maximum reactivity.

3.0 Determine whether there is any synergetic effect between the coal char and waste tyre char reactivity.

4.0 Come up with a model which describes the reactivity data.

In order to achieve these objectives, the following will be done:

i. Select two coals (one inertinite-rich and the other vitrinite-rich)
ii. Produce coal and waste tyre chars by pyrolysis, using a Packed Bed Reactor.
iii. Carry out gasification experiments with carbon dioxide on a sample of coal char, waste tyre char, and blends of waste tyre char and coal char in different mixing proportions, and experiments will be performed at different temperatures.
iv. Process the experimental results of the char conversion reaction rate data.
v. Evaluate the kinetics, using a suitable model.

1.3 Scope of This Study

The work of this study is presented in six chapters, which each contribute to the achievement of the objectives and to execute the methods set out in Section 1.2.

A general introduction to this work is presented in Chapter 1. The background and motivation for this study is presented, discussing the problems that are to be addressed and the possible opportunities that may arise from the success of this study.

A study of the literature on both coal and tyre is presented in Chapter 2. The nature of these two feedstocks is explored, their pyrolysis and gasification reactions are also studied and progress of these fields of research is briefly presented. Co-gasification is also discussed in Chapter 2 and, finally, kinetic models, which could possibly be used in this study, are discussed.

In Chapter 3, all the practical and experimental work done in this study is reported. The methods, apparatus and standards used and procedures followed are presented. The work ranges from sample selection and preparation to characterisation and gasification experimentation.

All the results of the experimental work conducted and presented in Chapter 3 are presented and discussed in Chapter 4. The answers to some of the questions presented in the objectives

are explored in this chapter. The results are modelled in Chapter 5 using the random pore model, and the kinetic parameters are evaluated.

Finally, conclusions are made in Chapter 6, in view of the objectives of this study. Recommendations are also made for future studies, which can answer some of the questions that arose during the course of this study and at the conclusion.

CHAPTER 2: LITERATURE REVIEW

2.1 Tyre Composition

Tyres are mainly composed of rubber, which makes up about 41% of the mass of a tyre (tire), as well as some inorganic components (fillers), reinforcing material, vulcanizing material, plasticisers and other additives. The materials and chemical components that make up each of these fractions are discussed in the sub-sections of this section.

2.1.1 Material Composition

Both natural rubber (NR) (cis-1,4-polyisoprene) and synthetic rubbers are used in the manufacturing of tyres. The most common synthetic rubbers are styrene–butadiene rubber (SBR), a copolymer of styrene and butadiene, and butadiene rubber (BR), which consists of polybutadiene. Natural rubber and the synthetic rubber components mostly end up in the volatile fraction in tyre pyrolysis, yielding only 4 weight% char when pyrolysed individually, compared to about 40% from tyre pyrolysis. Brazier (1980) has described styrene–butadiene rubber and butadiene rubber as non-charring rubbers (Williams & Besler, 1995).

Fillers make up about 30% of the tyre composition. Carbon black can come in many different types, and is the main source of char in tyre pyrolysis. Clay and silica gel are other fillers, which also remain with the char after pyrolysis, and in the ash after gasification or combustion, where they play a catalytic role during these reactions.

Reinforcing steel and fabric cord material make up to about 15% of the tyre composition - it reinforces the rubber, and can be in a twisted form or braided into strong cables. Both steel and fabric are usually removed from the tyre before pyrolysis and gasification.

Sulphur, zinc oxide, stearic acid and various other chemicals are used for rubber vulcanization in the tyre making process (6%). Sulphur acts as a cross-linking agent - it hardens and prevents excessive deformation of the tyre at elevated temperatures. Zinc oxide and stearic acid also enhance the physical properties of the rubber (Williams & Besler, 1995). Vulcanization accelerators are typically organosulphur compounds which act as catalysts for the vulcanization process (Williams & Besler, 1995). Sulphur and zinc, which are also catalytic in the reactions of the tyre waste, remain in the char after pyrolysis, and with the ash after gasification.

Plasticisers include processing oil and resins. The extender oil is a mixture of aromatic hydrocarbons. which serves to soften the rubber and improve workability (Williams & Besler, 1995), and is another source of carbon and hydrogen.

Other additives include antioxidants and anti-aging agents.

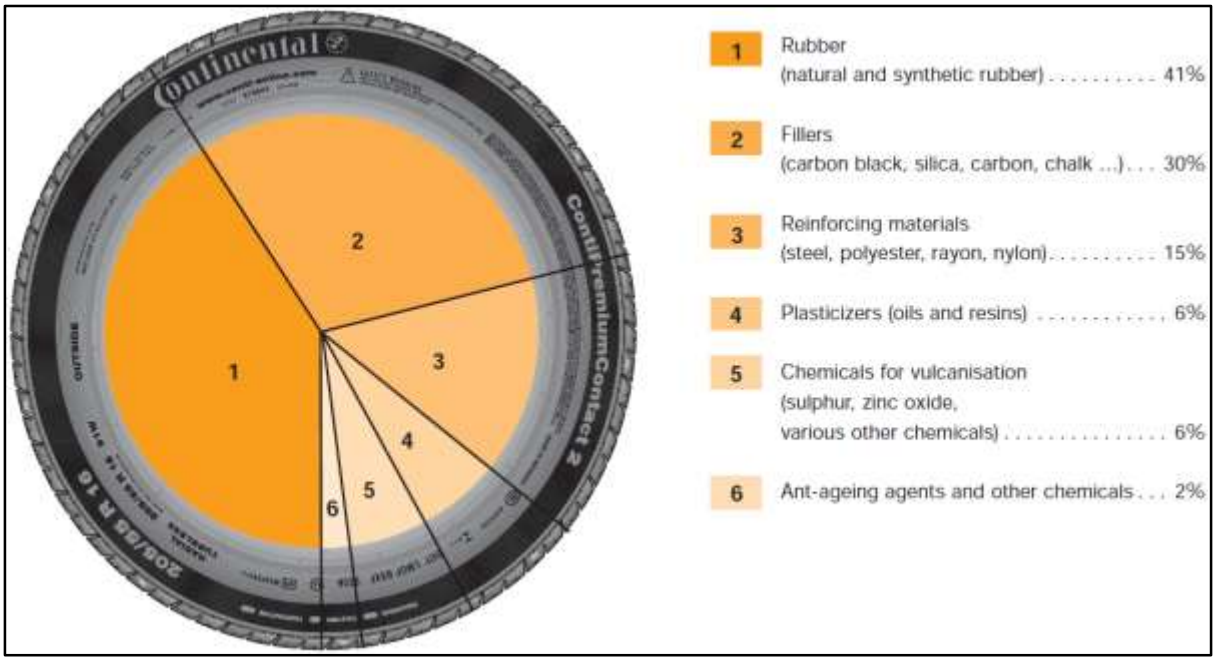

Figure 2.1: Tyre composition (Continental AG, 2008)

2.1.2 Chemical Analysis of Tyre

Chemical analysis shows that the dominant element present in tyres is carbon (73%), which is present in the organic rubber, oils and in the filler carbon black. Oxygen and hydrogen make up 9.8% and 6.9% respectively. Volatile matter is above 60% compared to around 35% of some coals. The ash content of waste tyres is about 7%, which is lower than that of most coals, and fixed carbon is low (below 30%), owing to the high volatile matter content (Talab *et al.*, 2010, Venter, 2012). Metals such as zinc, iron and calcium can be present in low concentrations. Trace metals are also present in low concentrations, ranging from 0.88 – 13,49mg/kg, these include silver, aluminium, magnesium, sodium, lead, potassium and titanium (MWH New Zealand Ltd, 2004), and they are part of the ash content in the chemical analyses.

Tyres are 100% recyclable because they do not contain any significant amounts of hazardous material (UNEP, 2000). The net calorific value of a tyre is between 32 and 34 MJ/kg, which is

higher than for coal (MWH New Zealand Ltd, 2004)**,** and it gives them great potential as a fuel. The high heating value, high volatile content and low ash content make scrap tyre a good candidate for thermal disposal applications (Karatas *et al*., 2012; 2013).

Most of the tyre work in this study is going to be based on a used passenger car tyre, which weighs about 6.5kg on average (Case, 2011).

2.2 The Nature of Coal

Coal is a sedimentary rock, which consists mainly of organic components, with minor mineral components, and has glassy physical behaviour (Osborne, 1988; Smith *et al.*, 1994). The general nature and properties, and the chemical composition of coal are explored in the sub-sections of this section.

2.2.1 General Nature and Properties

The composition, physical and chemical properties, and therefore chemical behaviour vary widely depending on maturity of the coal or extent of alteration from the plant matter from which the coal was derived. Coals are classified into ranks according to the extent of alteration; the younger and less altered coals are the low rank coals, and the more altered or mature coals are the high rank coals. Calorific value of coal also varies widely with rank.

According to their appearance, the medium to high-rank coals are described as black coals and the low rank coals are described as brown coal.

Table 2.1: ASTM rank classification of coals (Schobert, 2011)

Rank Level	**Class**	**Group**	**Fixed Carbon %**mmmf	**Volatile Matter %** mmmf	**Calorific value kJ/kg**
High	Anthracite	Meta-anthracite	>98	<2	
		Anthracite	92·98	2-8	
		Semi-anthracite	86-92	8-14	
	Bituminous	Low volatile	78-86	14-22	
		Medium volatile	69-78	22-31	
		High volatile A	<69	>31	>32 000
		High volatile B			30 000 – 32 000
		High volatile C			24 400 - -30 000
	Subbituminous	Subbituminous A			24 400 – 28 000
		Subbituminous B			22 000 - 24 400
		Subbituminous C			19 000 - 22 000
	Lignite	Lignite A			15 000 - 19 000
Low		Lignite B			<15 000

The carbon content of coal increases with rank, while the hydrogen content shows a slight decrease. Coal oxygen content decreases with rank, for example from nearly 30% in medium rank coals to as low as 2% in anthracites, and as the oxygen content decreases for a given amount of carbon content, the calorific value increases because the presence of oxygen in a coal may imply, in a sense, that a part of the carbon content is already oxidised (Schobert, 2011). This observation is in agreement with the increase in calorific value with increasing rank, since high rank coals have very low oxygen content. Volatile matter content decreases with increasing rank from about 40% to less than 2% (Schobert, 2011; Osborne, 1988).

2.2.2 Chemical Composition of Coal

Coal is a complex heterogeneous mixture of different organic and inorganic components with moisture content. The inorganic components of coal are termed as minerals, while the organic components are termed as macerals, and they are classified into different macerals groups (Smith *et al.*, 1994).

2.2.2.1 Organic Components

The study of macerals is important for the study of coal because the chemical structure of macerals and the maceral groups and types present determine the chemistry of the coals (Smith *et al.*, 1994). Notable chemical differences between different macerals are (i) variation in aliphatic hydrogen content, (ii) variation in molecular structures, particularly carbon aromaticity, and (iii) differences in reactivity. As a result, coals of the same rank may also vary greatly in reactivity as a result of differences in maceral composition. Maceral analysis is a major factor of consideration when selecting coals for different applications. The macerals present in a coal can be used to predict the chemical behaviour and reactivity of the coal (Schobert, 2011; Smith *et al.*, 1994).

Macerals are described and classified on the basis of their optical appearance and evident relationship to botanical structures from which they were derived (Schobert, 2011).

The vitrinite group of macerals was derived from plant cell substances and may still, in some cases, exhibit tissue structure, or may be structureless. Vitrinites are rich in oxygen and moderate in hydrogen and aromaticity. They are the most reactive maceral in most coal reactions (Osborne, 1988). The reflectance of vitrinites is high, and are characterised by a shiny

glass-like appearance, which makes vitrinite reflectance a useful parameter in determining coal rank, since it varies with rank.

The liptinite or exinite group is derived from secretions and waxy coatings of plants (Osborne, 1988). Liptinites are lower in reflectance than vitrinite - they are rich in hydrogen and highly aliphatic. In a particular coal, exinite has a higher volatile matter content than vitrinite, and such differences in volatile content can be used to classify coals according to differences in tar and gas yield on pyrolysis (Osborne, 1988).

The inertinite group has lower reflectance than the vitrinite group, and is dull in appearance, and has lower volatile content. Inertinites may show plant structures, and the group includes the macerals, macrinite, micrinite, semifusinite and fusinite. Inertinites, however, are generally more oxygenated and aromatic than vitrinites, rich in carbon and highly aromatic.

Lithotypes and Microlithotype maceral groups, however, do occur in association with each other, and these maceral associations are known as lithotypes and appear as bands of varying thickness and appearance, i.e. some are dull, while others are bright. Lithotypes contain microcomponents known as microlithotypes. Of the four lithotypes, vitrain and clarain are bright in appearance, and the main microlithotypes in them are vitrite and clarite, respectively. Durain and fusain are dull in appearance, and the main microlithotypes in them are durite and fusite, respectively (Williams *et al.*, 2000).

2.2.2.2 Mineral Matter in Coal

Minerals play an important role in coal utilisation. Besides ash production, mineral matter in coal affects the rate of reaction of the organic constituents of coal in gasification and combustion through catalysis. Some mineral species catalyse the reaction, while others are non-catalytic. Hattingh *et al* (2011) found that the reactivity of a coal sample in carbon dioxide gasification depended on ash content and the ash constituents as well. Relative reactivity was found to increase with increasing calcite, dolomite and CaO content, which corresponds with literature describing the important catalytic role of Ca^{2+} during CO_2 gasification (Hattingh *et al*, 2011).

The inorganic component of coal constitutes mineral matter of various composition, origin and modes of occurrence, and some trace elements. *Inorganic constituents* in coal can occur as

discrete mineral grains, cations associated with ionized functional groups, and cations held in coordination complexes (chelates) with the heteroatoms in the coal structure (Schobert, 2011). Discrete grains of inorganic substances incorporated in coal as a separate and distinct phase are referred to as mineral matter, and they include minerals such as anatase, quartz or clay, calcite, dolomite, kaolinite, illite, muscovite, pyrite, rutile and siderite (Schobert, 2011; Hattingh *et al.* 2011; Smith *et al.,* 1994).

Low-rank coals contain relatively large amounts of organically associated elements, which are eliminated in higher-rank coals. Some inorganic constituents of coal are chemically bound to the organic components, and most of these originate from the plant matter from which the coal is derived. Other inorganic constituents are dispersed within the coal in varying degrees of association with the organic part of coal from finely dispersed particles to distinct bands and grains, and these originate from sources other than the plant matter (Smith *et al.,* 1994; Williams *et al.,* 2000; Osborne, 1988).

Mineral matter undergoes some reactions during the reactions of coal. The weight of ash produced during the gasification of coal does not necessarily equal the total weight of inorganic constituents originally present in the coal. It is difficult and time-consuming to measure mineral matter content directly, and formulae have been developed to calculate the mineral matter content of a coal from the amount of ash that is produced based on the reactions that occur when mineral matter is converted to ash. In South Africa the National Institute for Coal Research formula is given as (Schobert, 2011):

$$MM = 1.1A + 0.55\ CO_2$$

Where: *MM = mineral matter*
A = ash
CO_2 = carbon dioxide
As percentages on air-dried basis.

2.3 Pyrolysis

Pyrolysis is the thermal degradation process where carbonaceous material is heated in an inert atmosphere, volatile matter is evolved and residual solid char remains. Understanding pyrolysis and its products is important for gasification studies, since the products formed are

intermediates in the gasification process. The pyrolysis conditions determine the quality of char obtained, and this in turn influences the reactivity of the char (Cloke and Lester, 1994).

2.3.1 Tyre Pyrolysis

Pyrolysis of rubber/tyres is an old concept, and it is a rational approach to recover the hydrocarbons for re-use but it has been uneconomical for commercial application due to poor quality of the products (Zabaniotou & Stavropoulos, 2003). In recent years there has been a great deal of research aimed at improving the economics of the process and commercial application of the products (Martinez *et al.*, 2013).

Pyrolysis of tyres yields pyrolytic oil, pyrolytic gas and a high-carbon solid char residue. The exact composition of each of these fractions is dependent on the pyrolysis conditions, such as temperature, heating rate, pressure and residence time (Conesa *et al.*, 2004; López, *et al.*, 2012). Oil and gas yield in the pyrolysis process increases with increases in temperature and heating rate, while char yield decreases with increasing temperature (Conesa *et al.*, 2004; Karatas *et al.*, 2013). From pyrolysis and kinetic experiments with tyre it has been observed that the temperature range for pyrolysis is between 300^{o}C and 500^{o}C (Mitta *et al.*, 2006), and it is an endothermic process. Karatas *et al.*, (2012) observed in a study in the temperature range of 200–800^{o}C that the degradation rate of tyre increased with an increase in temperature, but this effect was weak above 400^{o}C.

2.3.1.1 Tyre Pyrolysis Studies and Products

Conesa *et al.*, (2004) studied pyrolysis of waste tyre using a semi-continuous pilot plant reactor at three different temperatures 450°C, 750°C, and 1000 °C, and N_2 flow rate approximately 1.54L/min. The yields of the different fractions obtained when nitrogen was used as the purge gas are presented in Table 2.2.

Table 2.2: Pyrolysis product yield at 450^{o}C, 750^{o}C and 1000^{o}C (Conesa *et al.*, 2004).

Pyrolysis Temperature ^{o}C	Gas %	Tar %	Char %	Soot %
450	25	38.6	36.4	0
750	53.97	9.23	36.8	0
1000	37.93	<0.01	36.7	25.1

The analysis results of the gas, liquid and solid products showed a wide variety of chemicals in the oil and gas fractions. The main products identified in the gas phase were H_2, methane, ethane, ethylene, propane, propylene, isoprene, benzene, toluene, CO and CO_2. The yield of the gas phase products was higher at 750^{o}C than at 1000^{o}C, except for methane, hydrogen and benzene. The major liquid phase products were limonene, styrene, 5,5-dimethylhexanal, naphthalene and benzocycloheptatrien, indene and R-methylstyrene. At 750^{o}C styrene production was maintained, while limonene decreased and Indene increased (Conesa *et al.*, 2004).

Aylon *et al.*, (2008) studied tyre pyrolysis products up to a final temperature of 600 °C from a fixed bed and a moving bed reactor at pilot plant scale. Char yield was 38% in both reactors, suggesting total rubber conversion in both systems, but differences were observed in the liquid and gas yields. Liquid yield was higher (54.6%) in the fixed bed reactor than in the moving bed reactor (43.2%), while gas yield was lower (7.5%) in the fixed bed reactor than in the moving bed reactor (17.1%). C_4 compounds, mainly the isobutylene, were found to be dominant in the gas product. In the liquid fraction, similar composition was found for both experimental installations, and the main products were aromatic hydrocarbons with a significant percentage of polar compounds. Further analysis of the oils by GC/MS revealed that the most abundant products are the benzene, toluene, xylene (BTX) fraction, other substituted mono-aromatic compounds with two or more short aliphatic chains and limonene. From their work and from the work of others in the literature (Fernández *et al.*, 2009) it can be concluded that composition of pyrolytic gases is affected by the reaction temperature, experimental installation, the raw material and heating rate. Char yield was not influenced by experimental installation and the high ash content of 13.82 % and 13.17 % is consistent with that reported by other workers (Fernández *et al.*, 2009).

2.3.1.2 Uses of Tyre Pyrolysis Products

Uses of pyrolysis volatile products include use as fuel oil for burners and as fuel gas. The oil and the gas are used in some plants as fuel to provide energy for pyrolysis, which makes tyre pyrolysis an energy integrated and cost effective process. The gas has a high calorific value which makes it provide sufficient energy required for the tyre pyrolysis process in an exclusively tyre-pyrolysis plant (Aylon *et al.*, 2008; Williams & Besler, 1995).

Pyrolytic oil has a high calorific value, approximately 42MJkg^{-1}, and a sulphur content of 0.8-1.65 wt% depending on tyre source and process conditions. The oil is highly aromatic and contains high concentrations of potentially valuable chemicals such as benzene, xylene, toluene, styrene and DL-limonene. The oil can be added to petroleum refinery feedstock, and it can be an important source of refined chemicals (Williams & Besler, 1995; Zabaniotou & Stavropoulos, 2003).

The char is useful as a solid fuel, substitute carbon black or activated carbon, in which case they would have to be demineralised, since they have a high ash (±13 wt%), and sulphur (about 3 wt.%) content [compared with a maximum of 1 – 2 % for commercial carbon blacks (Aylon *et al*, 2008)] and/or activated, since they have a low surface area (around 60 m^{2}g^{-1}) (Berrueco *et al.*, 2005; Díez *et al.*, 2004; López *et al.*, 2009). The requirements of demineralisation and activation make commercial application unviable. However, pyrolytic char is a good candidate for gasification, the ash content is similar to or lower than that of many coals which are used in gasification processes.

2.3.2 Coal Pyrolysis

Pyrolysis of coal yields a solid char, liquid coal tar and pyrolytic gas. In the absence of air, minor decomposition of the aromatic molecule layers yields the liquid tars, while gases such as methane and H_2 are derived from the breakage of bonds to peripheral substituent groups and combination of the resulting radicals (Osborne, 1988). Devolatilization is the first step in thermally driven coal conversion and utilization processes, and it is one of the most critical sub-processes, it has a profound effect on the gasification processes (Howard, 1981; Brewster *et al.*, 1988; Nelson *et al.*, 1988 in Smith *et al.*, 1994).

Devolatilization of coal depends on many factors such as peak temperature, heating rate, pressure, particle size and coal type, and these are discussed below (Bell *et al.*, 2010).

Peak temperature and heating rate: X-ray diffraction measurements by Lu *et al.* (2000) showed that the chars become more crystalline and ordered with increasing pyrolysis temperature. With increasing pyrolysis temperature, H/C and O/C ratios in the chars decreased (Bell *et al.*, 2010).

Pressure: An increase in the pressure system will lead to lower fuel devolatilization, as the pressure exerted from the inside by the volatile matter is counteracted by the external pressure; at atmospheric pressure, volatile evolution is higher and faster (López *et al.*, 2012). The pressure system affects the way the char evolves during the devolatilization process and, therefore, affects the char outside surface and macropore morphology, which all affect the gasification reactivity of the char (López *et al.*, 2012; Yu *et al.*, 2004; Yang *et al.*, 2007 in Bell *et al.*, 2010).

Coal type and rank: Coal devolatilization behaviour and the proportions of each of the fractions that are evolved are affected by coal rank, organic properties and structural characteristics (Smith, *et al.*, 1994). The tar and gas yield of coal decreases as the rank increases. Bituminous coals exhibit high tar yields and moderate gas yields. Anthracites evolve less than 10% of their weight as volatile matter, almost all in the form of gas (Schobert, 2011; Williams *et al.*, 2000).

Coal pyrolysis proceeds in three basic stages (Schobert, 2011):

Stage 1 occurs at temperatures below 200^{o}C. It is usually a slow reaction, and the principal volatile products are water (from thermal dehydration of functional groups), carbon dioxide, carbon monoxide, and hydrogen sulphide. These products arise from a loss of functional groups or through condensation reactions.

Stage 2 occurs between about 350^{o}C and 550^{o}C. These reactions tend to be fast. The principal products are light hydrocarbon gases, including methane, as well as a variety of organic compounds which condense at room temperature to a tarry mixture; maximum tar yield occurs at approximately 500^{o}C – 550^{o}C (Saxena, 1990). Early tar evolution occurs from components of the coal that were not covalently bonded, but just trapped by slow diffusion rates and strong non-covalent bonds (Larsen, 1988; Yun *et al.*, 1991; Yurum *et al.*, 1991; Nishioka & Larsen,

1990 in Smith *et al.*, 1994). Evolution of hydrogen begins in this stage. During this stage, caking coals pass through a plastic state in which the coal appears to soften, swell, and then re-solidify into a porous mass.

Stage 3 begins above 550^{o}C. A variety of small gaseous molecules are formed, including water, carbon monoxide, carbon dioxide, hydrogen, methane, ethane, ethene, ethyne, acetylene, and ammonia. From 700^{o}C, the volume of gases increases, while most hydrocarbons decrease (Saxena, 1990). The other product is the char, which is a graphite-like solid of high carbon content.

2.4. Gasification

2.4.1 Gasification Overview

Gasification is a thermochemical process by which carbonaceous material is converted partially or completely into combustible gases (syngas) by reaction with a gasifying agent. The gasifying agent can be air, carbon dioxide, steam, oxygen or a mixture of two or more of these gases. Carbonaceous materials that can be gasified include coal, crude oil, biomass, natural gas and waste material such as waste tyres and waste plastics. Coal is the most common carbonaceous feedstock used in gasification and has been reported from as far back as 1792 (Littlewood, 1977 cited by Okolo, 2010). The use of waste material is increasing and is expected to continue to increase as the world seeks to convert more of its waste into energy.

Syngas generally consists of CO, H_2, CO_2, CH_4, and impurities such as H_2S and NH_3 (Liu *et al.*, 2010; Williams *et al.*, 2000), but the exact composition and calorific value will depend on the feedstock, the gasifying agent and the process conditions (Karatas *et al.*, 2012).

Syngas is used in one of three ways (Liu *et al.*, 2010):

(1) Combustion in a gas turbine to produce electricity as in the Integrated Gasification Combined Cycle (IGCC); a more efficient electricity generation technology which combines gasification and coal combustion.

(2) Raw material for chemical syntheses, such as ammonia synthesis (as a source of hydrogen), Fischer-Tropsch synthesis for liquid fuel production, and methanol production; or

(3) Methanation for synthetic natural gas production.

During coal gasification, both homogeneous and heterogeneous reactions occur. Homogeneous gas phase reactions are relatively simple, while heterogeneous reactions are more complicated (Liu *et al.*, 2010).Gasification proceeds in a number of steps, some of which depend on others, but which may occur simultaneously:

(1) Evaporation of moisture; the effect of this stage on the overall gasification thermodynamics is only substantial when low grade, high moisture coal is gasified, or when coal is fed to the gasifier as a coal-water slurry (Bell *et al.*, 2010).

(2) Pyrolysis, releasing volatile matter (tar, hydrocarbon liquids and gases), this is a rapid process and it leaves a char that is mainly composed of carbon and ash (Tomaszewicz *et al.*, 2013).

(3) Homogeneous reaction of volatiles released in the pyrolysis process in the gas phase; oxidation and partial oxidation reactions with the oxidant surrounding the coal particles. These reactions are very exothermic (Liu *et al.*, 2010).

(4) Heterogeneous reaction of char with gas-phase species (such as H_2O, O_2 and CO_2); carbon oxidation and partial oxidation, char gasification and hydrogenation are the reactions that take place at this stage, and they happen at a much lower rate than that of pyrolysis (Tomaszewicz *et al.*, 2013); and

(5) Mineral matter release and reaction forming ash (Liu *et al.*, 2010).

Gasification of the char or carbon with carbon dioxide (Boudouard reaction) is usually the prime process together with the partial oxidation steps, which produce CO (Williams *et al.*, 2000), and it is more important in CO_2-enriched gasification processes.

2.4.2 Gasification Reactions

The char gasification stage is the rate-controlling step because the reaction rate is much slower than that of pyrolysis (Tomaszewicz *et al.*, 2013), and it is also lower than the volatiles gas phase reactions rates, since it is a heterogeneous reaction and it is complicated by heat and

mass transfer effects (Liu *et al.*, 2010). It is therefore important to study char reactivity since it is a decisive factor in coal conversion processes, and it determines the volume and design of the gasifier (Song, 2005; Tomaszewicz *et al.*, 2013).

When oxygen is present in the gasifying gases, it reacts with carbon according to the following reactions (Liu *et al.*, 2010):

$C(s) + O_2 \rightarrow CO_2$	ΔH^o_{298K} = -393.98 kJ/mole	Equation (2.1)
$2C(s) + O_2 \rightarrow 2CO$	ΔH^o_{298K} = -221.31 kJ/mole	Equation (2.2)
$2CO + O_2 \rightarrow 2CO_2$	ΔH^o_{298K} = -566.65 kJ/mole	Equation (2.3)

These reactions are exothermic and the heat which they produce is useful for the endothermic gasification reactions. Since the above reactions are exothermic and result in low energy value gases, the quantity of oxygen feed to the gasifier must be controlled so that the reactions are not excessive (Bell *et al.*, 2010).

The carbon dioxide fed as gasifying agent, and any that is produced in carbon oxidation processes reacts with carbon in the reverse Boudouard reaction:

$C(s) + CO_2 \rightarrow 2CO$	ΔH^o_{298K} = +172.5 kJ mol^{-1}	Equation (2.4)

This is an endothermic reaction and it proceeds very slowly at temperatures below 1000K (727^{o}C).

Methanation reactions occur when the hydrogen produced by earlier reactions reacts with carbon, or the carbon containing gases to produce methane as the product of interest:

$C(s) + 2H_2 \leftrightarrow CH_4$	ΔH^o_{298K} = -74.94 kJ/mole	Equation (2.5)
$CO + 3H_2 \leftrightarrow CH_4 + H_2$	ΔH^o_{298K} = -206.3 kJ/mole	Equation (2.6)
$CO_2 + 4H_2 \leftrightarrow CH_4 + H_2O$		Equation (2.7)

These reactions are exothermic and generally slow, and they increase the calorific value of the product gas, since methane has a high heat of combustion, and they are important as substitutes of natural gas (Liu *et al.*, 2000).

A detailed understanding of char reactivity toward CO_2 and the reaction kinetics is considered essential for the mathematical and process modelling of gasifiers. (Tomaszewicz *et al.*, 2013)

2.4.2.1 Carbon Dioxide Gasification

Carbon dioxide gasification is described by Equation 2.4 the Boudouard reaction. This is an endothermic reaction and it proceeds very slowly at temperatures below 1000K (727^{o}C).

Char reactivities in CO_2 at temperatures of 1100 - 1300 K (827 – 1027^{o}C) for particle sizes less than 300µm are controlled by the intrinsic chemical reaction process with high activation energies. For a given char in the absence of a catalyst and at the same temperature they are much slower than char–O_2 reactions, which are pore-diffusion controlled, at the same temperature. Studies (Goetz *et al.*, 1982; Harris & Smith, 1989) have shown that the char-O_2 reaction is five orders of magnitude faster than the char-CO_2 reaction (Smith *et al.*, 1994). Char-CO_2 reactions are also slower than char-H_2O reactions.

2.4.2.2 Char-CO_2 Gasification Reaction Mechanisms

Char-CO_2 gasification reactions are heterogeneous reactions. Gas-solid reactions start with diffusion of reactant gas from the gas phase to solid surface, and into the solid internal surface through pores. The reactant gas adsorbed on the surface of the solid where the reaction subsequently takes place before desorption of the product from the surface of the solid. Finally, gaseous products diffuse from the internal surface to the solid surface and finally into the gas phase (Liu *et al.*, 2010).

Ergun and Mentser (1968) proposed a two-step process model for the Boudouard reaction

$C_{fas} + CO_2 \leftrightarrow C(O) + CO$ Equation (2.10)

$C(O) \rightarrow CO + C_{fas}$ Equation (2.11)

Where C_{fas} is a carbon free active site.

Dissociation of a CO_2 molecule at a carbon active site (C_{fas}), releasing CO and forming an oxidized surface complex [C(O)]. The carbon-oxygen complex subsequently produces CO and a new free active site; this is the actual carbon gasification step. Desorption of the carbon-oxygen surface complex is the rate-limiting step.

The rate for this mechanism can be described by the Langmuir-Hinshelwood rate equation

$$R = \frac{k_1 p_{co_2}}{1+\frac{k_1}{k_2}p_{co_2}+\frac{k_2}{k_3}p_{CO}}$$ Equation (2.12)

Intrinsic char reactivity is postulated to depend on the concentration of carbon edges and defects, or active sites, mineral matter, trace elements, oxygen, and hydrogen content (Laurendeau, 1978). These chemical parameters, along with the char porosity, account for variations in overall reactivity; as the gasification reaction proceeds the structure of the solid evolves spatially and temporally, affecting available surface area, active-site concentrations, and pore diffusion characteristics (Smith *et al.*; 1994).

In general, the chemical structures and elemental compositions of the fully devolatilized chars are much more similar than the diversity exhibited by the carbonaceous material feedstocks. Differences in char reactivity may be attributed to second-order variations in the carbon skeletal structure (physical structure), that produce variations in active sites, surface area and pore structure, or to differences in mineral content (Fletcher *et al.*, 1990; Pugmire *et al.*, 1991). Differences that affect char reactivity are impurities, dislocations and irregularities, different arrangements of edge atoms; reactant gases tend to preferentially adsorb on edge atoms. Hydrogen content on the surface of chars may also have an important role in their reactivity by generating nascent active sites (Radovic *et al*., 1985; Best *et al*., 1987; Khan, 1987).

The total surface area (TSA) of a char can be divided into three regions (Essenhigh, 1981): (1) the basal planes where there is little or no reaction, with no chemisorption film; (2) the reacting fraction of the active surface area (ASA), where there is little chemisorption film because the reaction is fast and the residence time of the oxygen atoms is negligible; and (3) the unreactive fraction of the ASA which is covered by adsorbed oxide film (Li *et al.*, 1998).

Carbon active sites are sites of intermediate reactivity which are sufficiently active to chemisorb the reactant gas and they are important for predicting gasification rates. Chars have a higher active surface area and are more reactive than chars produced under more severe conditions because they contain more edge carbon atoms; hydrogen content on the surface of chars also generates some nascent active sites (Smith *et al.*, 1994).

Tyre chars contain relatively high amounts of ash (12.5 wt.%) as well as 2.8 wt.% of sulphur. Because of the large amount of hydrocarbons driven off as volatiles during pyrolysis, the ash contains Si, Al, Ca, Mg, Na, Ti, Fe and Zn. The presence of crystals of zinc silicate (Zn_2SiO_4)

and zincite (ZnO) or zinc sulphide ZnS (depending on pyrolysis conditions) within the char has been confirmed by scanning electron microscopy and by XRD Analysis (Ucar *et al*. 2005; Olazar *et al*. 2009; López *et al.*, 2012).

2.4.3 Tyre Gasification

The gasification of waste tyres has been investigated at both laboratory and pilot plant scales (López *et al.*, 2012), and the general gasification behaviour of tyre char is similar to that of other carbonaceous material, with only differences in reaction kinetics, specific product composition and calorific value. As is the case with coal char, un-catalysed CO_2 gasification of tyre-char is an endothermic reaction, the rate is relatively slow and easy to measure. The chemical reaction is also the rate-controlling step when the particle size is smaller than 0.65 mm (Lee & Kim, 1996), and tyre char could also be co-gasified at existing coal gasification plants without any modification of the gasifier (López *et al.*, 2012).

2.4.3.1 Approaches to Tyre Gasification

The first approach to tyre gasification involves feeding tyre crumbs to the gasifier. In the first approach it is important to understand pyrolysis of tyres because it gives insight into a stage of gasification and the intermediate products that it produces, that is, the volatiles and the char. An alternative approach to tyre gasification involves separation of the pyrolysis and gasification steps, whereby pyrolysis is performed in a stand-alone pyrolysis plant and the product gases and oils are collected for various uses and the carbonaceous char is then fed to the gasification or co-gasification process (Zabaniotou & Stavropoulos, 2003; Conesa *et al.*, 2004). In the second approach, pyrolysis is a separate process and, therefore, it has to be studied, understood and controlled individually.

2.4.3.2 Tyre Gasification Studies

Song (2005) investigated the steam gasification reactivity of three carbonaceous materials (waste tyre, bituminous coal and sewage sludge) and found that the CO_2 gasification reaction rates follow the order: waste tyre > bituminous coal > sewage sludge. For the waste tyre gasification, the activation energy was 39.1 kJ/mol and the pre-exponential factor was 0.2669 s^{-1} over a temperature range of 550 - 800°C and a steam partial pressure of 50 kPa. The reaction order was 0.87 for tyre-char.

In experiments in an externally heated tubular stainless steel reactor at temperatures up to 1000°C, Lee & Kim (1996) found that the CO_2 reactivity of tyre char is lower than that of a bituminous coal (Datung coal), which is not particularly reactive in gasification, which is similar with the findings of Venter (2012). They also observed that tyre gasification conversion at 800-850°C is low, only ≈12% w/w daf conversion is achieved, even for a 90 minute reaction time at 800°C. Increasing the temperature to 850°C only produced a slight improvement in reactivity, but increasing the temperature to 900-950°C increased the reaction rate and improved conversion by three to five times (Lee & Kim, 1996).

Zabaniotou & Stavropoulos (2003) found that waste tyre char was less reactive than coal char and other carbonaceous materials, and they attributed this to the low content of heteroatoms (H, O, etc.), which act as active sites for gasification reactions, and of inorganic constituents [for example K, Na, Li, Ca (Lee & Kim, 1996)], which have catalytic activity in gasification reactions, in tyre char when compared to their content in coal char. The lower reactivity of tyre chars was also attributed to the orderly crystalline structure of tyre char which presents very little structural imperfections which are preferred centres for gasification reactions.

2.4.3.3 Co-gasification Studies

Venter (2012) studied the gasification and co-gasifcation of waste tyre char and coal char in a thermogravimetric analyser (TGA) and found that waste tyres were much less reactive than a vitrinite-rich coal from the New Denmark mine in South Africa. The activation energies of the tyre char and coal char were found to be 243 kJ/mol and 254 kJ/mol respectively (Venter, 2012). A blend of the tyre char and coal char in 1:1 ratio was initially slightly more reactive than the coal char up to a carbon conversion of about 80% ,where it slowed down and became slightly less reactive than the coal char; the activation energy of the blend was found to be 220 kJ/mol (Venter, 2012). He also found that there was a relative increase in reaction rate with an increase in isothermal reaction temperature, and that the char-CO_2 reaction followed Arrhenius type kinetics for the tyre, for the coal and for the blend.

Straka & Bučko (2009) investigated the co-gasification of waste tyre and a dried lignite from the Jiří open-pit mine in The Czech Republic on a laboratory scale by thermogravimetry. The gasifying agents used were steam and carbon dioxide. For CO_2 gasification, the results of the experiments showed that the temperature for the beginning of the gasification reaction was

significantly higher in the case of the coal and waste tyre mixture, than that of the coal alone. It was also found that the rate of gasification of the coal and tyre mixture was lower than that of the coal alone.

The rate of steam gasification of waste tyre was found by means of thermogravimetric analysis to be 1.59 wt.% min^{-1} , while that of the lignite coal was 3.49 wt.% min^{-1}, which shows that the lignite coal is more reactive than the waste tyre (Straka & Bučko, 2009). These results are comparable with the works of Murillo *et al.* (2006) and Murillo *et al.* (2004) (Murillo, et al., 2004) who studied the CO_2 reaction kinetics of a lignite coal char and waste tyre char, respectively, in a thermobalance reactor. Their results showed that the reaction of the lignite coal is significantly faster than that of the waste tyre char.

Talab *et al.*, (2010) modelled the co-gasification of coal and tyre shred with CO_2 and steam in a two-stage air blown gasifier using the multiple surface reactions model. The simulations revealed 100% conversion of both volatiles and char reactions, and particle burnout rate (reaction rate) results (Figure 2.2) showed that the reaction rate of the coal-tyre blend was higher than that of the coal alone and that the blend reacts more homogeneously along the gasifier centreline.

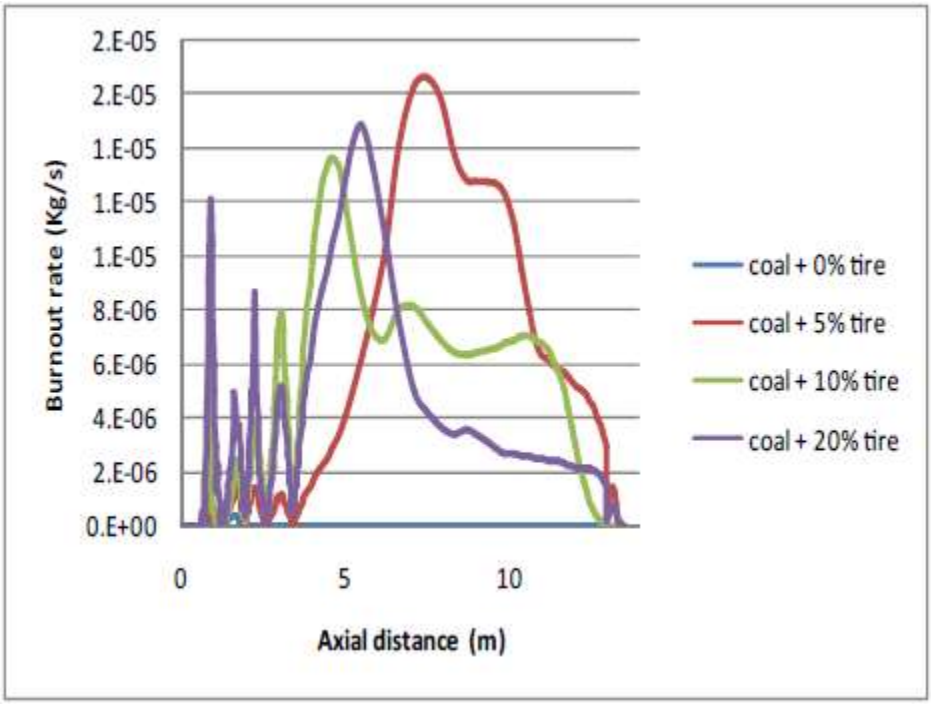

Figure 2.2: Centerline particle burnout rates (Talab *et al.*, 2010).

2.4.3.4 Char-Gas Reaction Regimes

Heterogeneous char-gas reactions are controlled by chemical kinetics at low temperatures and by gas diffusion/mass transfer at high temperatures. At moderate temperatures there is intermediate behaviour giving rise to three reaction regimes (zones) under which the char-gas heterogeneous reactions occur. There are three principles that control gas-solid reaction rate; i.e. external mass diffusion, internal diffusion, and the rate of the chemical reaction (Levenspiel, 1999). Each of these three principles dominates in each of the three reaction zones. The zones can be described as follows (Smith *et al.* 1994):

Zone I: Occurs at low temperature and is characterised by slow surface reaction and faster diffusion into the particle interior. Diffusion occurs into the particle centre and reaction takes place internally with constant particle diameter and changing density.

Zone II: Higher temperature than in Zone I therefore intrinsic reaction is also faster. Since the rate of reaction is faster than internal diffusion, gas only diffuses into outer layers of the particle and therefore reaction takes place in the outer layers and there will be a shrinking unreacted core inside the particle.

Zone III: At high temperatures there is fast intrinsic reaction on the surface and no significant diffusion into particle interior, therefore the particle reacts with constant density and decreasing diameter. Char chemical reactivity and porosity have less significance in overall rate of reaction in this zone.

The rate of mass transfer has weaker dependence on temperature than the surface reaction rate. Therefore, changes in the reaction regimes are mainly determined by changes in the surface reaction rate. The transition points between these zones depend on the reactant gas being used. Mass transfer into particle interior occurs by a combination of bulk gas flow and diffusion, and the reaction is determined by diffusion and reaction both in the surrounding gas phase and in the particle interior (Bell *et al.* 2010; Smith *et al.* 1994).

Kajitani *et al.* (2006) found that the overall carbon dioxide gasification rate for four coal chars was affected by mass transfer rates (Zone III) when the temperature was above 1,300 ^{o}C; and by surface reaction rate (Zone I) below 1200^{o}C. The range 1200^{o}C – 1300^{o}C is the transition and may represent Zone II behaviour. The effect of diffusion rates was indicated by the fact

that char particle sizes did not affect the gasification rate at low temperatures, but at high temperatures smaller particles reacted faster than larger particles (Bell *et al.* 2010).

As reaction proceeds, the internal surface area of particles increases as pores grow, and it decreases when pores begin to coalesce. These trends will also be observed in the char reaction rates especially in zone I and II where the effect of porosity is more significant. All modes of reaction have been observed in experiments depending on the conditions, and in practice reactions are known to occur in different zones depending on the gasifier type and operating conditions. Non-slagging gasifiers are typically operated below 1100^{o}C and therefore the overall reaction rate is probably limited by the surface reaction rate, while in slagging gasifiers, which are operated at 1300^{o}C to 1500^{o}C, mass transfer rate may limit the overall reaction (Bell *et al.* 2010).

2.5 Structural Kinetic Models

The overall reaction rate for char-gas reactions depends on the intrinsic surface reaction r_s, and the structure of the char particles (structure factor, $f(X)$), which are determined by the coal properties, char preparation conditions and operating conditions. This can be expressed by the equation given by Lu and Do (1992):

$$\frac{dX}{dt} = r_s(T, C) f(X) \qquad \text{Equation (2.13)}$$

The structural properties of chars that affect gasification rate include surface area, porosity, concentration of active sites on the surface and the catalytic effect of mineral matter; some of these properties for the samples used in this study are presented and discussed in Section 4.2. Models have been developed to predict the evolution of char surface area with conversion with the aim of predicting its behaviour and modelling gasification reactions. Some of the models that have been developed that incorporate structural evolution are: the volume reaction model, the shrinking core model and the random pore model (Bhatia & Perlmutter, 1980 and 1981; Everson *et al.*, 2008; Everson *et al.*, 2011; Miura *et al.*, 1990; Muhlen & Sulimma, 1987; Radovic *et al*, 1985; Kaitano, 2007; Okolo, 2010). For the purposes of this study, the random pore model and the volumetric model were selected and they will be discussed briefly in the section 2.5.1 and section 2.5.2

2.5.1 The Random Pore Model

The random pore model (RPM), initially proposed by Bhatia and Perlmutter (1980) and Gavalas (1980), has been used successfully by several investigators to model heterogeneous char-CO_2 reactions, combustion and other gas-solid reactions (Okolo, 2010; Everson *et al.*, 2008; Radovic *et al.*, 1985; Kaitano, 2007). The RPM takes into account internal structural changes in the reacting char, such as the change in the in active surface area, and it assumes that the reaction sites occur in cylindrical pores of arbitrary pore size distribution, which transform from being non-overlapped to being overlapped as the reaction progresses.

The random pore model can describe reactions that show a maximum rate at certain conversion levels, i.e. where rate of reaction initially increases due to pore growth as the reaction progresses and then decreases due to pore coalesecence, as well as reactions that do not exhibit this behaviour.

The random pore model is applicable to reactions in the chemical reaction kinetics controlled regime (regime I). For cases of reactions in regimes I and II where chemical reaction and pore diffusion effects are important, the RPM equation would be applicable at a particular point in the particle with a varying gas concentration profile along the radius, and the Thiele Modulus can be used to characterise the diffusion effect. The experimental conditions used in this study as described in Section 3.7.3 and Section 3.7.4 are such that the reactions are occuring under the chemical reaction controlled kinetics regime, and therefore the basic form of the random pore model with modifications defined by Kaitano (2007) and Everson *et al.*, (2008) will be used to model the results.

The equation of the random pore model is given as (Bhatia & Perlmutter, 1980):

$$f(X) = \frac{S_o(1-X)\sqrt{1-\Psi \ln(1-X)}}{1-\varepsilon_o} \qquad \text{Equation (2.14)}$$

The structural parameter (Ψ), which is a function of the physical properties of the char, is defined as:

$$\Psi = \frac{4\pi L_o(1-\varepsilon_o)}{{S_o}^2} \qquad \text{Equation (2.15)}$$

2.5.2 The Volumetric Model

The volumetric model (VM), also called the homogeneous model, is based on the assumption that the solid reactant is highly porous and therefore has enough space for the fluid reactant and the fluid product to difuse through freely, and that the active sites of the solid reactant are distributed homogeneously throughout the solid phase (Njapha, 2003). Apart from the assumption of a linearly decreasing reaction surface area with conversion, the volumetric model does not consider the structural changes of the char during gasification, and the reactions between the fluid and the solid are considered to be occurring homogeneously throughout the solid phase (Njapha, 2003; Zhang *et al.*, 2010; Fermoso *et al.*, 2010; Ishida & Wen, 1971). The model is, therefore, independent of particle size and shape and the reaction rate is determined by the chemical reaction rate. This means that the model is generally valid for reactions occuring in the chemical controlled regime (regime I) (Levenspiel, 1999). The rate expression of the volumetric model is given as (Zhang *et al.*, 2010):

$$\frac{dX}{dt} = r_s(1 - X) \qquad \text{Equation (2.16)}$$

Where r_s is the rate constant and X is the conversion.

With respect to time, the volumetric model can be written as:

$$t = -\frac{1}{r_s}\ln(1 - X) \qquad \text{Equation (2.17)}$$

This relationship can be used to evaluate the applicability of the volumetric model by comparing with experimental data.

Several researchers have successfully used the volumetric model to model reactions of coal or carbonaceous chars (Fermoso *et al.*, 2010; Njapha, 2003; Du Toit, 2013).

While the volumetric model can only represent systems where conversion rate decreases from its maximum at the beginning of the reaction to zero when the reaction is complete, the random pore model can represent the behaviour of a system that shows a maximum rate at certain conversion levels ($X < 0.393$) as well as one that does not. When $\Psi = 0$, the random pore model becomes the same as the volumetric model. Therefore, the random pore model is considered to be more flexible than the volumetric model (Zhang *et al.*, 2010).

CHAPTER 3: EXPERIMENTAL

3.1 Introduction

The experimental procedures and methods used to execute the gasification work are presented in this chapter. The nature and origin of the samples are discussed as well. Descriptions of materials used and various equipment used to execute the experimental work is also given in this chapter.

3.2 Origin of Tyre and Coal Samples

Waste tyre samples used in this study were obtained from Harry's Tyres in Potchefstroom, South Africa. The waste tyre samples were delivered already ground into granules in preparation for recycling in tyre retreading, and the reinforcing steel chords and textile fabrics were removed by the tyre company. The particle size ranged from -100µm to +1000 µm at delivery.

Two coal samples, one inertinite rich and the other one a vitrinite rich coal were also utilised in this work. The inertinite-rich coal (SF) is a run-of-mine coal from the Highveld coalfield in the Mpumalanga Province, and has a high ash content. Coals from this area are mainly used for electricity generation by ESKOM and for the production of petrochemical products by Sasol (Hattingh B. , 2009).

The vitrinite-rich coal (GG) is a washed coal from the Waterberg coalfield in the Limpopo Province. The coal is beneficiated and has a low ash content.

3.3 Sample Preparation

Gasification experiments were conducted on chars of the three samples with particle sizes below 75µm, the three samples were subjected to size reduction before being charred.

3.3.1 Size Preparation

Tyre samples were screened, and particles below 2000µm were collected and thereafter washed with water to remove sand and residual wire and other metallic material, which would distort the ash/mineral content and composition of the tyre and affect gasification reactivity of the tyre samples. After washing, the tyre samples were dried in air with direct sunlight. No size reduction was done at this point, because of the rubbery nature of tyre, until after charring.

The two coal samples were obtained in a particle size range greater than 40mm, and were first crushed using a jaw crusher to reduce the particle size to less than 10mm, and then milled with a hammer mill to obtain particles sizes below 3mm (3000µm). The coal samples were then milled again to below 75µm using a Fritsch P-14 rotary mill in a 6 litre ceramic jar with 10mm ceramic balls.

The - 75µm particles from each run were mixed in one 5 litre plastic bucket which was sealed tightly to avoid free contact with air before further processing.

The two coal samples were milled separately in turns in order to avoid contact and contamination of the samples with each other, the ceramic ball mill jar and the balls were cleaned by blowing with compressed air before and after use also to avoid sample contamination.

3.4 Char Preparation

The tyre and coal char samples were subjected to pyrolysis to obtain the tyre and coal chars which were used in the experiments. Charring experiments were carried out ex situ in order to avoid condensation of volatiles on the delicate Thermogravimetric Analyser used in the gasification experiments (Kaitano, 2007). The use of char for experimental work is motivated by the fact that in commercial gasification the reaction proceeds in three broad stages, i.e. evaporation, devolatilization, and gasification. Heterogeneous char gasification is the slowest stage, and is the reaction rate-controlling step (Tomaszewicz *et al.*, 2013, Bell *et al.*, 2010, Liu *et al.*, 2010).

3.4.1 Charring Procedure

Chars were prepared by devolatilization of the tyre and coal samples in a Packed Bed Balance Reactor (PBBR), shown schematically in Figure 3.1.

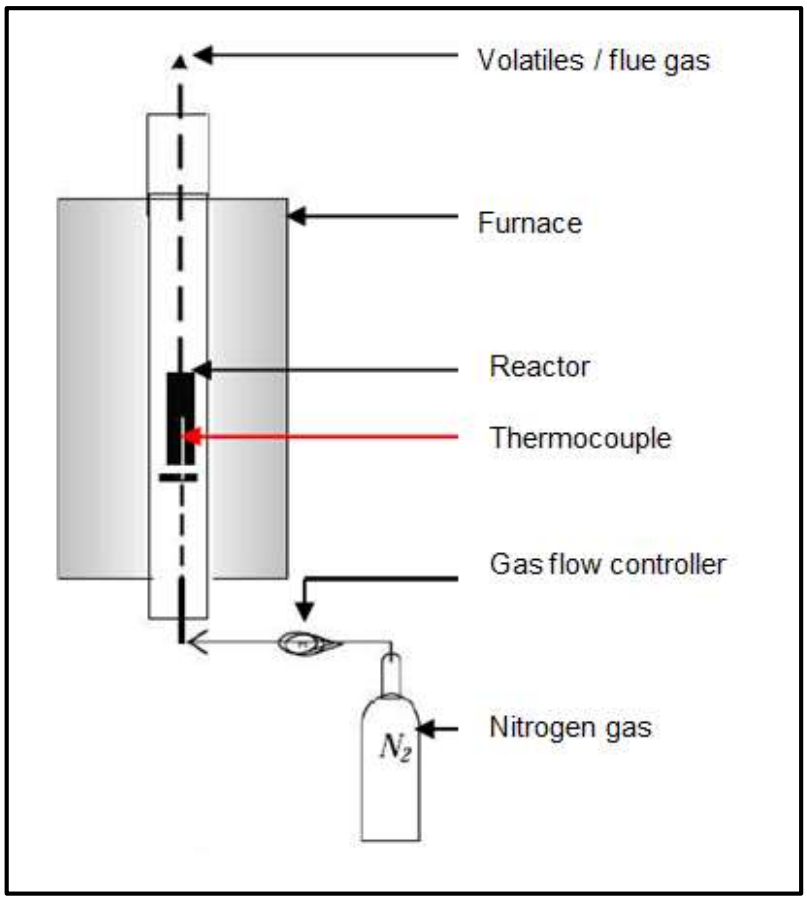

Figure 3.1: Experimental set-up for char preparation (Adapted from Kaitano, 2007).

The apparatus was ramped at 11 ºC/min until a temperature of 1000ºC where the sample was kept under inert nitrogen atmosphere for one hour. The procedure followed for each charring run is as outlined below:

1. 75g of tyre, 113g of GG coal or 124g of SF coal were weighed and fed into the reactor separately and the reactor was tightly sealed and placed into the furnace,
2. The purge gas (nitrogen) was turned on and set at a flow-rate of approximately 1.5litre/minute.
3. The furnace was started up and heated up at a rate of 11 ºC/minute to a final temperature of 1000ºC.In order to ensure complete devolatilization the temperature was held constant for 1 hour.
4. After the 1 hour holding time, the furnace was allowed to cool down naturally to ambient temperature.

5. When ambient temperature was reached, the nitrogen gas was turned off and the sample was removed from the reactor.
6. The chars obtained were weighed, placed in a re-sealable plastic pack (GLAD® Zip Seal) and sealed tightly and placed in a desiccator to prevent them from oxidising in air and absorbing moisture.

The average char yield results from the devolatilization of each sample are presented in Chapter 4.

After charring the tyre chars were then milled to particle sizes less than 75µm with the same rotary ball mill with a ceramic jar and ceramic balls that were used to mill the coal samples.

Due to the softening and swelling nature of the high vitrinite GG coal upon heating, the resulting char from the devolatilization process was agglomerated into lumps and had to be milled down to below 75µm once again. The SF coal did not show any agglomerating behaviour and the chars were collected in the same powder form as the coal that was fed.

The total chars obtained for each sample [waste tyre (WT) - 225g, SF - 249g and GG - 220g] were mixed to make one big batch of each sample in order to get one uniform sample of each. After the final size preparation by milling the samples were split into smaller representative batches of each sample using a rotary splitter pictured in Figure 3.1. The final SF, GG and waste tyre char samples were separately packaged in polytop vials and stored in a desiccator, one of the polytop vials will be taken out for experimental runs, characterisation or blending, at a time so that the larger proportion of the samples are always in the protected environment until they are required for use.

Figure 3.2: Rotary splitter

3.5 Char Blending

Blends were made on a mass basis to percentage proportions of waste tyre to coal chars of 75:25, 50:50 and 25:75. Each batch of the blends was a total of 8g made by mixing 6g & 2g, 4g & 4g, and 2g & 6g of waste tyre char and each of the coal chars respectively in a manually operated blender and mixing thoroughly in order to achieve a mixture as homogeneous as possible without reducing the particle sizes of the chars much further. Mixing time was standardised to four minutes so as to achieve the same level of blending and maintain similar particle size ranges. A total of 30g of each of the blend samples was made and packaged in polytop vials. The blend samples were named according to the proportions of the coal and waste tyre char that were mixed, thus they were named:

- 75% waste tyre to 25% GG coal blend – "GG25:WT75"
- 50 % waste tyre to 50% GG coal blend – "GG50:WT50"
- 25% waste tyre to 50% GG coal blend – "GG75:WT25"
- 75% waste tyre to 25% SF coal blend – "SF25:WT75"
- 50% waste tyre to 50% SF coal blend – "SF50:WT50"
- 25% waste tyre to 75% SF coal blend – "SF75:WT25"

Each of these samples was packaged in polytop vials and labelled accordingly, and they were all stored in a desiccator until required for experimentation, whereupon one of the vials with the required sample will be taken at a time for each run and returned to the desiccator immediately after weighing out the required sample.

3.6 Coal and Tyre Characterisation

The origins of the samples have been described in Section 3.2. All three samples have been used within the North West University School of Chemical and Minerals Engineering Coal Research Group for various studies previously, and both the raw samples and their chars were characterised (Coetzee, 2011; Nel, 2011; Monnaemang, 2013; Venter, 2012; Du Toit, 2013). Coal and waste tyre samples for this study were taken from the same batches that were used and characterised in the earlier studies.

3.6.1 Characterisation Tests and Standards

The coal samples were characterised by the chemical analyses - proximate analysis, ultimate analysis and calorific value determination – mineral analysis, petrographic analysis and structural analysis. Tyre samples were characterised by the chemical analyses, mineral analysis and structural analysis. The tests and standards used and the laboratories that carried out the analysis for each of the three samples are described below.

The proximate, ultimate and calorific value analysis of the two coals was conducted by Advanced Coal Technology Laboratories (Pty) Ltd. The ash composition analysis was conducted by UIS Analytical Services. The standards used for the chemical analyses and the mineral analysis are shown in Table 3.2 and Table 3.3 (Coetzee, 2011; Du Toit, 2013; Nel, 2011).

Table 3.1: Standards used for the chemical analyses and the mineral analysis of the SF coal and char (Coetzee, 2011; Du Toit, 2013).

Procedure	**Standard used**	
	SF coal	**GG coal**
Proximate Analysis		
Sample preparation	ISO 13909-4 :2001	SANS 18283: 2007 / ISO 18283: 2006
Moisture content	SANS 5925: 2007	SANS 5925: 2007
Ash content	SABS ISO 1171: 1997	SABS ISO 1171: 1997
Volatile matter content	SABS ISO 562: 1998	SABS ISO 562: 1998
Ultimate analysis		
Ultimate analysis	ISO 29541 : 2010	ISO 12902
Total sulphur	ISO 19579:2006	ISO 19579
Ash composition		
Mineral analysis (XRF)	ASTM D4326	ASTM D4326
Calorific value		
Calorific value	SABS ISO 1928:1995	SABS ISO 1928:1995

Table 3.2: Standards used for the chemical analyses and the mineral analysis of the GG coal (Nel, 2011).

Procedure	**Standard used**
Proximate Analysis	
Sample preparation	SANS 18283: 2007 / ISO 18283: 2006
Moisture content	SANS 5925: 2007
Ash content	SABS ISO 1171: 1997
Volatile matter content	SABS ISO 562: 1998
Ultimate analysis	
Ultimate analysis	ISO 12902
Total sulphur	ISO 19579
Ash composition	
Mineral analysis (XRF)	ASTM D4326
Calorific value	
Calorific value	SABS ISO 1928:1995

Chemical analysis of the GG char was conducted at North West University School of Chemical and Minerals Engineering laboratories as summarised in Table 3.4.

Table 3.3: Chemical analysis of GG chars (Monnaemang, 2013).

Proximate analysis	**Method/ Apparatus**	**Conditions**
Moisture content (wt. %)	Mettler Toledo HR83 Halogen	Sample weight: 1.0 +/- 0.1 g Temperature: 105°C for 180 min
Volatile matter content (wt. %)	LJ-Therm-Volatile oven	Sample weight: 1.0 +/- 0.1 g Temperature: 900°C for 7 min
Ash content (wt. %)	LJ-Therm-Volatile oven	Sample weight: 1.0 +/- 0.1 g Temperature: 900°C for 180 min
Fixed carbon content (wt. %)	100-(moisture+ volatile matter+ ash)	-
Ultimate analysis	CE-440 Elemental analyzer	-
Calorific value	IKA C5000 bomb calorimetric meter	Sample weight: 1.0 +/- 0.1 g

Chemical analysis of the waste tyre and the waste tyre char was conducted at the SANAS testing laboratory (Venter, 2012).

Petrographic analysis of the two coals was conducted by Petrographics SA. Samples for analysis were prepared according to the ISO Standard 7404-2 (1985). The Vitrinite random reflectance was done on 100 readings according to ISO Standard 7404-5 (1994), whereas ISO standard 7404-3 (1994) was followed to analyse the group macerals (500 point-count technique). The total maceral reflectance scan was done on 250 random reflection readings and the coal microlithotype, carbominerite and minerite analysis was done according to ISO Standard 7404-4 (1988) (Coetzee, 2011; Du Toit, 2013).

Structural analysis was carried out at the North West University School of Chemical and Minerals Engineering laboratories. CO_2 gas adsorption analysis was conducted using the Micromeritics ASAP2010 Analyser. The Micromeritics ASAP 2010 Analyser software was used to determine the surface area using the BET and Langmuir gas adsorption models (Coetzee, 2011).

3.7 Gasification Experiments

3.7.1 Experimental Material

The primary experimental materials for this study are waste tyre char (-75µm), a vitrinite-rich coal char, GG coal (-75µm) and an inertinite-rich coal char, SF coal (-75µm). The coal and tyre samples are described in detail in Section 3.2 and their characteristic properties are presented in Section 3.5. The reactant gas is technical grade carbon dioxide of 99.0% purity supplied by African Oxygen Limited (AFROX) South Africa.

3.7.2 Experimental Equipment and Set-up

Gasification experiments are carried out on a thermogravimetric analyser (TGA) built at the North West University (Potchefstroom Campus), School of Chemical and Minerals Engineering. A schematic representation of the experimental equipment is shown in Figure 3.2.

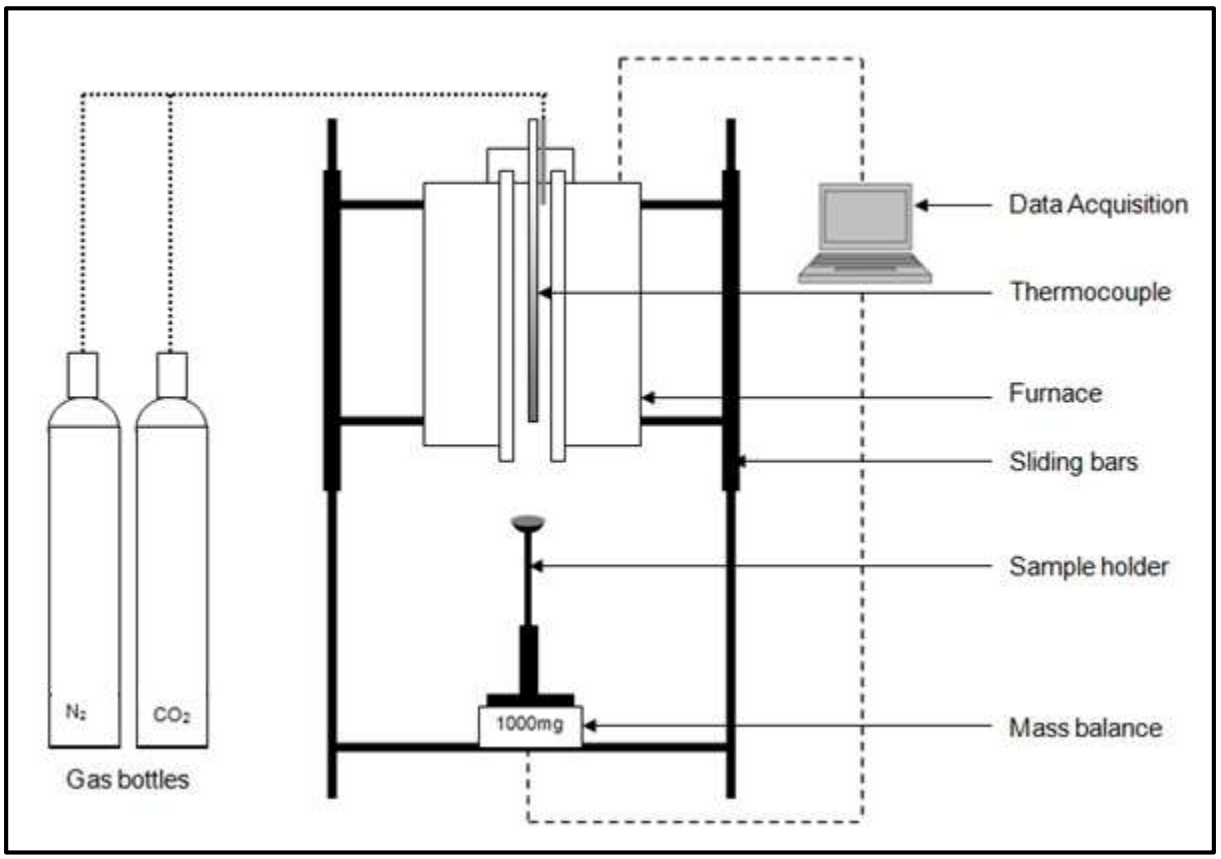

Figure 3.2: Schematic presentation of the TGA set-up (Monnaemang, 2013).

The reaction chamber in the set-up is a vertical pipe (52mm in diameter), in which the sample holder will be positioned, within a Lenton® TSV 15/50/180 furnace with a heating rate capability of 1 - 25^{o}C/min and a maximum possible temperature of 1500^{o}C. The furnace

temperature is monitored by a 6mm K-type thermocouple which is connected to a data logger. Reactant gas is fed from the top of the reaction chamber and it is controlled by a Brooks® 5850 TR Series mass flow controller with a range of 0 – 2L/min. The mass flow controller is calibrated for the CO_2 gas that is to be used in the experiments under ambient conditions close to those at which experiments will be conducted.

The quartz sample holder sits on a Sartorius® ED4202S balance which measures the weight of the sample during an experimental run. The mass reading from the balance and the temperature reading from the thermocouple are logged on the computer using Advantech VisiDAQ Runtime software, which records the temperature (°C) and mass (mg) values every five seconds, the saved data can be retrieved into a Microsoft Office Excel file for processing.

3.7.3 Experimental Procedure

A 2g sample was placed on the alumina sieve lined with quartz wool to prevent the powder samples from leaking through the sides of the sieve. The quartz sample holder with the sample on it was placed on the Sartorius balance and carbon dioxide gas was turned on and set to flow at 2L/min. The cold furnace was lowered, onto the loaded sample holder and the balance was then switched on or tarred so that it reads "0.00g" with the sample holder and gas flow on. The thermogravimetric analyser (TGA) reactor oven was raised again and set to the isothermal temperature required for the particular experimental run, and it was heated up at a rate of 20°C/min until the required isothermal temperature (900°C, 925°C, 950°C or 975°C) was reached.

When the TGA oven reached the required isothermal temperature, the oven was lowered to a position where the thermocouple in the oven was 4mm above the loaded sample holder so that it read the correct temperature at which the sample would be reacting. Immediately after the reactor furnace was lowered, the data collection software was logged so that it started recording the mass and temperature data.

When the reaction was complete, data logging was stopped and the data was saved on the computer and on external storage for processing of results; CO_2 gas flow was stopped. The ash that was left in the sample holder, which consists primarily of mineral matter, was weighed on the Mettler Toledo balance.

3.7.4 Experimental Programme

Reactivity experiments were carried out on the waste tyre and coal. According to the aim of determining the reactivity and kinetics of blends of the two coal-derived chars with the waste tyre-derived char (Section 1.2); experiments were done on the blends of the tyre with each of the two coals in five different compositions of tyre and coal at four different temperatures (900^{o}C, 925^{o}C, 950^{o}C, 975^{o}C).

All experiments were conducted at atmospheric pressure with a carbon dioxide flow rate of 2000ml/min. Two experimental runs were conducted for each of the sample proportions at one of the four temperatures. Table 3.12 sets up a summary of the experimental programme.

Table 3.4: Experimental Programme

Parameters		Gasification Reaction Conditions
Tyre:coal sample ratios	Tyre:SF coal chars	100:0, 75:25, 50:50, 25:75, 0:100
	Tyre:GG coal chars	100:0, 75:25, 50:50, 25:75, 0:100
Particle size		75µm
Mass of sample		2g
Reactant gas		100% CO_2
Reactant gas flow rate		2000 ml/min
Temperatures		900^{o}C, 925^{o}C, 950^{o}C, 975^{o}C
Pressure		1atm
Number of runs		38
Number of repeats		2

CHAPTER 4: RESULTS AND DISCUSSION

4.1 Introduction

Results from the experimental work presented in Chapter 3 are presented in this chapter. Results from the devolatilization/pyrolysis process are presented in Section 4.2, sample characterisation results are presented in Section 4.3 and CO_2 gasification results are presented in Section 4.4. The presentation of gasification results will focus on the influence of temperature on the CO_2 gasification reactivity of the samples, the reactivities of the three different samples, the effect of blending the waste tyre char with coal char and comparison of the effects of the two coal chars on the reactivity of the waste tyre char (WT). Discussions on the gasification results are also presented in Section 4.4.

4.2 Devolatilization Results

The yields of the three fractions obtained from the devolatilization or charring process are presented in Table 4.1.

Table 4.1: Devolatilization yields.

Sample	Feed (g)	Char yield (g)	Ash & Fixed Carbon (%)	Volatiles & Moisture (%)
Tyre	75	28	37.3	62.7
GG Coal	113	73.5	65.0	35.0
SF Coal	124	83	66.9	33.1

4.3 Characterisation Results

4.3.1 Proximate Analyses

Table 4.2: Proximate Analyses results for GG coal, SF coal, Tyre and their chars (Nel, 2011; Du Toit, 2013; Venter, 2012).

	GG coal		**GG char**		**SF coal**		**SF char**		**Tyre coal**		**Tyre char**	
	Proximate Analysis [wt%]											
	(a.d)	**(d.a.b)**	**(a.d)**	**(d.b.)**	**(a.d)**	**(d.b.)**	**(a.d)**	**(d.b.)**	**(a.d)**	**(d.b.)**	**(a.d)**	**(d.b.)**
Moisture content	5.0	-	1.1	-	5.6 ± 0.1	-	3.0 ± 1.2	-	0.5	-	0.2	-
Volatile matter content	27.0	30.2	1.6	1.9	23.8 ± 0.1	25.2 ± 0.1	1.9 ± 0.1	2.0 ± 0.1	63.8	64.1	0.4	0.4
Fixed carbon content[1]	55.4	56.8	83.4	83.8	49.1 ± 0.3	52.0 ± 0.3	70.4 ± 1.3	72.5 ± 1.3	29.1	29.2	84.7	84.9
Ash Content	12.6	13.0	13.9	14.3	21.6 ± 0.3	22.9 ± 0.3	24.8 ± 0.3	25.5 ± 0.3	6.6	6.7	14.7	14.7
Total	100	100	100	100	100	100	100	100	100	100	100	100
Gross calorific value (MJ/kg)	26.6	-	29.7	-	21.7 ± 0.3	-	24.2 ± 0.3	-	37.95	-	28.71	-

[1] Obtained by difference.

4.3.2 Ultimate Analyses

Table 4.3: Ultimate Analyses results for GG coal, SF coal, Tyre and their chars (Nel, 2011; Du Toit, 2013; Venter, 2012).

	GG coal	GG char	SF coal	SF char	Tyre coal	Tyre char
Ultimate Analysis [wt%] (dry ash-free basis)						
Carbon	67.1	80.4	78.4 ± 0.1	96.0 ± 0.1	89.7	96.9
Hydrogen	4.2	0.7	4.0 ± 0.1	0.1 ± 0.1	7.7	0.0
Nitrogen	1.7	1.2	2.0 ± 0.1	1.6 ± 0.1	0.4	0.2
Total sulphur	0.68	0.07	0.9 ± 0.3	0.7 ± 0.1	2.1	2.9
Oxygen [1]	8.8	17.6	14.7 ± 0.4	1.6 ± 0.2	0.1	0.1
Total	100	100	100	100	100	100

[1] Obtained by difference

4.3.3 Mineral Analysis

Mineral analysis is used to determine the mineral species present in the ash from the coal and tyre sample by means of XRF analysis and the results obtained for the two coal and the tyre samples are presented in Table 4.4.

Table 4.4: Mineral analysis results for GG coal, SF coal and Tyre (Nel, 2011; Coetzee, 2011)

Inorganic species	**Ash Sample**		
	GG coal Wt. % (d.b.)	**SF coal Wt. % (d.b.)**	**Waste tyre Wt. % (d.b.)**
Al_2O_3	29.0	23.99	17.30
CaO	7.9	14.62	5.27
Fe_2O_3	4.3	2.92	2.14
K_2O	0.5	0.38	1.32
MgO	2.7	3.35	0.99
Na_2O	0.7	0.84	11.70
P_2O_5	1.5	1.73	0.33
SiO_2	45.0	44.87	58.32
TiO_2	1.7	1.46	1.15
SO_3	2.8	3.25	1.15
Other	3.8	2.59	0.33
Total	99.9	100	100
Char Ash Content	13.9	24.8	14.7
Alkali Index (AI)	1.7	8.2	4.2

It can be observed that the ash of the GG coal sample consists mainly of SiO_2, Al_2O_3, CaO and Fe_2O_3 species, respectively, which make up a total of 86.2% of the ash. The results obtained from the XRF analysis are similar to the mineral analysis for other washed South African export coals (Pinheiro, 1999). In SF coal SiO_2, Al_2O_3, CaO and MgO, respectively, are the dominant species. Hattingh *et al*. (2011) also obtained high values for SiO_2, Al_2O_3 and CaO for South African Highveld coals. Coetzee (2011) compared his results with the works of Oberholzer (2009) and Pinheiro (1999) and all three sets of results were comparable. Pinheiro (1999)

obtained a significantly higher value for the major constituent SiO_2 and for Fe_2O_3, while their value for CaO was significantly lower (Coetzee, 2011).

4.3.4 Petrographic Analysis

Petrographic analysis is used to determine the vitrinite random reflectance, group macerals, reactive inertinite macerals, total maceral reflectance, microlithotype, carbominerite and minerite of the coals (Coetzee, 2011). The results obtained by Nel (2011) on 3mm GG coal particles and by Coetzee (2011) on 5mm SF coal particles are presented in Table 3.7 – Table 3.9 along with comparison with the results from Oberholzer (2009).

Table 4.5: Reflectance results for GG coal and SF coal and comparison.

	GG coal 3mm (Nel, 2011) **Vol%**	**SF coal 5mm** (Coetzee, 2011) **Vol%**	**Oberholzer (2009) Vol%**
Vitrinite random reflectance	0.69	0.62	0.57
Total maceral reflectance	0.71	1.12	1.11

According to the ISO 11760-2005 Classification of Coals, the three coals in Table 4.5 are classified as bituminous medium Rank C.

Table 4.6: Monomacerals analysis results for GG coal and SF coal and comparison.

	GG coal 3mm (Nel, 2011) **Vol% (m.m.f)**	**SF coal 5mm** (Coetzee, 2011) **Vol% (m.m.f)**	**Oberholzer (2009) Vol% (m.m.f)**
Vitrinite	86.3	25	24
Liptinite	6	3	4
Inertinite	7.7	71	72

GG coal is classified as a vitrinite rich coal, while SF coal is classified as an inertinite rich coal. The observations for SF coal agree with observations made for Highveld coals by other researchers (Van Niekerk, 2008; Hattingh *et al.*, 2011; Coetzee, 2011).

Table 4.7: Microlithotype analysis of GG coal and SF coal.

	GG coal 3mm (Nel, 2011) **Vol%**	**SF coal 5mm** (Coetzee, 2011) **Vol%**	**Oberholzer (2009)** **Vol%**
Pure vitrinite	55	12	9
Pure inertinite	2.3	37	40
Clarite	11.3	2	2
Durite	<1	3	11
Vitrinertite	6	16	9
Trimacerite	12.3	10	8
Carbominerite	7.7	16	14
Minerite	5.3	4	7

The pure vitrinite, pure inertinite and other microlithotype results reflected in Table 4.7, again, confirm GG coal as a vitrinite rich coal and SF coal as an inertinite rich coal.

4.3.5 Structural analysis

Table 4.8: CO_2 adsorption structural analysis results for GG coal, SF coal, Tyre and their respective chars.

	GG (Monnaemang, 2013)		**SF** (Du Toit, 2013)		**Tyre** (Venter, 2012)	
Variable	**Coal**	**Char**	**Coal**	**Char**	**Tyre**	**Char**
D-R Surface area [m^2/g]	136 ± 2	215 ± 2	161 ± 5	182 ± 5	25.65	44.38
BET / Langmuir S_o [m^2/g]	72 ± 2	113 ± 2	117 ± 5	126 ± 5	56.79	35.09
Pore Volume (cm^3/g)	0.03	0.046	$4.2 \pm 2 \times 10^{-5}$	$3.3 \pm 2 \times 10^{-5}$	0.00487	0.0104
Pore Diameter (Å)	4.05	3.8			4.486	4.271

CO_2 gas adsorption was used to characterise the surface area and pore structure of the coal and tyre using low-pressure adsorption of gases. The micro pore surface area was calculated using the Dubinin-Radushkevich (D-R) equation and Langmuir surface areas were calculated from isotherm data (Du Toit, 2013). It can be observed that the Dubinin-Radushkevich (D-R) surface

area increased from the raw sample to the char for both the coals and the tyre. This can be attributed to the creation of more micropores during the devolatilization process. BET Langmuir surface area showed the same trend in SF coal, but in tyre Venter (2012) observed a decrease in the surface area in the char, and this was explained by the CO_2 gas reacting with the fixed carbon on the surface area of the sample, thus decreasing the quantity of active sites.

Pore volume increased from raw sample to char for GG coal and for tyre, but the opposite was observed for the SF coal. Du Toit (2013) attributes this observation in the SF coal to the increase in the number of micropores which, although it increases the total surface area, it decreases the average pore diameter and volume.

SF coal surface area results are comparable with values obtained for three Highveld seam 4 coals which range between 181-197 m^2/g when calculated using the Dubinin-Radushkevich equation (Hattingh et al., 2011). The BET surface area of the waste tyre compares with the surface area (< 100 m^2/g) reported by Edward *et al.* (2004) and Wojtowicz *et al.* (1996) (30 – 90 m^2/g), however the BET surface area of the waste tyre chars is lower than the values obtained from literature (270 – 980 m^2/g) (Venter, 2012). The surface area values obtained do fall in the range obtained by Liu *et al.* (2000) in a study on six Australian bituminous coals.

4.4 Gasification Results

4.4.1 Normalisation of Experimental Results

A typical mass loss versus time plot of the raw experimental data obtained from the thermogravimetric analyser (TGA) is shown in Figure 4.1. The reaction shows a rapid mass loss at the beginning, which then slows down gradually as the reaction progresses and the reacting carbon decreases until a constant final mass is obtained. The final mass of the reacting sample in Figure 4.1 of 360mg (18%), which represents the ash content of the WT char, is close to the expected ash content of 18.4%, based on the proximate analysis of the waste tyre samples presented in Section 4.3. For further processing and presentation of the data, the mass is converted to grams and time is converted to minutes for convenience of handling and presentation.

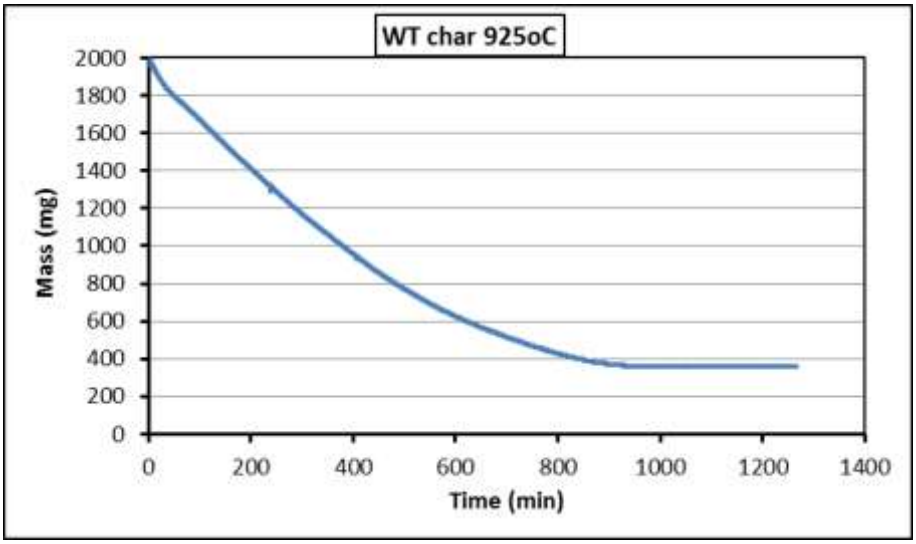

Figure 4.1: A typical mass loss curve for waste tyre char (WT) at 925ºC at atmospheric pressure.

Experimental results are normalised according to the initial mass (M_0) so that they can be compared on the same axis:

$$n = \frac{M}{M_0} \qquad \text{Equation 4.1}$$

Figure 4.2 presents a normalised plot for the reaction results of GG char at four different temperatures (900ºC, 925ºC, 950ºC, 975ºC) and it compares the reactivity of the char sample at the four given temperatures.

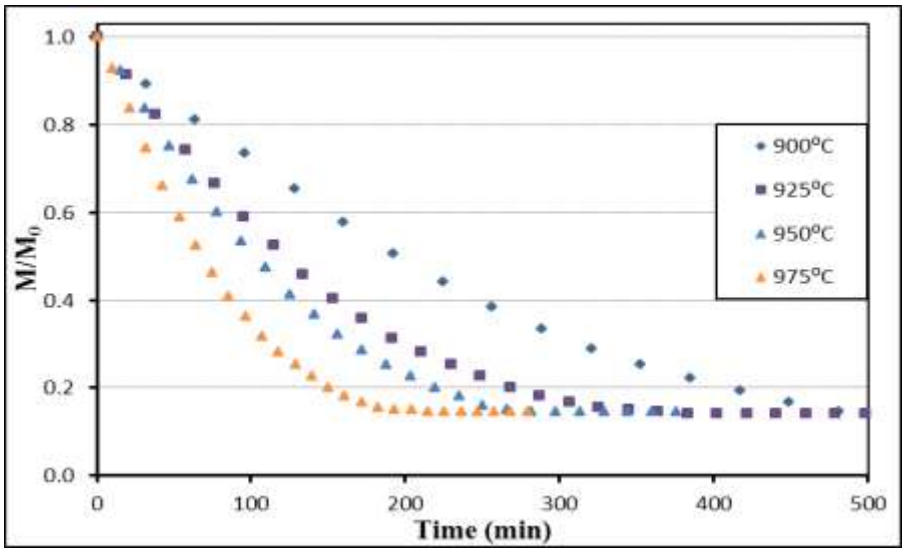

Figure 4.2: A normalised mass loss curve for the reaction of GG char at four temperatures.

To compare the reactivities of only the carbon content of the chars, the results were normalised on an ash-free basis, assuming that all significant mass loss occurring in the reacting sample was due to carbon conversion, i.e. neglecting all reactions or mass loss related to gas evolution by the mineral mater in the coal or waste tyre. The data was normalised according to the equation 4.1 (Kaitano, 2007),

$$X = \frac{m_0 - m_t}{m_0 - m_{ash}} \qquad \text{Equation 4.2}$$

The conversion rate or rate of reaction at a point in time during the reaction was calculated from the slope of the conversion graph at that particular point by Equation 4.3:

$$\frac{dX}{dt} = \frac{\Delta X}{\Delta t} = \frac{X_i - X_{i-1}}{t_i - t_{i-1}} \qquad \text{Equation 4.3}$$

A typical conversion versus time graph is presented in Figure 4.3. The conversion rate is highest at the beginning of the reaction - this is referred to as the initial reactivity of the sample and it varies with temperature, and at least four initial reactivities at different temperatures can be used to estimate the activation energy of the sample for the reaction with carbon dioxide. The conversion rate gradually decreases with time and progression of the reaction occurs until it is zero, when conversion is complete (X = 1). Conversion data is also the basis of the modelling work.

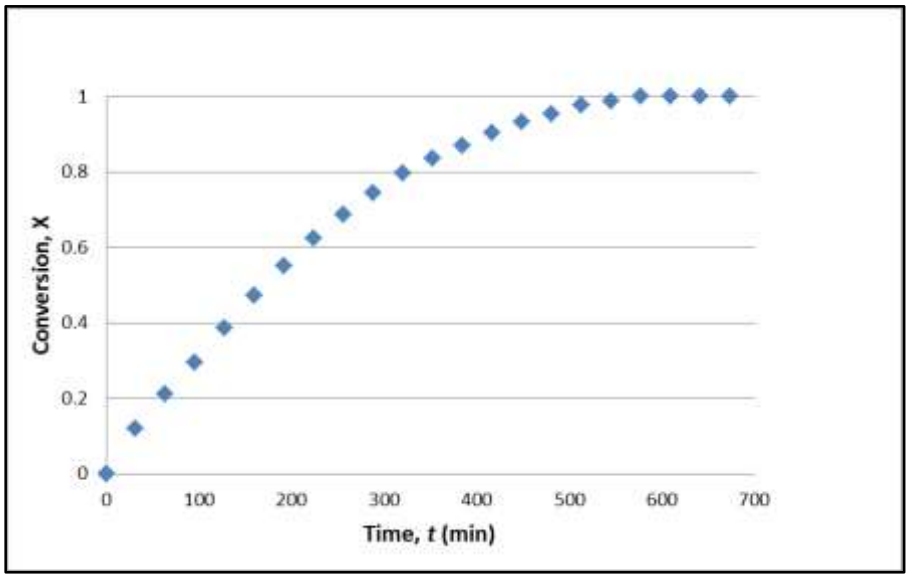

Figure 4.3: Conversion versus time plot for the reaction of GG coal char with CO_2 at 900^{o}C.

4.4.2 Repeatability of Experiments

Repeat runs were conducted for each of the nine samples in order to ascertain accuracy of the experiments and reliability of the experimental result. The two sets of results for each sample at a given operating temperature with constant gas flow rate (2L/min 100% CO_2) were compared by plotting the conversion curves on the same axis, and by calculating the initial reactivities, the times for 50% conversion ($t_{0.5}$), the structural parameters (Ψ), and the time factor (t_f) from the random pore model (RPM) for each of the experimental runs.

The results of this analysis for the three samples, Tyre (WT), one coal (GG) and one blend (GG50:WT50) at 975ºC, 950ºC and 925ºC respectively, are presented in Figure 4.5 and in Table 4.9.

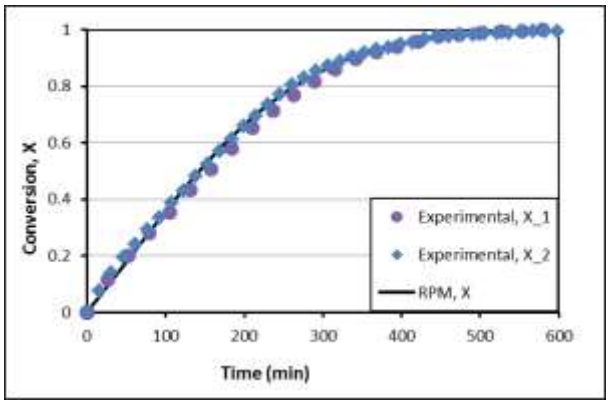

WT 975ºC

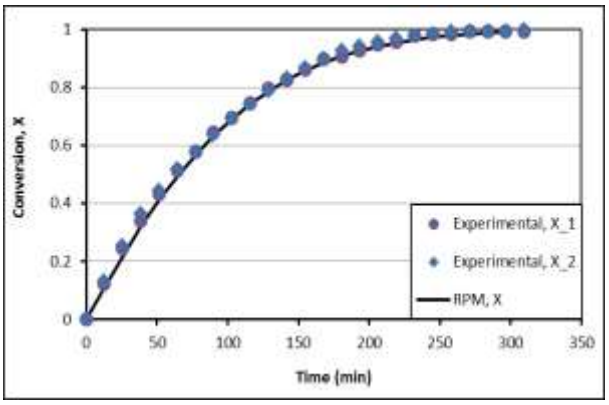

SF 950ºC

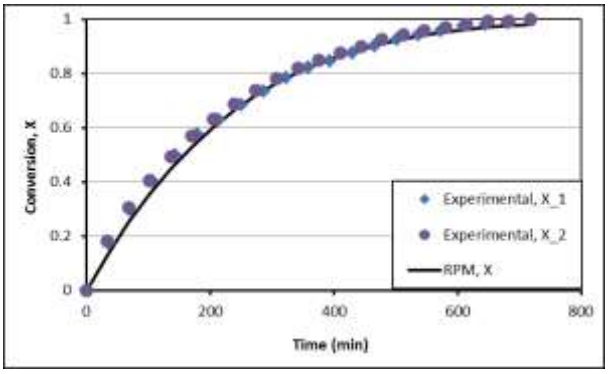

GG50:WT50 925ºC

Figure 4.5: Repeatability analysis - conversion versus time plots for WT (975ºC), SF (950ºC) and GG50:WT50 (925ºC) along with the random pore model (RPM) conversion curves.

Table 4.9: Repeatability analysis – comparison of reaction parameters for WT (975°C), SF (950°C) and GG50:WT50 (925°C).

Sample	Run	Ψ	t_f (min^{-1}) x 10^{-3}	Initial Reactivity (min^{-1}) x 10^{-3}	$t_{0.5}$ (min)
WT	1	4.94	3.39	5.06	155
	2	2.97	3.6	4.74	143.1
SF	1	1.1	9.09	9.79	60
	2	1.32	7.59	10.4	61.25
GG50:WT50	1	0.302	3.9	4.87	143
	2	0.212	4.09	5.36	136.8

Figure 4.5 and Table 4.9 show that both the experimental and model conversion curves as well as the calculated reaction parameters are sufficiently close to each other, hence the experimental results are repeatable and reliable.

4.4.3 Effect of Operating Temperature on Gasification Reactivity

Char-CO_2 gasification experiments were conducted at four different temperatures (900°C, 925°C, 950°C, 975°C) with all other conditions being kept constant for all the samples investigated in this study. The results are presented as plots of conversion versus time for each experimental run. The results are also presented in the form of specific reaction rate versus conversion plots. The plots for four selected samples (WT, GG coal char, GG50:WT50 and SF25:WT75) are shown in Figures 4.6 and 4.7.

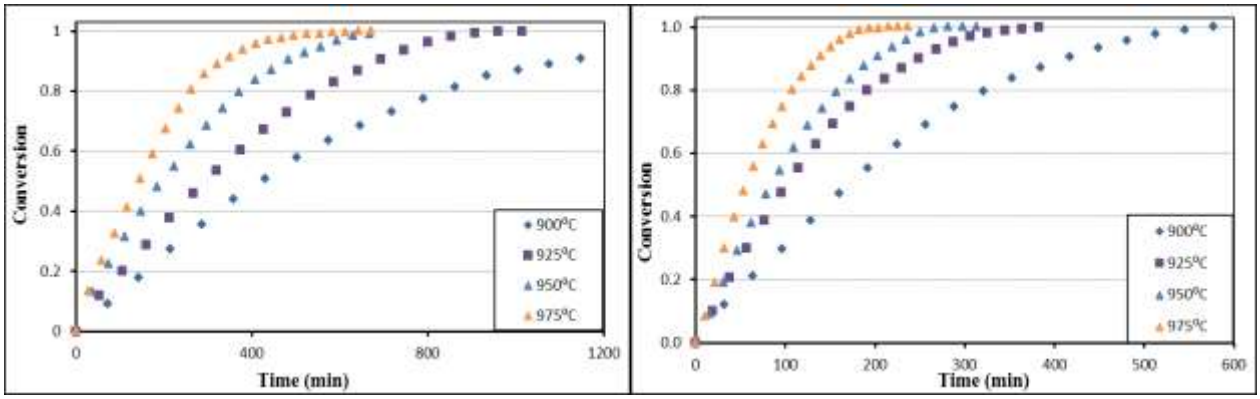

WT GG

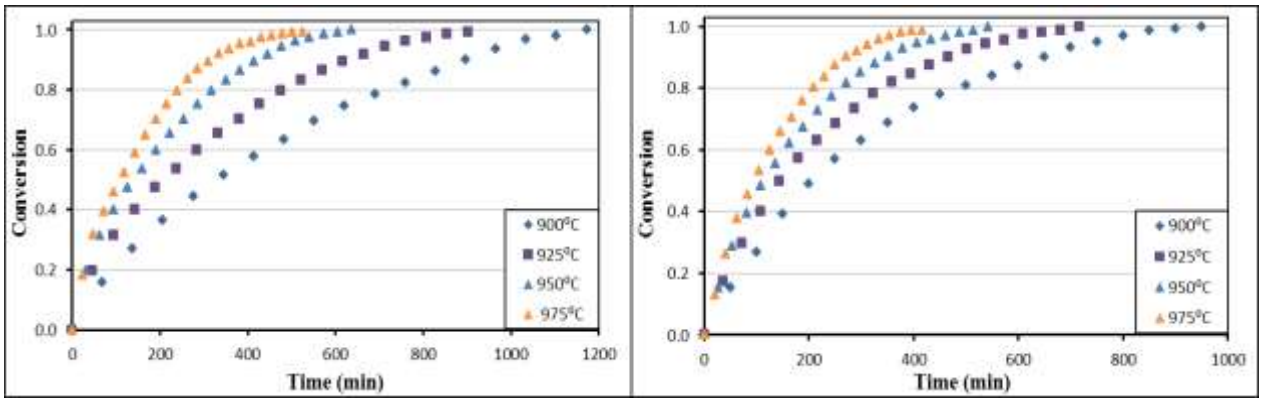

SF25:WT75 GG50:WT50

Figure 4.6: The effect of temperature on CO2 gasification reactivity of waste tyre (WT), coal (GG) and two blends of waste tyre and two coals (GG50:WT50 and SF25:WT75).

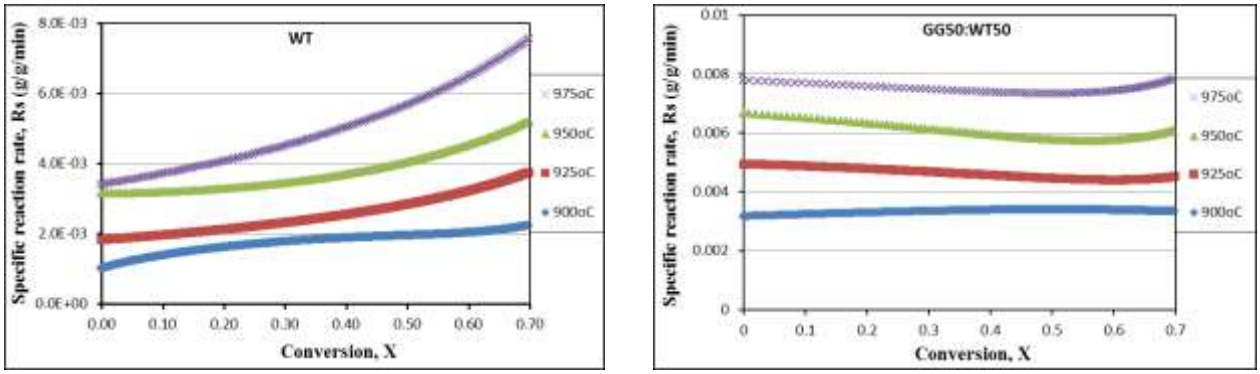

Figure 4.7: The effect of temperature on **s**pecific reactivity of waste tyre (WT) and a blend of waste tyre and GG coal (GG50:WT50).

The trends in Figure 4.6 show that an increase in reaction temperature results in lower conversion times for all the samples under investigation (results for the other samples in Appendix A.1). The specific reaction rate versus conversion plots in Figure 4.7 show that at

any given point of carbon conversion the specific reaction rate gets higher with increase in temperature. The char-CO_2 gasification reaction follows Arrhenius type of kinetics (Okolo, 2009). The effect of temperature on the gasification rate shows that intrinsic reaction rate is more dominant than the mass transfer (gas diffusion) effects (Du Toit, 2013; Xu *et al.*, 2011). The findings agree with the trends in literature on coal as well as biomass (Kaitano, 2007; Xu *et al.*, 2011; Hattingh B., 2009; Radovic *et al.* 1985; Ochoa *et al.*, 2001; Everson, 2008; Njapha, 2003).

4.4.4 Reactivity of Samples

In this section the reactivity of the different samples used in this study is presented and compared using three methods, the conversion versus time plot, the specific reactivity versus conversion plot, and the initial reactivity, $\left(\frac{dX}{dt}\Big|_{t=0}\right)$. The reactivities of the pure samples are presented and discussed in Section 4.4.4.1, while the reactivities of blended samples are presented and discussed in Section 4.4.4.2. The influence of sample properties and the effects of blending coal and waste tyre are also discussed in the respective sections.

4.4.4.1 Pure Coal and Tyre Samples

Conversion – time and specific reactivity - conversion plots for the char-CO_2 gasification reactions of waste tyre char (WT), GG coal char and SF coal char at 975^{o}C are shown in Figure 4.8 (a) and (b) respectively in order to show the relative reactivities of the three char samples.

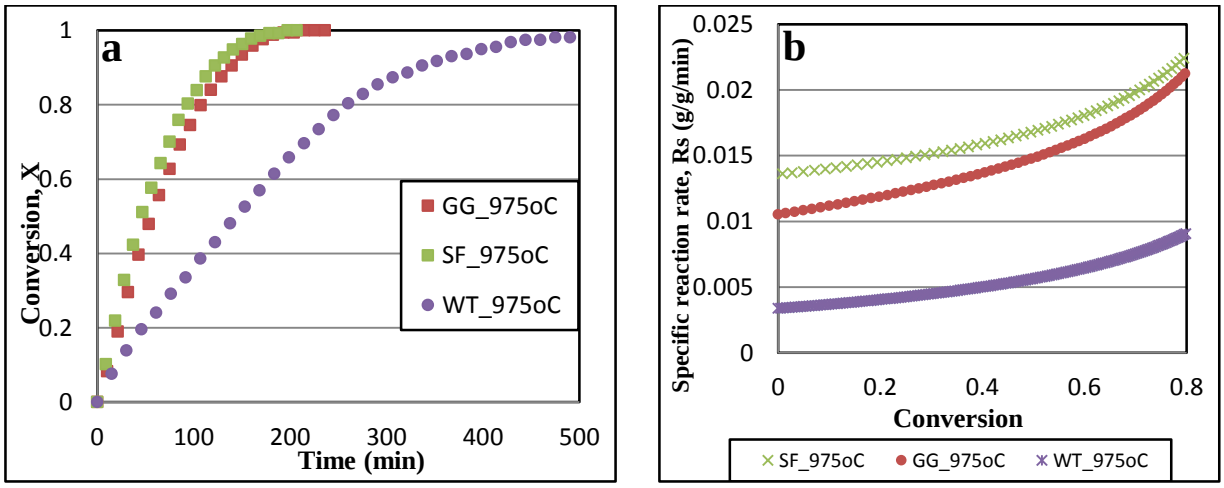

Figure 4.8: Conversion versus time (a) and specific reactivity versus conversion (b) plots for the CO_2 gasification reactions of waste tyre char (WT), GG coal char and SF coal char at 975^{o}C.

Figure 4.8 shows that the SF coal char is the fastest reacting of the three pure samples, followed by the GG coal char, and then lastly the waste tyre char (WT). These results are confirmed by the initial reactivities $\left(\frac{dX}{dt}\Big|_{t=0}\right)$ of the three samples given in Table 4.10. The observed reactivity trends can be explained from the properties of the three char samples presented in Section 4.3. Table 4.8 shows that the surface areas of the coal chars are three to four times that of waste tyre char. The greater surface area provides more active sites on which carbon-CO_2 reactions can take place (Walker *et al.*, 1983). As a result it is expected that the coal samples will be more reactive than waste tyre. SF char has higher ash content than GG char (Figure 3.5) and the mineral matter (ash) in coal is known to catalyse gasification reactions (Hattingh, 2009; Hüttinger & Nattermann, 1994; Ye *et al.*, 1998; Walker *et al.*, 1983; Kaitano, 2007; Everson, 2008) hence, it is expected that for the coals of the same rank, a higher ash coal will be more reactive during gasification. These results are similar to the findings by Venter (2012) on CO_2 gasification of waste tyre and an inertinite-rich bituminous coal, and by Monnaemang (2013) on partial gasification of waste tyre and a vitrinite-rich bituminous coal.

Table 4.10: Initial CO_2 gasification reactivities of WT, GG and SF chars at 975ºC

Temperature	Sample	Initial Reactivity X 10^3 (min^{-1})
975ºC	WT	4.75
	GG	7.95
	SF	11.3

4.4.4.2 Effects of blending

4.4.4.2.1 Reactivity of Pure Samples and Blends

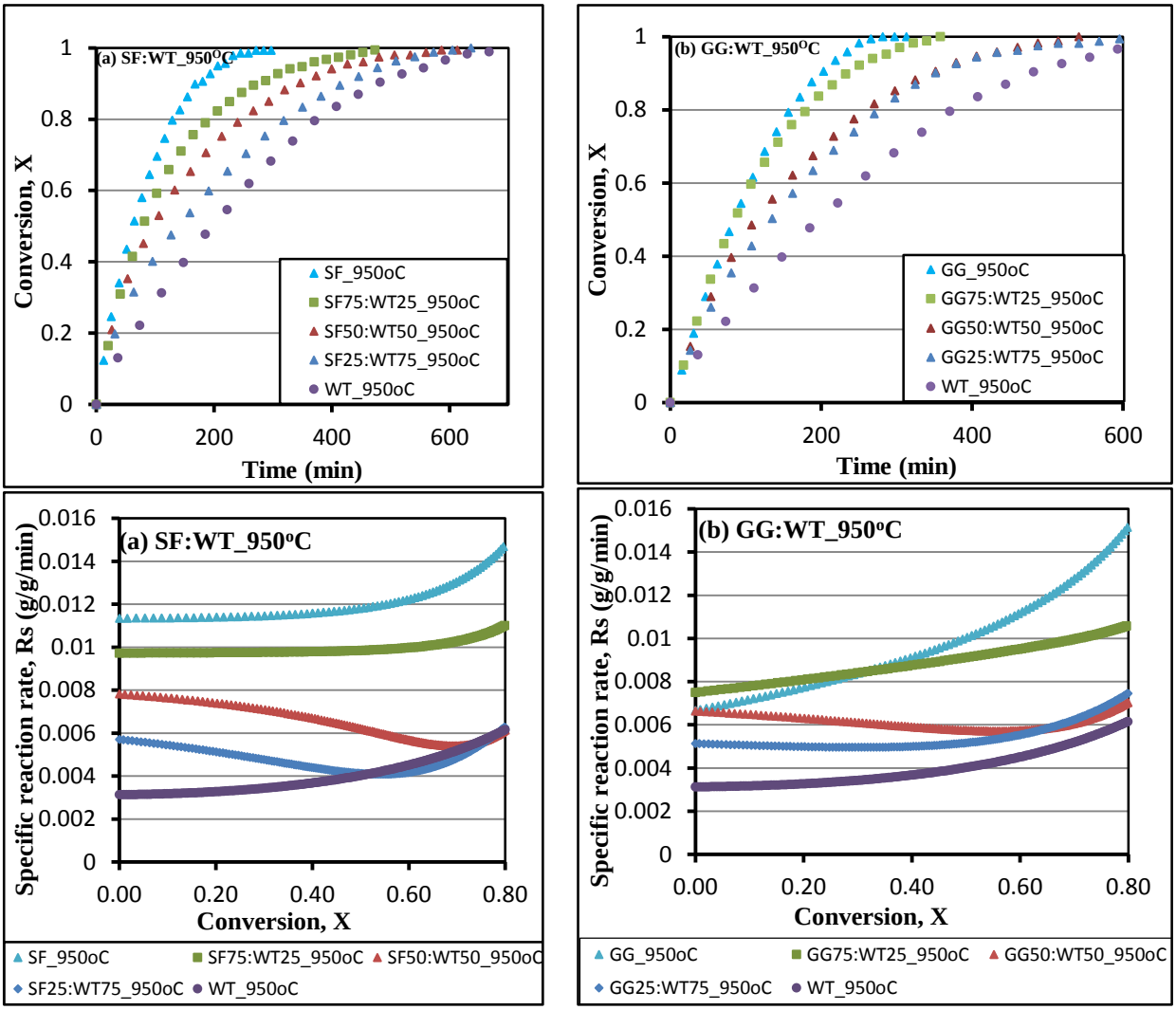

(a) SF coal char (b) GG coal char

Figure 4.9: Effect of blending coal char with waste tyre char on CO_2 gasification reactivity at 950°C.

In all cases for a given isothermal operating temperature, WT char is the least reactive of all the samples. The results in Figure 4.9 show for both coal char samples that the greater the ratio of coal char in the coal/tyre char mixture, the higher the rate of reaction, and this is confirmed by the initial reactivity results given in Table 4.11. This can be explained by the fact that waste tyre char (WT) is much less reactive than both coal chars (Figure 4.8). The same findings were made by Venter (2012) and Monnaemang (2013) as well.

The reactivity of the SF coal char is greater than that of all its blends and that of pure WT char. However, the relationship between the reactivities of GG char and its blends presents a different trend. The reactivity of GG75:WT25 is initially higher than that of the pure GG coal, then GG char reactivity overtakes that of the blend. At 950^{o}C this point occurs after 50 minutes, thus around 26% conversion. The initial reactivity of GG50:WT50 char blend is also very close to that of the pure GG char sample. These reactivity trends can be observed in Figure 4.9 (b) for the experiments done at 950^{o}C. Results similar to the ones presented in Figure 4.9 and Table 4.11 for the other temperatures are given in Appendix B.

The observed trend for the GG coal blends suggests the presence of synergism between the two samples during the gasification reactions. This possibility will be explored and discussed further in Sections 4.4.4.2.2 and 4.4.5 using different methods.

Table 4.11: Effect of blending on gasification reactivity of coal char and waste tyre char – initial reactivity$\left(\frac{dX}{dt}\Big|_{t=0}\right)$.

Sample	Initial Reactivity at 925^{o}C X 10^3 (min^{-1})	Sample	Initial Reactivity at 925^{o}C X 10^3 (min^{-1})
WT	2.25	WT	2.25
GG25:WT75	4.64	SF25:WT75	4.08
GG50:WT50	5.36	SF50:WT50	5.15
GG75:WT25	5.66	SF75:WT25	6.54
GG	5.31	SF	7.69

4.4.4.2.2 Reactivity of GG blends and SF Blends

To compare the effect of blending each coal with tyre has on reactivity, conversion versus time plots for reactions of the various blends are plotted against temperature in Figure 4.10. The three mixing ratios used in this study (75% coal, 50% coal and 25% coal) are considered in this analysis, and the plots for the pure samples are also included on the same axis in each case for comparison purposes.

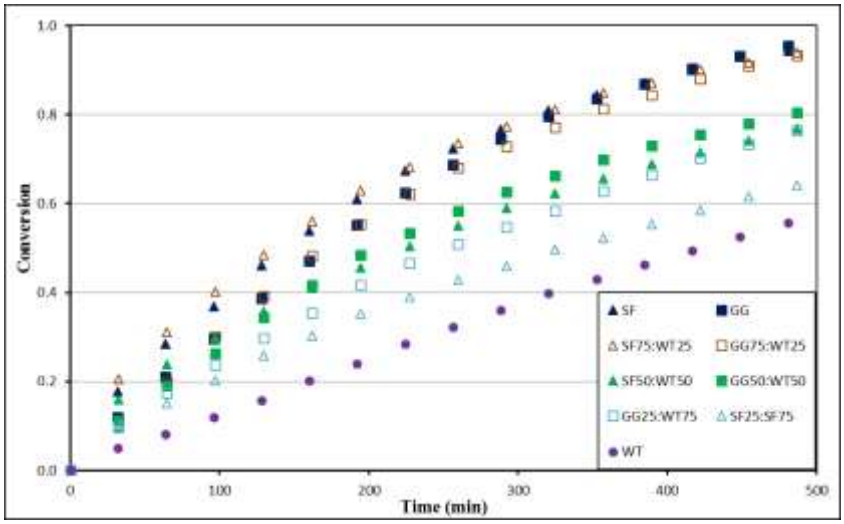

(i) Effect of blending on relative reactivity at 900°C

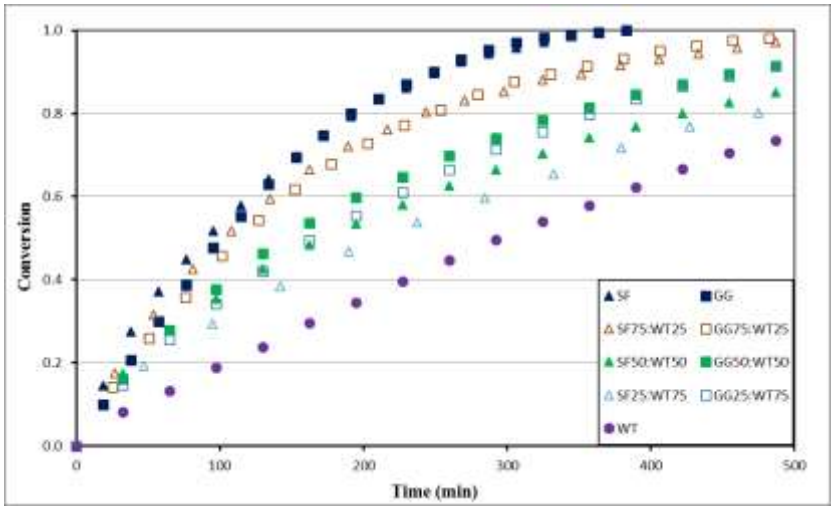

(ii) Effect of blending on relative reactivity at 925°C

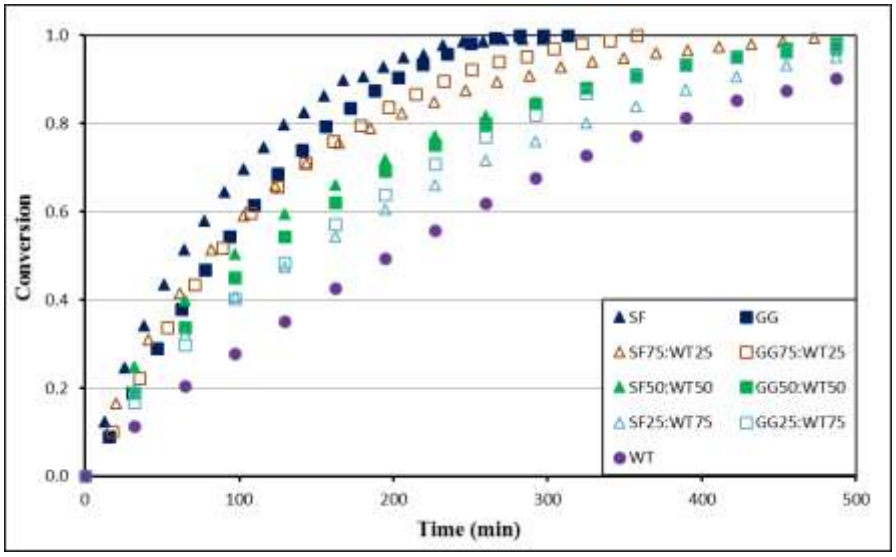

(iii) Effect of blending on relative reactivity at 950°C

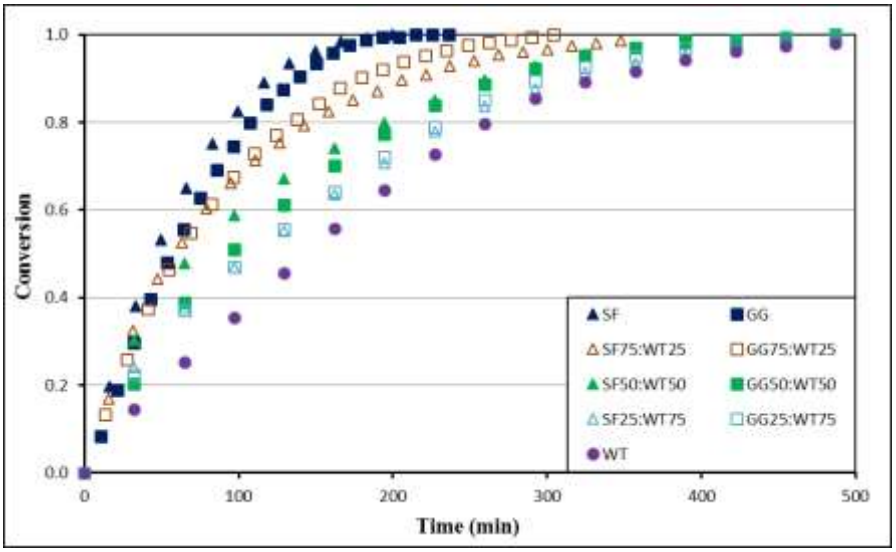

(iv) Effect of blending on relative reactivity at 975°C

Figure 4.10: The effects of WT blending on the relative reactivity of GG coal char and SF coal char at four different temperatures.

For both coal chars, the reactivity of the 75% coal blends is closer to that of the pure coal for all the four temperatures investigated. The 75% SF blend is more reactive than the 75% GG blend, but only up to a point between 50% conversion and 100% conversion, depending on the reaction temperature. This change in the relation between the reactivity of the GG blend and that of the SF blend occurs at higher conversions for lower temperatures, and at lower conversions for higher temperatures.

The behaviour of the 50% blends and the 25% blends is more departed from that of the pure coal chars. At lower temperatures (900°C and 925°C), the GG/WT blends are more reactive than the SF/WT blends, and the difference between the 25% GG and the 25% SF blends is wider than the difference between the 50% GG blend and the 50% SF blend at these temperatures. This can be observed in Figure 4.10. These observations and those in the preceding paragraph set the trend that, at lower temperatures, the addition of waste tyre char to the coal/WT blend causes the reactivity of GG/WT blend to improve relative to that of SF/WT blend. In such an instance the GG/WT blend is more reactive than the SF/WT blend at the 50% coal proportion, and it is even more reactive at the 25% coal proportion, although the pure SF coal char is more reactive than the pure GG coal char.

However, at the higher temperatures (950^{o}C and 975^{o}C), the reactivities of the blends follow the same order as that of the pure samples, that is, SF/WT blends are more reactive than GG/WT blends for all the mixing proportions, and no clear trends in the order of reactivity are observed.

4.4.5 Coal –Waste Tyre Gasification Synergism

In an attempt to determine if there is any synergism between the coal and waste tyre chars CO_2 in gasification reactions, two methods were used. The first approach was based on analysis of the relationship between the conversion rates of pure samples and those of their blends, and the relationship between the blends of the two coals with WT according to the results presented in Sections 4.4.4.2.1 and 4.4.4.2.2. The second approach involved predicting the conversion rate of a coal/waste tyre blend at a certain temperature using the conversion data of the pure samples at that temperature, and then comparing it with the experimental conversion data for that blend at the same temperature.

4.4.5.1 First Approach

The results presented in Section 4.4.4.2.1 indicated the possibility of synergism between coal char and waste tyre char which was more pronounced for the GG char. This is seen from the fact that the initial reactivity of GG75:WT25 is greater than that of the pure GG char, and that of GG50:WT50 is still very close to that of the GG char. In Section 4.4.4.2.2 the change in the relationship between the conversion rates of the GG blends and those of the SF blends at lower temperatures with an increase in WT char content in the blends showed that there was a synergistic effect between coal char and waste tyre char, which was greater in GG blends than in the SF blends. The conclusions based on this approach, however, are not conclusive on the presence of a synergistic effect in SF/WT blends, therefore the use of the second approach is justified.

4.4.5.2 Second Approach

The prediction of theoretical conversion of mixtures by using the pure samples for the 50% coal blends was done by adding and then averaging the conversion values for the reactions of the coal and WT chars at similar times in Microsoft Excel®, for the 75% coal and 25% coal blends prediction was done using the following formulae, respectively:

$$X = 0.75X_C + 0.25X_{WT}$$ Equation (4.4)

$$X = 0.25X_C + 0.75X_{WT}$$ Equation (4.5)

It is expected that if there is synergism between the coal and WT chars, the experimental conversion rate for the blend will be higher than the predicted rate. If there is no synergism the respective conversion curves will lie on top of each other. In the case where there is inhibition, the experimental conversion curve will lie below the predicted curve. The results are shown in Figures 4.11 and 4.12.

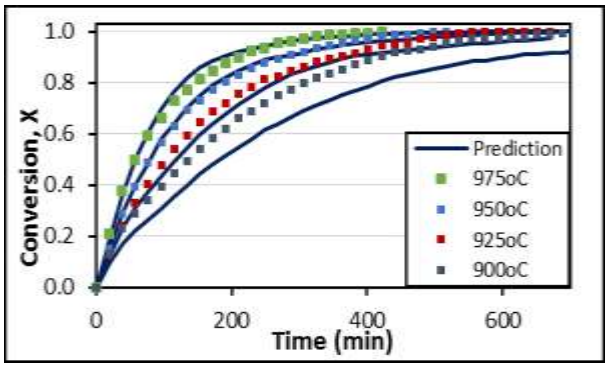

SF75:WT25

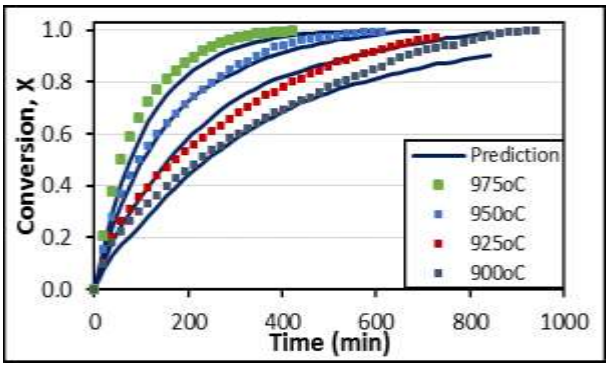

SF50:WT5

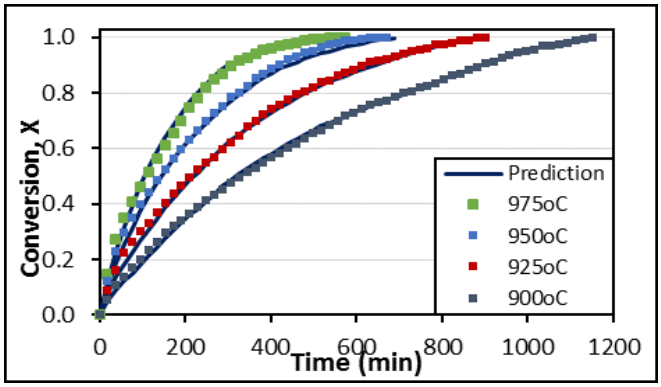

SF25:WT75

Figure 4.11: Comparison of predicted conversion rate with experimental conversion rate for SF/WT blends

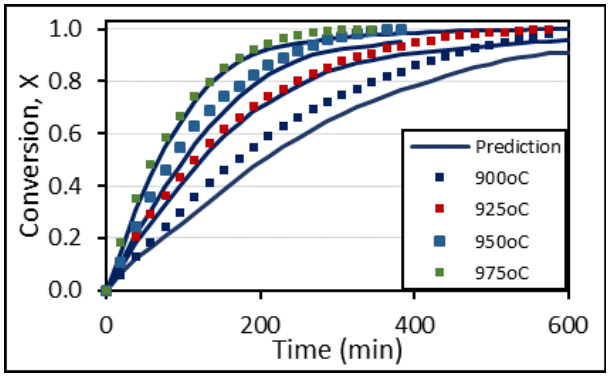

(i) GG75:WT25

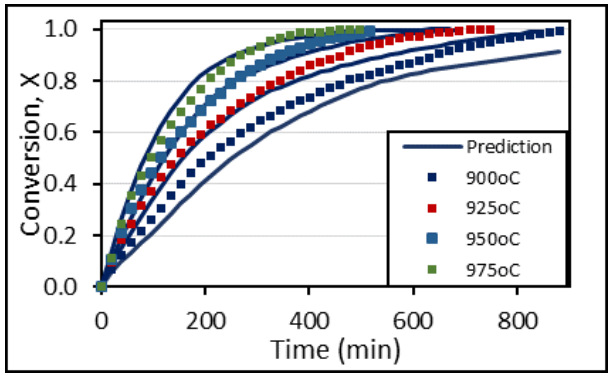

(ii) GG50:WT50

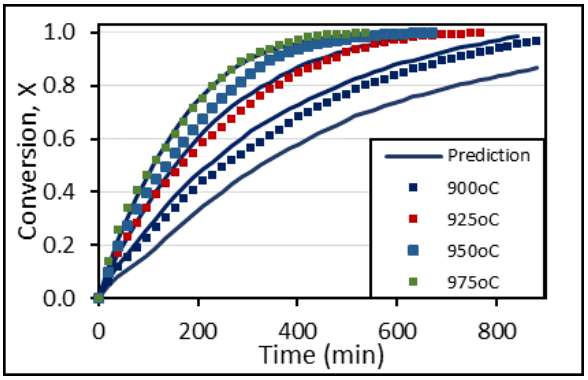

(iii) GG25:WT75

Figure 4.12: Comparison of predicted conversion rate with experimental conversion rate for GG/WT blends.

Figure 4.11 shows that for the blend with highest coal content (SF75:WT25), the experimental data is above the predicted data for the lower temperatures, 925ºC and 900ºC. The highest difference is at 900ºC. This suggests that there is synergism between the SF coal and the waste tyre at the lower temperatures. For the SF50:WT50 blend there is no clear trend in the relationship between the predicted and the experimental conversion rates, i.e. the observed difference may be a result of experimental error. The experimental curves for the 25% SF coal blend lie on top of the prediction curves, therefore the experimental conversion rate is just as predicted.

However, the GG blends' results present a different trend with respect to blend ratios from the one observed for the SF blends (Figure 4.12). The blend with the lowest coal and highest tyre content (GG25:WT75) shows the greatest departure from the predicted conversion rate. The difference between the experimental and the predicted conversion rates increases with decreasing temperature, the differences are wider for the GG25:WT75 than for the SF75:WT25 blend. For the GG50:WT50 blend, the experimental conversion rate is also observed to be higher than the predicted conversion rate at lower temperatures and the difference is only clear at 900^{o}C. These observations show that there is synergism between the coal and the waste tyre in the 25% and 50% GG coal blends, especially at the lower temperatures. The 75% GG coal blend's conversion curves do not show clear trends, and it can be concluded that any synergism present in this blend is not strong enough for the temperature dependence of synergism to be observed.

In Figures 4.11 and 4.12 there is no case where the experimental conversion rate is clearly less than the predicted rate, which shows that there is no significant reaction inhibition effect in the blends.

4.4.5.3 Discussion

Coal/Tyre Concentration Effect

The fact that an increase in the proportion of WT char in the GG/WT char blends results in a better performance of the blend (above the predicted conversion rate) shows that the synergism present in the reactions of these blends is primarily a result of enhancement by the tyre char or a component of the waste tyre char in the mixture. The opposite trend observed with the concentration effect in the case of the SF/WT char blends, while the temperature effect is constant, suggests that in these blends synergism is primarily driven by enhancement by a component of the SF coal char in the mixture. It is possible that the enhancing factor is catalysis by mineral matter in the samples.

Mineral matter in coal is known to catalyse carbon gasification reactions (Kaitano, 2007; Everson, 2008; Hattingh, 2009; Hüttinger & Nattermann, 1994; Ye *et al.*, 1998; Walker *et al.*, 1983). Mineral analysis of the coal and the tyre samples used in this study and presented in Section 4.3.3 (Table 4.4) show that the major minerals present in coal are also present in waste

tyre, and it is expected that they will also have a catalytic effect in carbon gasification reactions. Proximate analysis results in Section 4.3.1 (Table 4.2), closely supported by devolatilisation results in Section 4.2, and by the gasification reactions' final mass, show that the ash content of the three chars is WT char 14.7%, GG char 13.9%, and SF char 24.8%.

Hattingh (2011) noted that different constituents in the ash have different effects on the gasification reactivity of coal. Basic compounds in the ash (CaO, MgO, K_2O, Na_2O and Fe_2O_3) are known to have a catalytic effect, while the acidic compounds (SiO_2 and Al_2O_3) are non-catalytic. The effect of the ash content of coal on gasification reactivity may be more properly quantified by the use of a lumped parameter for the ash, the alkali index (AI) (Sakawa *et al.*, 1982; Zhang *et al.*, 2006):

$$AI = ash\% * \left(\frac{CaO + K_2O + MgO + Na_2O + Fe_2O_3}{Al_2O_3 + SiO_2}\right) \quad \text{Equation (4.6)}$$

A higher alkali index will result in higher catalytic effect of the ash and higher gasification reactivity of the coal. The calculated alkali indices for the three pure char samples used in this study are SF – 8.2, WT – 4.2 and GG – 1.7 (Table 3.7).

Therefore it is expected that in GG/WT mixtures, since WT char has a higher ash content and a higher alkali index, the higher WT char content will result in greater catalysis than in a case with lower WT char content, and since SF char has higher ash content and a higher alkali index than the WT char, the higher SF char content will result in greater catalysis than in a case with low SF char. This explains the opposite trends of the concentration effect observed in synergism for the two blend types.

While the WT char will enhance the GG char in GG/WT blends, and the SF char will enhance the WT char in SF/WT blends, it can be noted that the effect of waste tyre char on coal char is greater than the effect of coal char on waste tyre char. This is seen in the fact that at the temperatures where synergism is strong, a clear effect can still be observed in the 50% blends, i.e. in the case where tyre is having the enhancing effect (Figure 4.12(ii)), unlike in the case where coal is having the enhancing effect (Figure 4.11(ii)). In Figure 4.10 plots of the 50% blends from the two coals on the same axis show that 50% GG blends, where tyre is enhancing the reaction, are more reactive than 50% SF blends where coal is enhancing the reaction at

900°C and at 925°C. This can be explained from the fact that the catalytic minerals in tyres will have a greater effect on the more porous and more reactive coal carbon than coal minerals will have on the less porous and less reactive tyre carbon.

Temperature Effect

It has been observed that synergism between the WT char and the coal chars, or enhancement of the CO_2 gasification reactions of the blends of the WT and the coal chars is clear and strongest at the lower temperatures, 900°C and 925°C; and it cannot be clearly observed at 950°C and at 975°C using both approaches that were used to assess synergism. The temperature effect is observed and is similar for both SF/WT blends and GG/WT blends. These observations can be explained, if the enhancement of the reactions is attributed to catalysis by mineral matter in the chars, by the fact that mineral phases in coal will undergo transformation at high temperatures as the reactions progress.

It is believed that CO_2 gas will oxidise some of the mineral phases in coal, such as metallic iron (Fe), pyrrhotite ($Fe_{1-x}S$) and oldhamite (CaS), at high temperatures as Fe catalyst is very highly active in CO_2 gasification reactions (Irfan *et al.*, 2011; Asami *et al.*, 1996). Although chars used in this study were prepared at temperatures up to 1000°C, this was done under an inert nitrogen atmosphere, and further mineral transformation is expected to occur under a reactive CO_2 atmosphere. Grigore *et al.* (2008) proved this with experiments on coke-CO_2 gasification and annealing in the absence of CO_2 at the same temperature, and found very high mineral transformation in the case of CO_2 gasification and only small changes in the case of annealing. The char - CO_2 reaction will have an impact on both the form and the quantity of mineral matter in the char, as the reaction progresses, with some pre-existent minerals disappearing and more new mineral phases being formed, and efficient gasification of a particular coal depends sensitively on the high-temperature behaviour of mineral matter in coal char (Grigore *et al.*, 2008; Irfan *et al.*, 2011).

Since the basic mineral matter present in waste tyre char is very similar to that present in coal char (Table 3.7), including the relative quantities, it is expected that the mineral matter in waste tyre char will undergo the same changes that coal char minerals undergo at the same temperature ranges.

The reduction in the enhancement effect in the coal/WT char blends, as reaction temperature increases, may therefore be explained by the loss of catalytic forms of the char minerals due to high temperature mineral transformation in the presence of CO_2.

CHAPTER 5:MODELLING

5.1 Introduction

In this section,the random pore model (RPM) is applied to the gasification experimental data. The reactions are occuring within the chemical reaction kinetics controlled regime (regime I), where the RPM is applicable, and has been used successfully by other researchers to model carbon gasification reactions (Kaitano, 2007; Radovic *et al.*, 1985; Okolo, 2010; Venter, 2012; Everson *et al.*, 2008). Subsequent evaluation of the parameters such as activation energy, k values are carried out in this section as well.

5.2 Random Pore Model

The equation of the random pore model, introduced in Section 2.5.1, is given as (Bhatia & Perlmutter, 1980):

$$f(X) = \frac{S_o(1-X)\sqrt{1-\Psi \ln(1-X)}}{1-\varepsilon_o} \qquad \text{Equation (2.14)}$$

The structural parameter (Ψ) is defined as:

$$\Psi = \frac{4\pi L_o(1-\varepsilon_o)}{{S_o}^2} \qquad \text{Equation (2.15)}$$

The overall reaction rate is given by (Bhatia & Perlmutter, 1980):

$$\frac{dX}{dt} = \frac{r_s S_o(1-X)\sqrt{1-\Psi \ln(1-X)}}{1-\varepsilon_o} \qquad \text{Equation (5.1)}$$

Equation (5.1) can be rewritten in terms of the dimensionless parameter, τ, as (Kaitano, 2007; Everson *et al.*, 2008):

$$\frac{dX}{d\tau} = (1-X)\sqrt{1-\Psi \ln(1-X)} \qquad \text{Equation (5.2)}$$

Where,

$$\tau = \frac{r_s S_o t}{1-\varepsilon_o} \qquad \text{Equation (5.3)}$$

Integration of Equation (5.2) gives the carbon conversion, X, as a function of time, *t*, or the dimensionless time, τ (implicit and explicit):

In terms of time, *t*:

$$t = \frac{2(1-\varepsilon_o)}{r_s S_o \Psi}\left(\sqrt{1 - \Psi \ln(1-X)} - 1\right) \qquad \text{Equation (5.4)}$$

In terms of dimensionless time, τ (implicitly):

$$\tau = \frac{2}{\Psi}\left(\sqrt{1 - \Psi \ln(1-X)} - 1\right) \qquad \text{Equation (5.5)}$$

Rearranging Equation (5.5) gives the carbon conversion, *X*, explicitly in terms of the dimensionless time, τ:

$$X = 1 - exp\left[-\tau\left(1 + \frac{\Psi\tau}{4}\right)\right] \qquad \text{Equation (5.6)}$$

Equation (5.6), the model equation, can be simplified by defining a time factor as (Everson *et al.*, 2008):

$$t_f = \frac{r_s S_o}{(1-\varepsilon_o)} \qquad \text{Equation (5.7)}$$

And substituting it back into Equation (5.6), giving:

$$X = 1 - exp\left[-t_f t\,.\left(1 + \frac{t_f t \Psi}{4}\right)\right] \qquad \text{Equation (5.8)}$$

A reduced time t/t_x, where t_x *is* the time for a fractional conversion of *X* can be defined, thus, $t_{0.9}$ is the time for 90% conversion (Kaitano, 2007; Everson *et al.*, 2008). The reduced time, t/t_x, can be used instead of the real time, *t*, in Equation (5.4) and it simplifies to the form:

$$\frac{t}{t_{0.9}} = \frac{\left(\sqrt{1-\Psi\ln(1-X)} - 1\right)}{\left(\sqrt{1-\Psi\ln(1-0.9)} - 1\right)} \qquad \text{Equation (5.9)}$$

It should be noted that:

$$\frac{t}{t_{0.9}} = \frac{\tau}{\tau_{0.9}}$$ Equation (5.10)

An n[th] order power rate law for the intrinsic reaction rate r_s will be used together with the Arrhenius equation for the temperature dependence:

$$r_s = k_{so}\, exp\left(\frac{-E_a}{RT}\right) y^m{}_{CO_2}$$ Equation (5.11)

To determine the time factor, t_f, Equation (5.4) can be rewritten as:

$$t = \frac{2}{t_f \Psi}\left(\sqrt{1 - \Psi \ln(1-X)} - 1\right)$$ Equation (5.12)

Then plotting real time, t, against $\sqrt{1 - \Psi \ln(1-X)} - 1$, the time factor can be calculated from the slope. The time factor was calculated for each experiment using the average structural parameter for each sample.

The intrinsic reaction rate parameters were calculated using of Equations (5.7) and (5.11). Equation (5.7) can be rearranged to:

$$r_s = \frac{t_f(1-\varepsilon_o)}{S_o}$$ Equation (5.13)

And since in this study the reagent was 100% CO_2 Equation (5.11) reduces to

$$r_s = k_{so}\, exp\left(\frac{-E_a}{RT}\right)$$ Equation (5.14)

Combining the two equations gives:

$$\frac{t_f(1-\varepsilon_o)}{S_o} = k_{so}\, exp\left(\frac{-E_a}{RT}\right)$$ Equation (5.15)

Defining a lumped pre-exponential factor, k'_{so} as:

$$k'_{so} = \frac{k_{so} S_o}{(1-\varepsilon_o)}$$ Equation (5.16)

And rearranging Equation (5.15) yields

$$t_f = k'_{so}\, exp\left(\frac{-E_a}{RT}\right)$$ Equation (5.17)

Taking logarithms both sides:

$$\ln(t_f) = \ln(k'_{so}) - \frac{E_a}{RT}$$ Equation (5.18)

Then the intrinsic reaction rate parameters can be determined by plotting $\ln(t_f)$ versus $^1/_T$,

Activation energy, E_a, is calculated from the slope of the plot and the lumped pre-exponential factor, k'_{so}, is evaluated from the y – intercept.

5.2.1 Determination of Kinetic Parameters

Kinetic modelling was conducted with the random pore model to quantify the effect of operational variables of the experiments - temperature, char type and char composition. This involved evaluation of the kinetic parameters:

- The structural parameter Ψ, through numerical modelling of the experimental data with the model [Equation (5.9)],
- The time factor t_f, for each of the experiments using Equation (5.18) and the structural parameter Ψ,
- The activation energy E_a, and the lumped pre-exponential factor, k'_{so} using Equation (5.18).

These kinetic parameters are useful in the validation of the model in Section 5.3

5.2.1.1 Evaluation of the Structural Parameter

The structural parameter Ψ was determined using Equation (5.9)

$$\frac{t}{t_{0.9}} = \frac{\left(\sqrt{1-\Psi \ln(1-X)} - 1\right)}{\left(\sqrt{1-\Psi \ln(1-0.9)} - 1\right)}$$ Equation (5.9)

The left-hand side of the equation, the dimensionless time $^t/_{t_{0.9}}$, was calculated using the experimental times (t) at different points of the experiment, set at intervals so as to get fifteen points from the total reaction time, and the time for 90% conversion for that particular experiment ($t_{0.9}$). On the right-hand side of the equation X was the conversion at every point

of time (t), the initial Ψ is chosen abitrarily between zero and two from the guidance of literature data. The equation was then regressed in Micrsoft Excel® using the Solver Add-In function by the error sum of squares method (ESS). The value of Ψ was iterated until the equation

$$ESS = \left[\left(\frac{t}{t_{0.9}}\right) - \left(\frac{\left(\sqrt{1-\Psi\ln(1-X)}-1\right)}{\left(\sqrt{1-\Psi\ln(1-0.9)}-1\right)}\right)\right]^2 \qquad \text{Equation (5.19)}$$

Converged to a minimum value.

Theoretically the structural parameter (Ψ) is only dependent on the physical properties of the parent char. The structural parameter guides one to understand how the surface area develops during the gasification reaction. A single structural parameter value should be applicable to all the experiments of a particular char, therefore the Ψ values evaluated for the four experiments of one char at different temperatures are averaged, and the average was used for further calculations including determination of the time factor. The average structural parameters for the nine samples are given in Table 5.1.

Table 5.1: The structural parameters for the nine samples.

Sample	**Ψ Range**	**Average Ψ**	**Sample**	**Ψ Range**	**Average Ψ**
WT	2.41 – 4.99	3.50	WT	2.41 – 4.99	3.50
GG25:WT75	0.96 – 1.64	1.17	SF25:WT75	0.66 – 1.3	0.86
GG50:WT50	0.30 – 0.87	0.50	SF50:WT50	0.12 – 0.8	0.34
GG75:WT25	0.55 - 1.65	1.00	SF75:WT25	0.21 – 0.42	0.33
GG	2.3 – 3.0	2.54	SF	0.66 – 1.6	1.10

The average structural parameters of all the coal/WT blend samples and of the SF char are less than two ($\Psi < 2$), which indicates that the maximum reactive surface area for these chars occurs at the point of fractional conversion $X = 0$ and decreases as the reaction progresses. This implies that for these chars pore coalescence is more significant than pore growth from the beginning of the reactions. Thus the rate of reaction decreases as the reaction progresses (Bhatia & Perlmutter, 1980). The rate of reaction rate versus conversion plot for SF25:WT75 char (Figure 5.1a) illustrates this point.

For the WT and GG chars, however, structural parameter values of 3.50 and 2.54 (Ψ > 2) indicate that the reactive surface area for these chars initially increases as the reaction progresses, until a maximum value is reached, then it decreases. The initial increase of the surface area occurs because pore growth is initially more dominant than pore coalescence, until a point where pore coalescence becomes more dominant. Thus the maximum rate of reaction occurs at a later point than fractional conversion, X = 0 (Bhatia & Perlmutter, 1980; Everson *et al.*, 2008). The rate of reaction rate versus conversion plot for GG char (Figure 5.1b) illustrates this point.

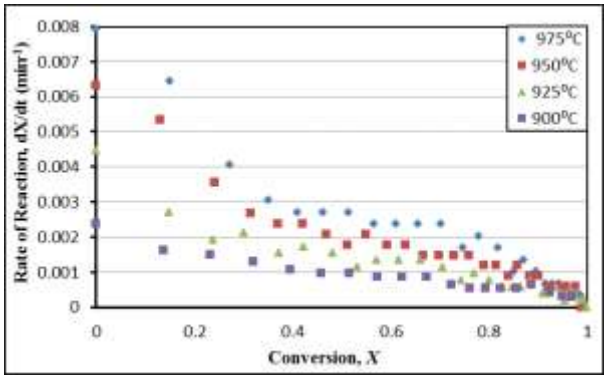

(a) SF25:WT75

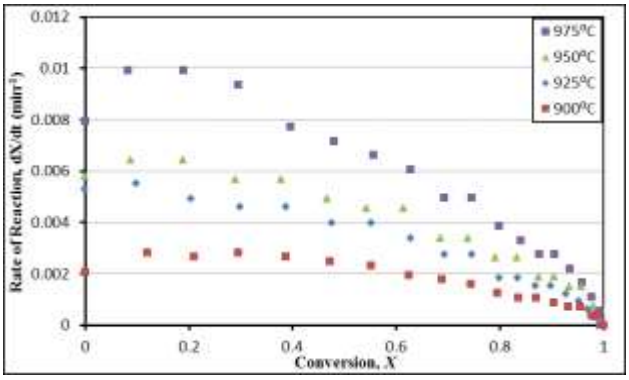

(b) GG

Figure 5.1: Rate of reaction versus fractional conversion for SF25:WT75 and GG chars at four different temperatures.

Reaction rate versus conversion plots for the other samples are presented in Appendix B.4.

5.2.1.2 Determination of Time Factor, t_f

The time factor (t_f), which is analogous to the initial apparent reactivity of the coals, was determined from Equation (5.12), for the different operating temperatures for each sample, using the average structural parameter (Ψ) for the sample.

$$t = \frac{2}{t_f \Psi}\left(\sqrt{1 - \Psi \ln(1 - X)} - 1\right) \qquad \text{Equation (5.12)}$$

The equation was plotted as real experimental time (t) against the linearised function of X, $\left(\sqrt{1 - \Psi \ln(1 - X)} - 1\right)$, the time factor can be calculated from the slope (S) of the plot as:

$$t_f = \frac{2}{\Psi S} \qquad \text{Equation (5.20)}$$

The evaluated time factors for the pure coal and tyre samples and for the 50% coal:tyre mixtures are presented in Table 5.2, along with the initial reactivity (R) and the time for 50% conversion ($t_{0.5}$) for each reaction. These parameters for the other samples are presented in Appendix C.

Table 5.2: Time factors, initial reactivities of selected samples.

WT			**GG75:WT25**	
Temp.	t_f X 10^{-3} (min^{-1})	R X 10^{-3} (min^{-1})	t_f X 10^{-3} (min^{-1})	R X 10^{-3} (min^{-1})
900ºC	1.05	1.59	3.66	3.17
925ºC	1.59	2.25	4.89	5.66
950ºC	1.72	3.56	6.98	5.82
975ºC	3.16	5.06	9.02	9.82
SF			**SF50:WT50**	
900ºC	3.83	5.58	2.77	4.19
925ºC	6.26	7.69	3.33	5.15
950ºC	9.44	9.79	5.46	7.94
975ºC	13.6	11.3	7.09	10.4
GG			**GG50:WT50**	
900ºC	3.03	3.76	2.79	3.09
925ºC	5.1	5.31	3.90	4.87
950ºC	6.33	5.79	5.26	5.75
975ºC	9.26	7.95	6.74	6.43

The results in Table 5.2 and in Appendix C show that the time factor and the experimentally determined initial reactivity are close to each other for each sample at the investigated temperatures, and both the time factor and the initial reactivity increase with increasing reaction temperature. These observations are similar to the observations in the work of Hattingh (2009), Kaitano (2007) and Okolo (2009). SF coal char has the highest time factor and initial reactivities and WT char has the lowest values, which is in agreement with the trends observed with the conversion rates given earlier in Section 4.4.3. In general, the addition of WT char to a coal char results in a reduction in the time factor and initial reactivity, with the exception of the 75% GG blend, where some of the values are higher than those for GG coal char. This is

also similar to observations made in the conversion rate plots in Section 4.4.4.2.1, also discussed in the discussion on synergism in Section 4.4.5.

5.2.1.3 Determination of Activation Energy, E_a

The activation energy was evaluated from Equation (5.18):

$$\ln(t_f) = \ln(k'_{so}) - \frac{E_a}{RT} \qquad \text{Equation (5.18)}$$

By plotting $\ln(t_f)$ against the reciprocal of the reaction temperature in Kelvins $\left({}^{1}/_{T}\right)$ – Arrhenius plot - activation energy was calculated from the slope of the plot (S) according to the relation:

$$S = -\frac{E_a}{R} \qquad \text{Equation (5.21)}$$

The Arrhenius plots for all the samples investigated are shown in Figure 5.1 and the obtained activation energies for the nine samples investigated for the four temperatures at which experiments were conducted, are given in Table 5.3.

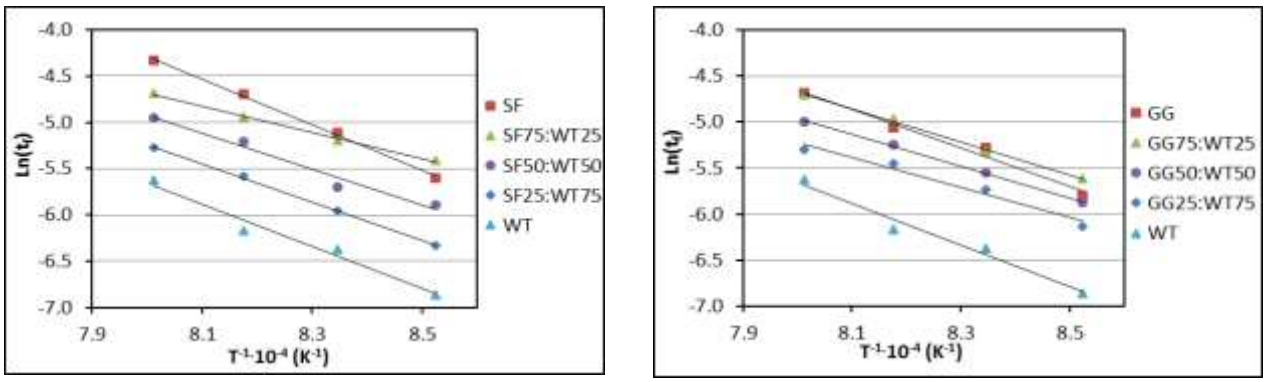

(i) SF, WT and SF:WT blends (ii) GG, WT and GG:WT blends

Figure 5.2: Arrhenius plots for the coal chars, WT chars and their blends.

Table 5.3: Activation energies *(E_a)* for the nine samples investigated.

Sample	E_a (kJ/mol)	Sample	E_a (kJ/mol)
GG	173.9	SF	205.3
GG75:WT25	149.4	SF75:WT25	118.6
GG50:WT50	143.2	SF50:WT50	161.1
GG25:WT75	135.4	SF25:WT75	172.6
WT	189.9	WT	189.9

The pure char samples have the three highest activation energies out of all the nine samples, in the order SF > WT > GG. The high activation energy of SF coal may be a result of the fact that the parent coal is a high inertinite coal. Inertinite macerals are known to form dense chars with poor ignition properties, implying high activation energies (Kaitano, 2007; Okolo, 2009; Everson *et al.*, 2008; Sun *et al.*, 2004), while that of the WT char may be attributed to its low surface area. Hattingh (2009) reported activation energies in the range 171 – 202 kJ/mol for high inertinite bituminous coals, and Monnaemang (2013) reported an activation energy of 173kJ/mol for waste tyre char gasification and 238.6 kJ/mol for vitrinite-rich coal. A summary of comparison of activation energies and other kinetic and structural parameters obtained in this study with similar samples by other investigators, is given in Table 5.4.

It is interesting to note that the blends of coal and waste tyre chars have lower activation energies than both the pure coal and the pure waste tyre chars. This makes a case for synergism or catalysis between the coal char and the waste tyre char. Further, for the GG/WT blends, it can be observed that increasing the WT char proportion in the blend lowers the activation energy, and for the SF/WT blends, increasing the SF coal char proportion, lowers the activation energy. These observations agree with the observations made with the conversion rates, which were presented in Sections 4.4.4.2.2 and 4.4.5.2, and support the arguments for synergism or catalysis presented in Section 4.4.5.

Clearly, the activation energies of both coals are reduced by blending with waste tyre, even in cases where there is no observable improvement in the conversion rate. Monnaemang (2013) and Venter (2012) also reported lower RPM activation energies for their 50% coal/tyre blends

than for both their coal and tyre respectively in CO_2 gasification at temperatures between 900°C and 1000°C.

5.2.1.4 Determination of the Lumped Pre-exponential Factor, k'_{so}

The lumped pre-exponential factor, k'_{so} was determined from the plot of $\ln(t_f)$ against the reciprocal of the reaction temperature in Kelvins $\left({}^{1}/_{T}\right)$ for Equation (5.18) for each sample - the Arrhenius plots in Figure 5.1. k'_{so} is calculated from the y – intercept of the plot from the relationship:

$$y - intercept = \ln k'_{so} \qquad \text{Equation (5.21)}$$

The k'_{so} values obtained for each sample are presented in Table 5.4.

5.2.2 Synergism

The third approach used to assess the possibility of synergism between waste tyre and coal chars in CO_2 gasification is the analysis of of the kinetic paramenters evaluated with the random pore model, namely the time factor (t_f) and the activation energy (E_a).

The time factors (t_f) evaluated in Section 5.2.1.2 follow the same trend as the initial reactivities obtained experimentally, and presented in Table 4.11.Therefore the same conclusions on the presence of synergism in GG/WT blends that were made with the first approach in Section 4.4.5.1 can also be made with the time factors.

It was noted in Section 5.2.1.3 that blending coal char with WT char results in activation energies that are lower than those of both the pure coal and pure tyre, and that the trend of these reductions is similar to the trend observed with the effect of blending on conversion rates in Sections 4.4.4.2.2 and 4.4.5.2. The fact that the synergism in the blends results in lowering of activation energy, supports the idea that this synergism is driven by catalysis, since catalysis basically works by lowering of the activation energy of a chemical reaction. However, other reaction enhancing factors may also be present in the char blend, or in the reacting char – gas mixture.

Table 5.4: Summary of structural and kinetic parameters for the nine samples used in the studies and comparison to literature values.

Coal						
	Sample type	Model used	Activation energy (E_a), kJ/mol	Average structural parameter (Ψ)	Lumped pre-exponential factor (k'_{so}), min^{-1}	Time factor (t_f) x 10^3
This Study	Bituminous coal (GG)	RPM	173.9	2.54	1.76×10^5	3.03 – 9.26
Monnaemang (2013)	Bituminous coal (GG)	RPM	238.6	2.48 ± 0.39	1.49×10^8	1.25 – 9.12
This Study	Medium rank-C bituminous coal (SF)	RPM	205.3	1.1	5.45×10^6	3.83 – 13.6
Du Toit (2013)	Bituminous coal	L-H model	243 ± 32	0.5	-	-
Hattingh (2009)	Bituminous coal	RPM	171-202	1.23 – 1.43	$0.02 – 2.1 \times 10^7$	
Koekemoer (2009)		RPM	163 - 225	1.0 – 2.5	-	1.3 - 10.1

Waste Tyre						
	Sample type	Model used	Activation energy (E_a), kJ/mol	Average structural parameter (Ψ)	Lumped pre-exponential factor (k'_{so}), min^{-1}	Time factor (t_f) x 10^3
This study	Waste Tyre	RPM	189.9	3.5	3.05×10^5	1.05 – 3.16
Monnaemang (2013)	Waste Tyre	RPM	176	6.05 ± 0.79	$8.64 \cdot 10^7$	2.8 – 8.9
Venter (2012)	Waste Tyre	RPM	243.3	1.23±0.04	1.35×10^8	3.36 – 14.1
Blends						
This study	GG75:WT25	RPM	186	2.41	4.9×10^5	2.3 – 7.9
This study	GG50:WT50	RPM	119	2.07	4.56×10^2	2.1 – 4.3
Monnaemang (2013)	GG:Tyre 50%	RPM	223.8	0.88 ± 0.06	3.04×10^7	1.25 – 9.12
Venter (2012)	Coal:Tyre 50%	RPM	220.52	1.19 ± 0.05	6.67×10^7	-
This study	GG25:WT75	RPM	136	2.49	2.05×10^3	1.8 – 4.3
This study	SF75:WT25	RPM	156	1.64	2.59×10^4	2.7 - 7.2
This study	SF50:WT50	RPM	219	1.88	9.15×10^6	1.5 - 5.6
This study	SF25:WT75	RPM	195	2.34	5.95×10^5	1.2 - 4.0

5.2.3 Validation of Kinetic Model

The model equation, Equation (5.8), the kinetic and structural parameters evaluated in Section 5.2.1 are used to calculate the model's conversion data for each sample, which is a prediction of the conversion of the sample under consideration.

$$X = 1 - exp\left[-t_f t \,.\left(1 + \frac{t_f t \Psi}{4}\right)\right] \qquad \text{Equation (5.8)}$$

The calculated conversion data is fitted to the experimentally determined conversion data by plotting the two data sets in a conversion versus time plot on the same axis. The fitted curves for the pure samples and the 50% blends are shown in Figure 5.2. It can be observed that the random pore model adequately describes the char-CO_2 reactions under the investigated conditions (regime I). The fitted curves for the other blends are presented in Appendix C.2.

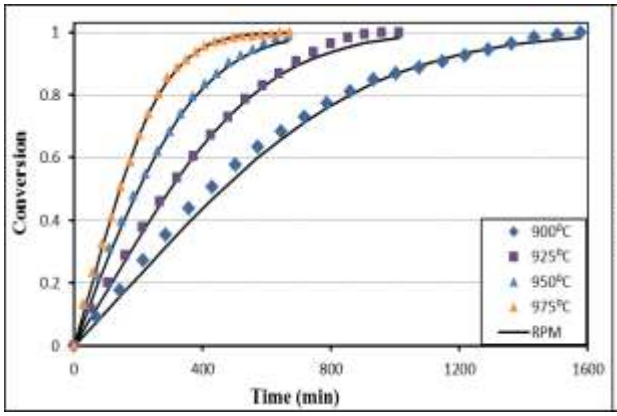

RPM fitting for WT char reactions

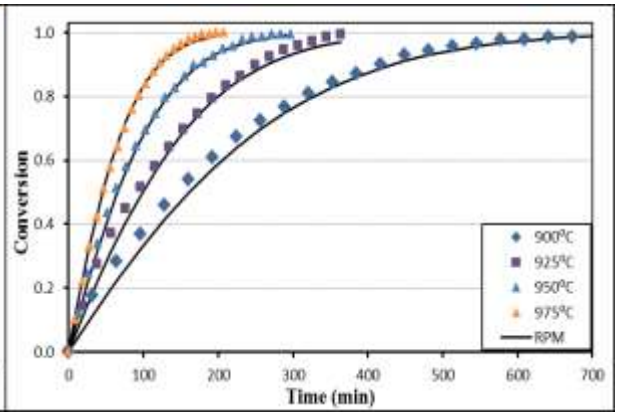

RPM fitting for SF char reactions

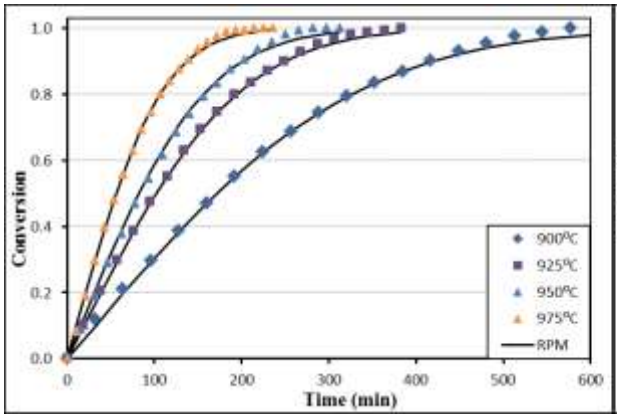

RPM fitting for GG char reactions

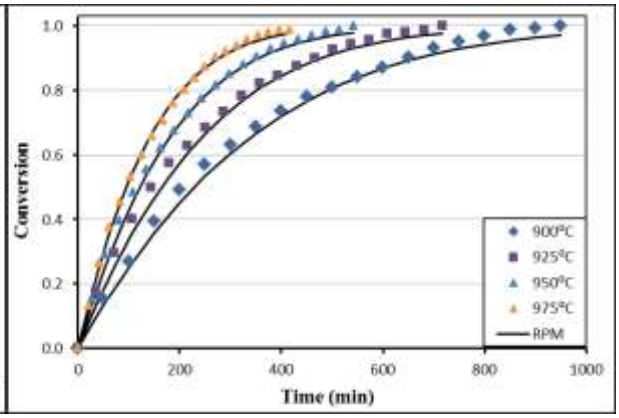

RPM fitting for GG50:WT50 blend reactions

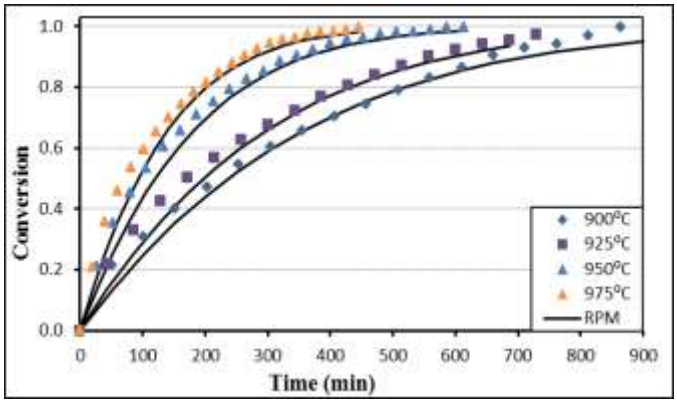

(i) RPM fitting for SF50:WT50 blend reactions

Figure 5.3: Random pore model fitting on conversion curves for five samples each at four different temperatures.

CHAPTER 6: CONCLUSIONS AND RECOMMENDATIONS

6.1 Introduction

The carbon dioxide gasification kinetics of a waste tyre sample and that of two coal samples were investigated in this study. The gasification kinetics of the blends of the coals with the waste tyre in 25:75%, 50:50% and 75:25% proportions were also investigated at four different temperatures (900^{o}C, 925^{o}C, 950^{o}C and 975^{o}C). The effects of operating temperature and of blending were investigated. Results of this investigation are presented in Chapter 5 and in this chapter a summary of the major findings and conclusions as well as recommendations for further studies are presented.

6.2 General Conclusions

1. Pyrolysis of the waste tyre and coal samples indicated that the waste tyre sample had the highest volatile content of 62.7%, followed by GG coal with 35% and SF coal being the lowest at 33.1%. These results are close to the proximate analysis of the three samples. The WT char has a higher ash content when compared with the GG char, though waste tyre has a lower ash content than for the GG coal.
2. XRF analysis results of waste tyre sample showed that the ash contained all the major minerals present in coal ash. The percentages of the minerals in tyre were comparable with those present in the coal samples used in this study. The Alkali index for the three char samples was in the same order as the ash content of the chars: SF char – 8.2, WT char – 4.2 and GG char – 1.7.
3. The rate of reaction for all three char samples was dependent on operating temperature and increased with increase in temperature. All experiments in this study were confirmed to have been conducted in the chemical reaction controlled regime (regime I). Rate of reaction of the char samples at a constant isothermal operating temperature was in the order SF > GG > WT, and the reaction was established to be dependent on three factors: ash content, alkali index and surface area of the char. The rates of reaction for the two coal chars, SF and GG were close to each other. However, the SF char was

relatively more reactive which can be attributed to its higher ash content and alkali index than the GG char.

4. The reactivity of the coal/WT blends was found to be mainly between that of the pure coal and WT chars. The greater the percentage of the WT chars in the blend the lower the reactivity of the blend. The GG75:WT25 blend, however, was an exception - it was initially more reactive than the GG coal up to a point around 50% conversion, which differed among the four different operating temperatures. This observation for the 75% GG blend was the first indicator that pointed that there might be synergism between coal and waste tyre CO_2 gasification reactions.
5. At 900^{o}C and 925^{o}C, the addition of WT char to the coal lead to the reactivity of the GG/WT blend improving, compared to that of the SF/WT blend. These observations were pointers to synergism between WT char and coal char in CO_2 gasification reactions, and the effect was greater on the reactivity of the GG char than on the reactivity of the SF blend. However, no clear synergistic relationship was observed between WT char and SF char.
6. The possibility of synergism was also checked by predicting a conversion rate from the experimental conversion data of the pure samples and comparing it with the conversion rates of the blends. At lower temperatures (900^{o}C and 925^{o}C) the experimental conversion curves deviated above the predicted curves. For the GG blends, the deviation increased with increase in WT percentage such that the 25% GG/WT blend had the widest deviation above the predicted conversion curve. This shows that there was synergism between the WT char and the GG char at lower temperatures. The synergism was highest in the blend with the highest amount of WT char, thus showing that it was the WT char that enhanced the reactivity of the GG/WT blend.

   For the SF coal blends, the deviation increased with increase in WT percentage, so much that the 75% SF/WT blend had the widest deviation above the predicted conversion curve. This shows that there was synergism between the WT char and the GG char, and the synergism was highest in the blend with the highest amount of SF char, thus showing that it is the SF char that enhances the reactivity of the SF/WT blend. At the higher temperatures (950^{o}C and 975^{o}C) no clear trend was observed on the relationship between the experimental and the predicted conversion curves.

The experimental conversion rate was always above the predicted conversion rate for all blends at all temperatures which shows that there was no inhibition between the WT char and coal chars in CO_2 gasification reactions between 900°C and 975°C.

7. The random pore model (RPM) adequately described all the experimental data and variables, i.e. structural parameters (ψ), activation energy, time factor and lumped pre-exponential factor, for all the samples could be determined from the model. The structural parameters for each of the samples did not show any temperature dependence and the average values for WT, GG, GG75:WT25, GG50:WT50 and GG25:WT75 were 3.5, 2.54, 1.0, 0.5 and 1.17 respectively. The average structural parameter values for SF, SF75:WT25, SF50:WT50 and SF25:WT75 were 1.1, 0.33, 0.34 and 0.86. The structural parameters of the blends were all lower than those of the respective pure samples. The time factors (t_f) were close to the initial reactivity values for each of the experiments conducted. They were also affected by reaction temperature and followed the same trends in the blends as the initial reactivity. The lumped pre-exponential factors for WT, GG, GG75:WT25, GG50:WT50 and GG25:WT75 were 3.05×10^5, 1.76×10^5, 4.9×10^5, 4.56×10^2 and 2.05×10^3 min^{-1} respectively, and those for SF, SF75:WT25, SF50:WT50 and SF25:WT75 were 2.59×10^4, 9.15×10^6 and 5.95×10^5 min^{-1} respectively.
8. The activation energies for the WT, GG and SF chars were 189.9kJ/mol, 173.9kJ/mol and 205.3kJ/mol, respectively. All the blends of the WT and each of the coals had lower activation energies than both the WT char and the respective coal char, which supported the presence of synergism between WT and coal char in CO_2 gasification reactions. For the GG/WT blends activation energy was found to decrease further with the increase of the WT char proportion in the blend (149.4kJ/mol, 143.2kJ/mol and 135.4kJ/mol respectively). This supports the conclusion reached with the conversion rates, that WT char enhances the gasification reactivity of the GG char. For the SF/WT blends the concentration effect was found to be opposite to that observed with the GG blends, i.e. activation energy was found to decrease further with the increase of the SF char proportion in the blend (172.6kJ/mol, 161.1kJ/mol and 118.6kJ/mol respectively). This supports the conclusion reached with the conversion rates that SF char enhances the gasification reactivity of the WT char.

9. The observed enhancement effect by the WT char (in GG/WT blends) and by the SF char (in SF/WT blends) may be explained by the ash content and alkali indices (AI) of the WT char and coal chars. The ash content and AI values of the pure samples are in the order SF > WT > GG (Conclusions 1 and 2). The higher ash content and alkali index of the SF char, when compared to the same values for WT char, is expected to cause it to have a greater catalytic effect than WT char in SF/WT blends' reactions. The higher ash and alkali index values for WT char, when compared with GG char, is expected to cause it to have a greater catalytic effect than GG char in GG/WT blends' reactions.

6.3 Recommendations for Future Study

Based on the findings from this investigation and the questions that still remain after the conclusion of this study, the following recommendations are made for future study in the field of waste tyre gasification and co-gasification with coal:

1. Investigate the influence of coal petrographics in coal and waste tyre co-gasification, by using coals with similar ash content and varying the petrographic characteristics, and by demineralising the coals that were used in this study and carrying out similar gasification experiments.
2. Study co-gasification with other high-ash coals to ascertain if high ash coals will always enhance coal/tyre co-gasification reactions and up to what extent of ash content.
3. Conduct structural characterisation of blends of waste tyre and coal chars to assess the effect of the mixing process on the structure of the chars and possibly find an explanation to the reactivity of char blends.
4. Study co-gasification with chars prepared from coal and waste tyre blended before charring, since this is the situation that would more closely represent a practical co-gasification process, and compare the results from the approach used in this study. Conduct structural characterisation of chars obtained from charring after blending and compare the results with those from chars blended after charring and assess the impact of the differences on co-gasification.
5. Study co-gasification with other gasifying agents – steam and air.
6. Investigate the effect of pressure and of particle size on the co-gasification kinetics of waste tyre and coal.

REFERENCES

Asami, K., Sean, P., Furimsky, E., & Ohtsuka, Y. 1996. Gasification of brown coal and char with carbon dioxide in the presence of finally dispersed iron catalysts. *Process Technology,* 47(2):139 - 141.

Aylon, E., Fernandez-Colino, A., Navarro, M. V., Murillo, R., Garcia, T., & Mastral, A. M. 2008. Waste Tire Pyrolysis: Comparison between Fixed Bed Reactor and Moving Bed. *Industrial and Engineering Chemistry Research,* 47(12):4029–4033.

Bell, D.A., Towler, B.F., & Fan, M. 2010. Coal gasification and its applications. 1st Ed. Oxford: William Andrew. http://www.sciencedirect.com/science/book/9780815520498 Date of access: 11 Mar. 2013.

Bhatia, S. K., & Perlmutter, D. D. 1980. A Random Pore Model for Fluid Solid Reactions: I. isothermal, kinetic control. *AIChE Journal,* 26(3):379-386.

Bhatia, S. K., & Perlmutter, D. D. 1981. A random pore model for fluid-solid reactions: II. Diffusion and transport effects. *AIChE Journal,* 27(2):247-254.

Botes, A. 2012. South African waste management tyre fee to generate R700 million per year to promote tyre recycling . *Urban Earth,* 19 Nov. http://urbanearth.co.za/articles/south-african-waste-management-tyre-fee-generate-r700-million-year-promote-tyre-recycling Date of access: 19 Mar. 2013.

Coetzee, G.H. 2011. The influence of particle size on the steam gasification kinetics of coal. Potchefstroom: NWU. (Dissertation - MEng).

Conesa, J. A., Martin-Gullon, A., Font, R., & Jauhiainen, J. 2004. Complete Study of the Pyrolysis and Gasification of Scrap Tires in a Pilot Plant Reactor. *Environmental Science Technology,* 38(11):3189-3194.

Copans, G., & Tyrer, L. 2008. SA's carbon emissions a cause for concern. *Engineering News,* 25 Jan. http://www.engineeringnews.co.za/article/sa039s-carbon-emissions-a-cause-for-concern-2008-01-25 Date of access: 27 Mar. 2013.

Du Toit, G. J. 2013. The influence of CO2 on the steam gasification rate of a typical South African coal. Potchefstroom:NWU. (Dissertation - MEng).

Everson, R. C., Neomagus, H., & Kaitano, R. 2011. The random pore model with intraparticle diffusion for the description of combustion of char particles derived from mineral- and inertinite rich coal. *Fuel,* 90(7):2347–2352.

Everson, R. C., Neomagus, H., Kaitano, R., Falcon, R., & du Cann, V. M. 2008. Properties of high ash coal-char particles derived from inertinite-rich coal: II. Gasification kinetics with carbon dioxide. *Fuel,* 87(15):3403-3408.

Feng, B., & Bhatia, S. (2002). On the validity ofthermogravimetric determination of carbon gasification kinetics. *Chemical Engineering Science,* 57(15):2907 – 2920.

Fermoso, J., Gil, M., Pevida, C., Pis, J., & Rubiera, F. 2010. Kinetic models comparison for non-isothermal steam gasification of coal–biomass blend chars. *Chemical Engineering Journal,* 161(1):276–284.

Fernández, A., Díez, M., Alvarez, R., & Barriocanal, C. 2009. Pyrolysis of tyre wastes. Paper presented at the First Spanish National Conference on Advances in Materials Recycling and Eco–Energy, Madrid, 12-13 Nov. 2008. http://digital.csic.es/bitstream/10261/18414/1/S01_2.pdf Date of access: 9 Jul. 2013.

Galvagno, S., Casu, S., Martino, M., Di Palma, E., & Portofino, S. 2007. Thermal and kinetic study of tyre waste pyrolysis via TG-FTIR-MS analysis. *Journal of Thermal Analysis and Calorimetry,* 88(2):507-514.

Gavalas, G. 1980. A random capillary model with application to char gasification at chemically controlled rates. *AIChE Journal*, 26(4):577-585.

Grigore, M., Sakurovs, R., French, D., & Sahajwalla, V. 2008. Mineral reactions during coke gasification with carbon dioxide. *International Journal of Coal Geology*, 75(4):213 - 214.

Hattingh, B. 2009. The determination of the reaction mechanisms involved in the CO2 gasification of inertinite-rich, high ash coal. Potchefstroom: NWU. (Dissertation - MEng).

Hattingh, B. B., Everson, R. C., Neomagus, H. W., & Bunt, J. R. 2011. Assessing the catalytic effect of coal ash constituents on the CO2 gasification rate of high. *Fuel Processing Technology,* 92(10):2048-2054.

Hüttinger, K., & Nattermann, C. 1994. Correlations between coal reactivity and inorganic matter content for pressure gasification with steam and carbon dioxide. *Fuel,* 73(10):1682–1684.

Irfan, M.F., Usman, M.R., & Kusakabe, K. 2011. Coal gasification in CO2 atmosphere and its kinetics since 1948: A brief review. *Energy*, 36(1):12-40.

Ishida, M., & Wen, C. 1971. Comparison of zone-reaction model and unreacted-core shrinking model in solid–gas reactions. I. Isothermal analysis. *Chemical Engineering Science*, 26(7):1031–1041.

Kaitano, R. 2007. Characterisation and reaction kinetics of high chars derived from inertinite-rich coal discards. Potchefstroom: NWU. (Thesis - PhD).

Karatas, H., Olgun, H., & Akgun, F. 2012. Experimental results of gasification of waste tire with air & CO2, air & steam and steam in a bubbling fluidized bed gasifier. *Fuel Processing Technology*, 102:166 - 174.

Karatas, H., Olgun, H., Engin B., & Akgun, F. 2013. Experimental results of gasification of waste tire with air in a bubbling fluidized bed gasifier. *Fuel Processing Technology*, 105:566 - 571.

Lee, J.S., & Kim, S.D. 1996. Gasification kinetics of waste tire-char with CO2 in a thermobalance reactor. *Energy*, 21(5):343-352.

Levenspiel, O. 1999. Chemical Reaction Engineering 3rd Ed. Oregon: Wiley & Sons.

Li, Y.H., Lu, G.Q. & Rudolph, V. 1998. The kinetics of NO and N2O reduction over coal chars in fluidised-bed combustion. *Chemical Engineering Science*, 53(1):1–26.

Liu, G., Tate, A., Bryant, G., & Wall, G. 2000. Mathematical modeling of coal char reactivity with CO2 at high pressures and temperatures. *Fuel*, 79(10):1145–1154.

Liu, K., Song, C., & Subramani, V. 2010. Hydrogen and Syngas Production and Purification Technologies. Hoboken: John Wiley & Sons; AIChE.

López, F. A., Centeno, T. A., Alguacil, F. J., Lobato, B., López-Delgado, A., & Fermoso, J. (2012). Gasification of the char derived from distillation of granulated scrap tyres. *Waste Management*, 32(4):743–752.

Mahlangu, M.L. 2009. Waste tyre management problems in South Africa and the possible opportunities that can be created through the recycling thereof. Pretoria: UNISA. (Dissertation - MA).

Martinez, D. J., Puy, N., Murillo, R., & Garcia, T. 2013. Waste tyre pyrolysis–A review. *Renewable and Sustainable Energy Reviews,* 23(2013):179–213.

Mastral, A.M., Murillo, R., Callen, M.S., & Garcia, T. 1999. Application of coal conversion technology to tire processing. *Fuel Processing Technology,* 60(3):231-242.

Matsuokaa, K., Akihoa, H., Xub, W., & Guptac, R. 2005. The physical character of coal char formed during rapid pyrolysis at high pressure. *Fuel,* 84(1):63–69.

Mavuso, Z. 2013. Recycling process possible solution to waste tyres. *Engineering News,* 15 Feb. http://www.engineeringnews.co.za/article/new-recycling-process-possible-solution-to-recycling-plan-2013-02-15 Date of access: 11 Apr. 2013.

Mitta, N.R., Ferrer-Nadal, S., Lazovic, A.M., Perales, E.V., & Puigjaner, L. 2006. Modelling and Simulation of a Tyre Gasification Plant for Synthesis Gas Production. (*In* Marquardt, W. & Pantelides, C., *Eds*. 16th European Symposium on Computer Aided Process Engineering, Garmisch-Partenkirchen. Amsterdam: Elsevier B.V. p. 1771 - 1776).

Miura, K., Makino, M., & Silveston, P. 1990. Correlation of gasification reactivities with char properties and pyrolysis conditions using low rank Canadian coals. *Fuel,* 69(5):580-582.

Monnaemang, W. 2013. Pyrolysis of ground scrap automotive tyres and the effect of partial gasification on char surface area. Potchefstroom: NWU. (Project - BEng).

Muhlen, H., & Sulimma, A. 1987. Thermogravimetric apparatus for characterisation of coal with regard to pyrolysis and gasification under pressures up to 100 bar. *Fuel Processing Technology,* 15:145-155.

Murillo, R., Navarro, M.V., Lopez, J.M., Aylon, E., Callen, M.S. & Garcia, T. 2004. Kinetic Model Comparison for Waste Tire Char Reaction with CO2. *Industrial and Engineering Chemistry Research,* 43(24):7768-7773.

MWH New Zealand Ltd. 2004. End-of-Life Tyre Management: Storage Options. A report prepared for The Ministry for the Environment. Wellington.

Nel, S. 2011. Catalytic steam gasification of large coal particles. Potchefstroom: NWU. (Dissertation - MEng).

Njapha, D. 2003. Determination of the kinetic models and associated parameters for the low temperature combustion and gasification of high-ash coal chars. Potchefstroom: NWU. (Thesis - PhD).

Ochoa, J., Cassanello, M., Bonelli, P., & Cukierman, A. 2001. CO2 gasification of Argentinean coal chars: A kinetic characterization. *Fuel,* 74(3):161-176.

Odendaal, N. 2012. Waste tyre plan approved for immediate implementation. *Engineering News*, 30 Nov. http://www.engineeringnews.co.za/article/waste-tyre-plan-approved-for-immediate-implementation-2012-11-30 Date of access 29 Mar. 2013.

Okolo, G. N. 2009. The effects of chemical and physical properties of chars derived from inertinite-rich, high ash coals on gasification reaction kinetics. Potchefstroom: NWU. (Dissertation - MEng).

Ondrey, G. 2011. Coal-to-chemicals. *Chemical Engineering:* 16 - 20, Feb.

Osborne, D. G. 1988. Coal Preparation Technology, Vol. 1. London: Graham and Trotman Limited.

Radovic, L., Steczko, K., Walker, P., & Jenkins, R. 1985. Combined effects of inorganic constituents and pyrolysis conditions on the gasification reactivity of coal chars. *Fuel Processing technology,* 10(3):311-326.

Sakawa, M., Sakurai, Y., & Hara, Y. 1982. Influence of coal characteristics on CO2 gasification. *Fuel,* 61(8):717-720.

Schobert, H. H. 2011. Coal Chemistry. Potchefstroom: NWU, Potchefstroom Campus. (Lecture Series CHEN622).

Smith, K.L., Smoot, L.D., Fletcher, T.H., & Pugmire, R.J. 1994. The Structure and Reaction Processes of Coal. New York: Plenum Press.

Song, B. H. 2005. Gasification kinetics of waste tire char and sewage sludge char with steam in a thermobalance reactor. *Journal of Industrial and Engineering Chemistry,* 11(3):361-367.

South Africa. 2008. Waste Tyre Regulations, 2008. (Notice 425). *Government gazette,* 30929:3, 1 Apr. 2008.

South Africa. Department of Energy. 2009. Digest of South African Energy Statistics. Pretoria.

StatsSA. 2013. Motor trade sales (Preliminary). Pretoria.

Straka, P., & Bučko, Z. 2009. Co-gasification of a lignite/waste-tyre mixture in a moving bed. *Fuel Processing Technology*, 90(10):1202–1206.

Sun, Q., Li, W., Chen, H., & Li, B. 2004. The CO2-gasification and kinetics of Shenmu maceral chars with and without catalyst. *Fuel*, 83(13):1787–1793.

Talab, I., Al-Nahari, Z., Qudaih, R., & Janajreh, I. 2010. Numerical Modeling of Coal Tire-Shred Co-Gasification. *Jordan Journal of Mechanical and Industrial Engineering*, 4(1):155- 162.

Tomaszewicz, M., Łabojko, G., Tomaszewicz, G., & Kotyczka-Moran´ska, M. 2013. The kinetics of CO2 gasification of coal chars. *Journal of Thermal Analytical Calorimetry*, 113(3):1327-1335.

U.S. EIA. 2011. International Energy Outlook 2011. U.S Department of Energy, Accessed from www.eia.gov/ieo/pdf/0484(2011).pdf.

UNEP. 2000. Basel Convention: Technical Guidelines on the Identification and Management of Used Tyre. Châtelaine.

United Kingdom. Department for Environment, Food and Rural Affairs. 2009. The hazardous waste (England and Wales) regulations 2005 (as Ammended by the hazardous waste (England and Wales) regulations 2009). London.

Venter, P. A. 2012. Determination of gasification kinetics of blends of used tyre-derived char and inertinite rich South African coal. Potchefstroom: NWU. (Project - BEng).

Walker, P., Matsumoto, S., Hanzawa, T., Muira, T., & Ismail, I. 1983. Catalysis of gasification of coal-derived cokes and chars. *Fuel*, 62(2):140–149.

Williams, H., Pourkashanian, M., Jones, J.M., & Skorupska, N. 2000. Combustion and Gasification of Coal. New York: Taylor and Francis.

Williams, P.T., & Besler, S. 1995. Pyrolysis-thermogravimetric analysis of tyres and tyre components. *Fuel*, 14(9):1277-1283.

Wojtowicz, M., & Serio, M. 1996. Pyrolysis of Tyres: Can it be Profitable? *Chemtech*: 48-54, Oct. 1996.

World Coal Association. 2012. Coal Facts 2012. London.

Xu, Q., Pang, S., & Levi, T. 2011. Reaction kinetics and producer gas compositions of steam gasification of coal and biomass blendchars, part 2: Mathematical modelling and model validation. *Chemical Engineering Science,* 66(10):2232–2240.

Ye, D., Agnew, J., & Zhang, D. 1998. Gasification of a South Australian low-rank coal with carbon dioxide and steam: kinetics and reactivity studies. *Fuel,* 77(11):1209–1219.

Zabaniotou, A. A., & Stavropoulos, G. 2003. Pyrolysis of used automobile tires and residual char utilisation. *Journal of Analytical and Applied Pyrolysis,* 70(2):711-722.

Zhang, L., Huang, J., Fang, Y., & Wang, Y. 2006. Gasification Reactivity and Kinetics of Typical Chinese Anthracite Chars with Steam and CO2. *Energy & Fuels,* 20(3):1201-1210.

Zhang, Y., Hara, S., Kajitani, S., & Ashizawa, M. 2010). Modeling of catalytic gasification kinetics of coal char and carbon. *Fuel*, 89(1):152–157.

APPENDICES

Appendix A: Reactivity of Samples

A.1:Conversion versus time plots

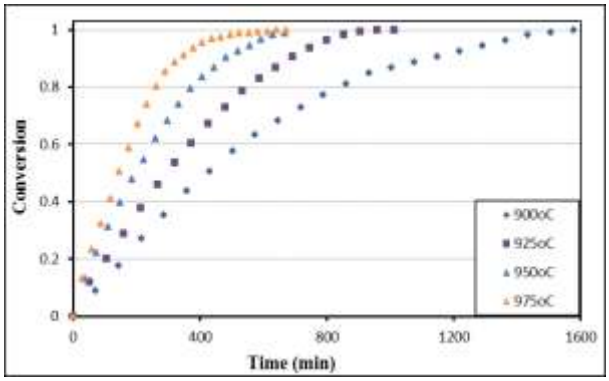

(i) WT

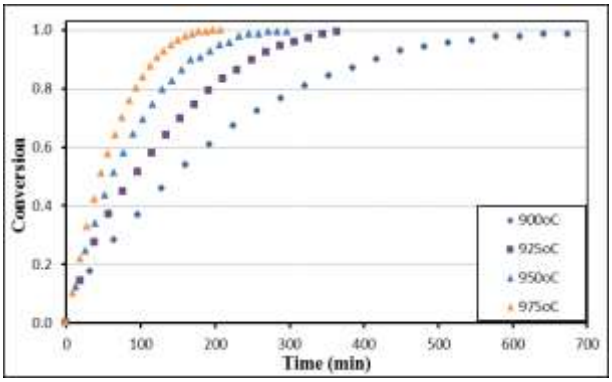

(ii) SF

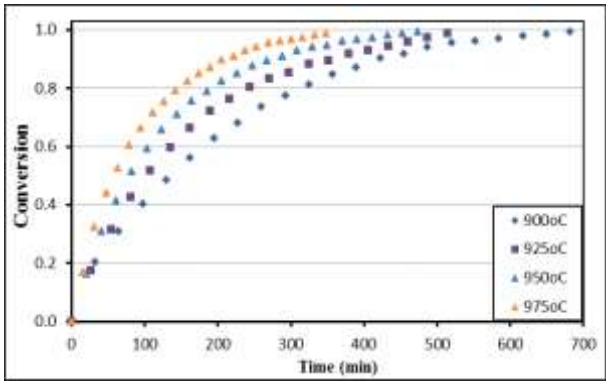

(iii) SF75:WT25

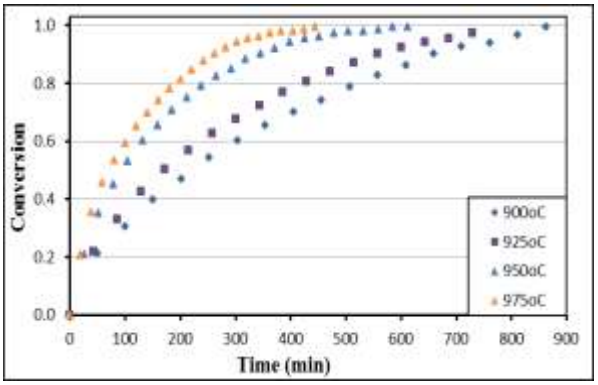

(iv) SF50:WT50

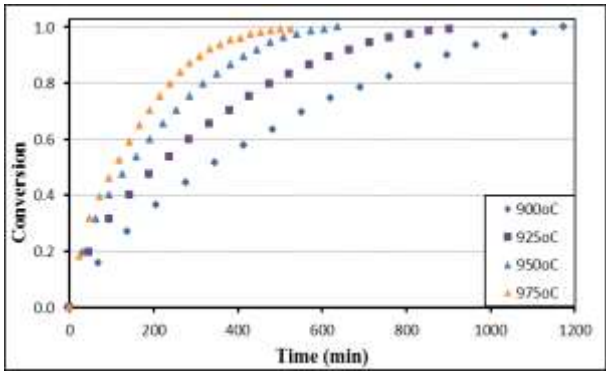

(v) SF25:WT75

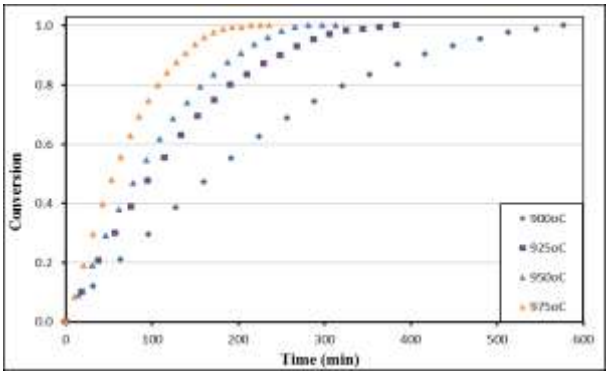

(vi) GG

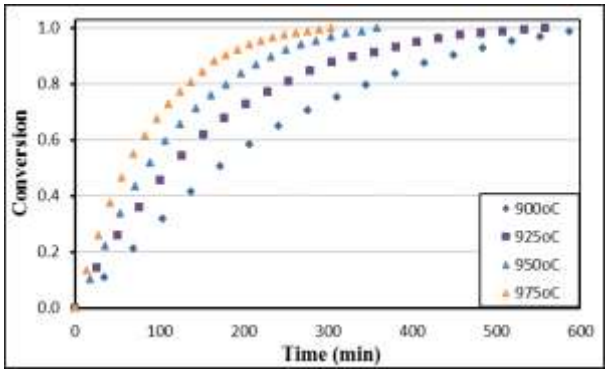

(vii) GG75:WT25

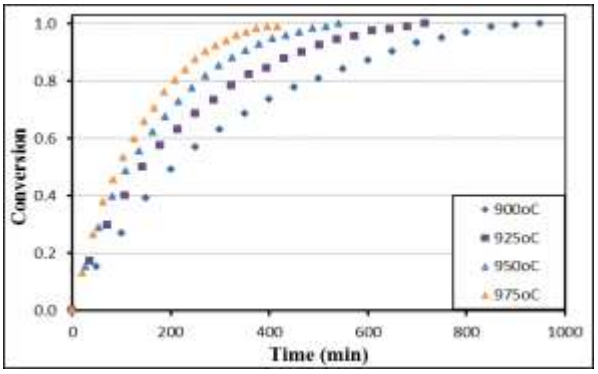

(viii) GG50:WT5

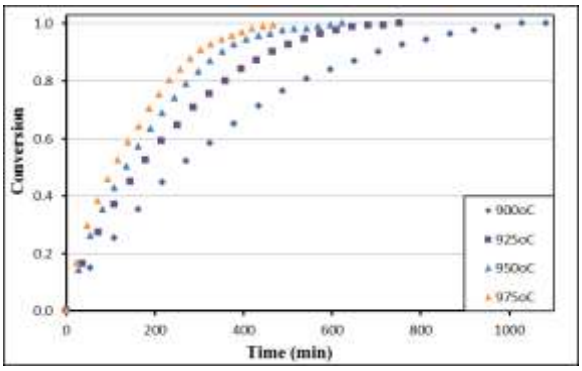

(ix) GG25:WT75

Figure A.1: Conversion versus time plots for the nine samples

A.2: Specific reaction rate versus conversion plots

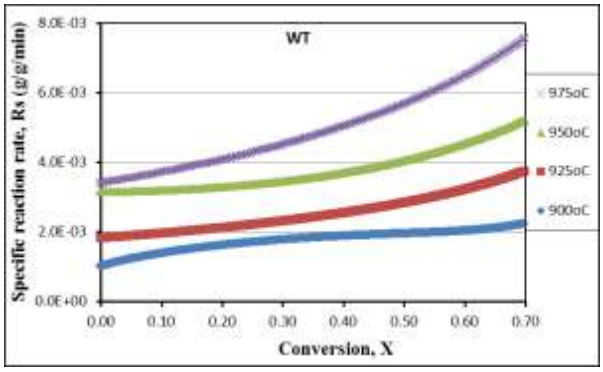

(i) WT

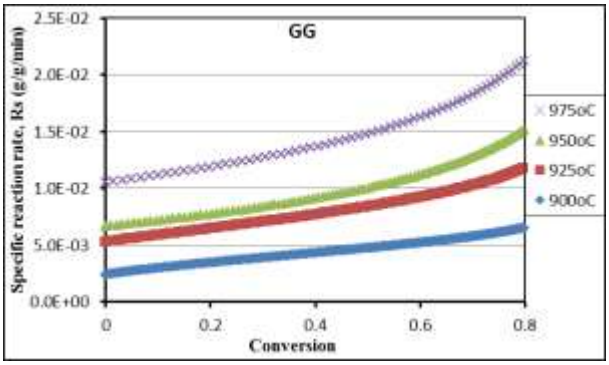

(ii) GG

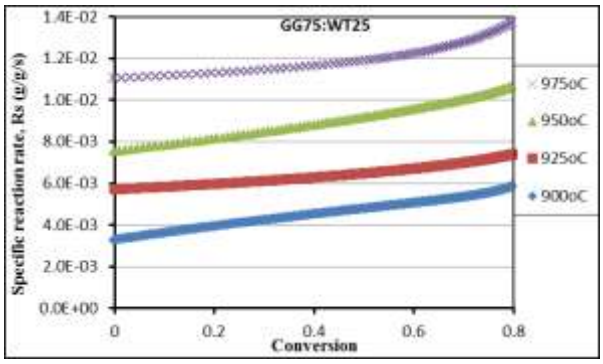

(iii) GG75:WT25

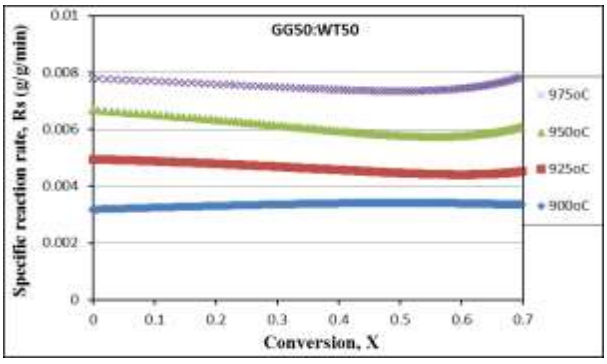

(iv) GG50:WT50

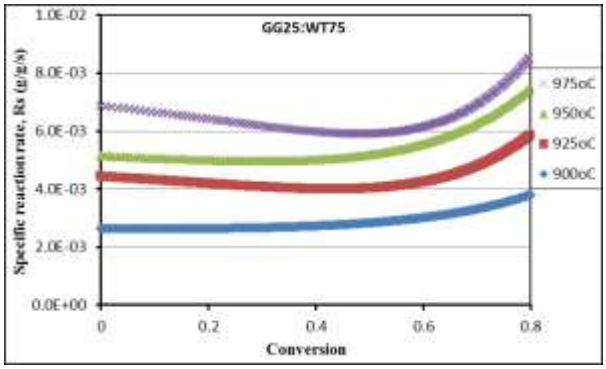

(v) GG25:WT75

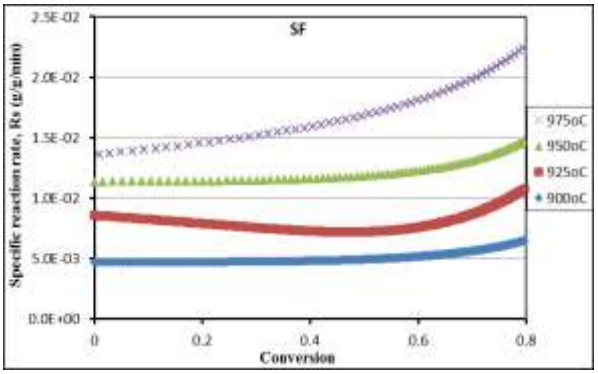

(vi) SF

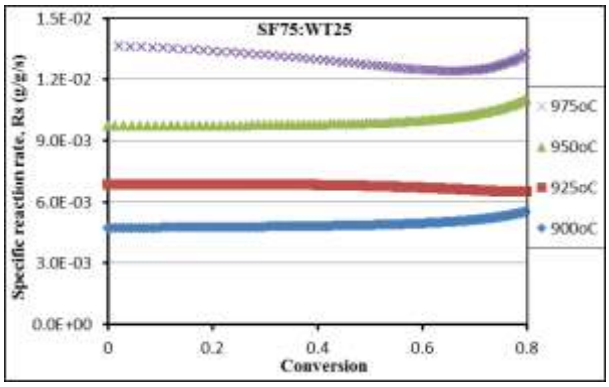

(vii) SF75:WT25

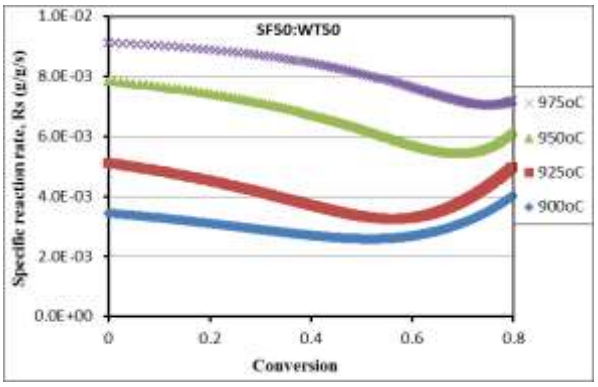

(viii) SF50:WT50

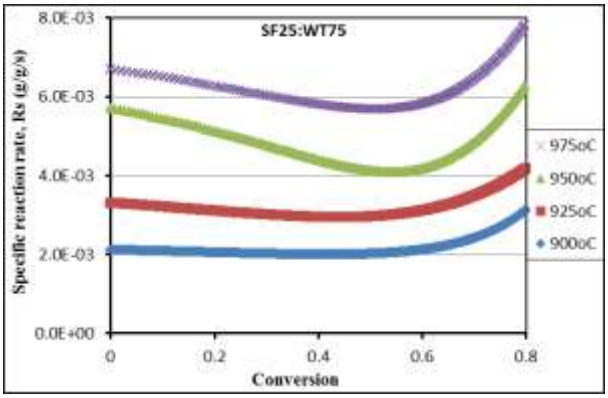

(ix) SF25:WT75

Figure A.2: Specific reaction rate versus conversion plots for the nine samples

A.3: Pure samples reactivity comparison

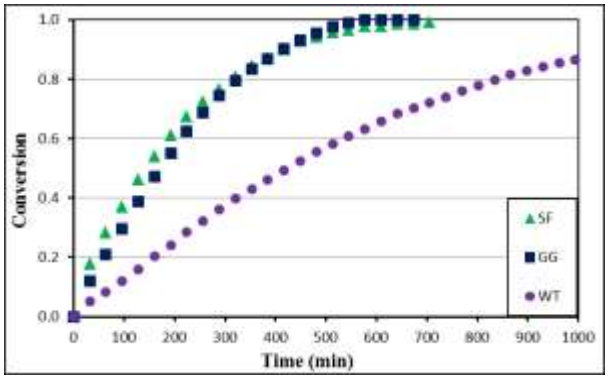

900ºC

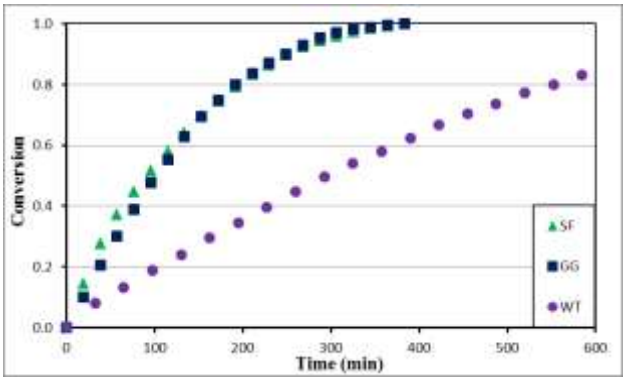

925ºC

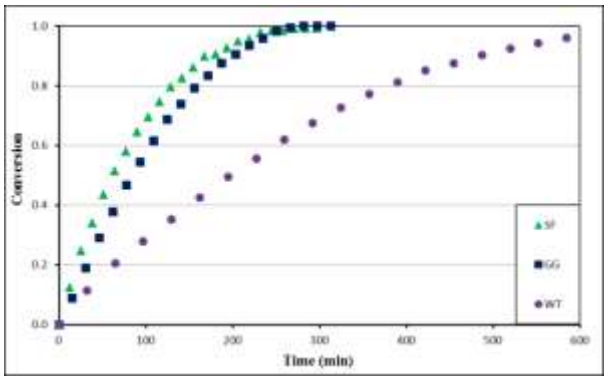

950ºC

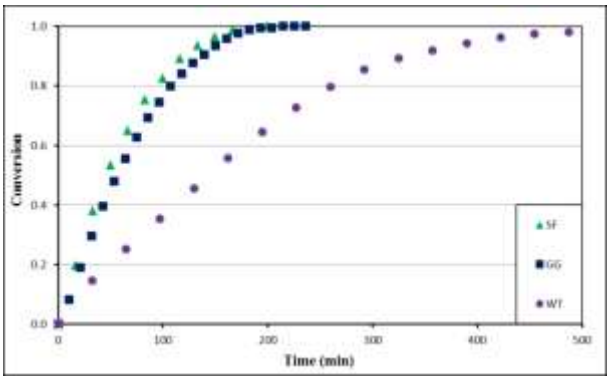

975ºC

Figure A.3: Pure samples reactivity comparison

Table A.1: Initial reactivities of the three pure samples

900ºC		925ºC	
Sample	Initial Reactivity X 10^3 (min^{-1})	Sample	Initial Reactivity X 10^3 (min^{-1})
WT	1.59	WT	4.75
GG	3.76	GG	6.15
SF	5.58	SF	7.39
950ºC		975ºC	
WT	3.53	WT	4.53
GG	5.37	GG	9.32
SF	9.59	SF	11.7

A.4: Reaction rate versus conversion plots

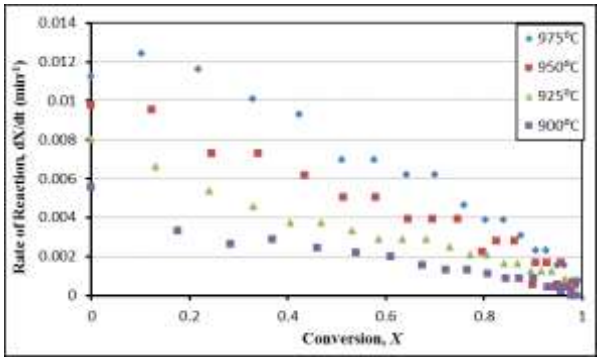

(i) SF

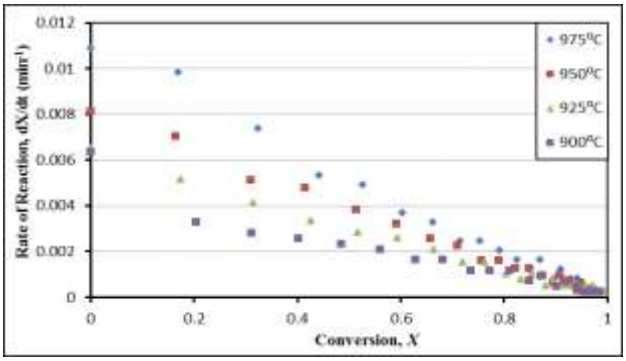

(ii) SF75:WT25

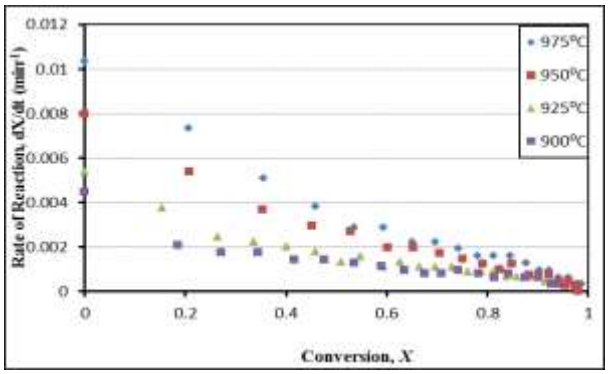

(iii) SF50:WT50

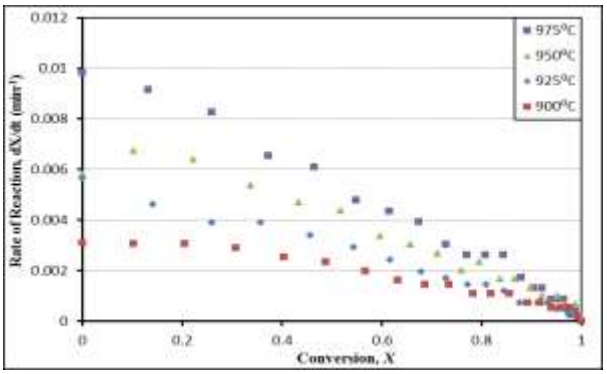

(iv) GG75:WT25

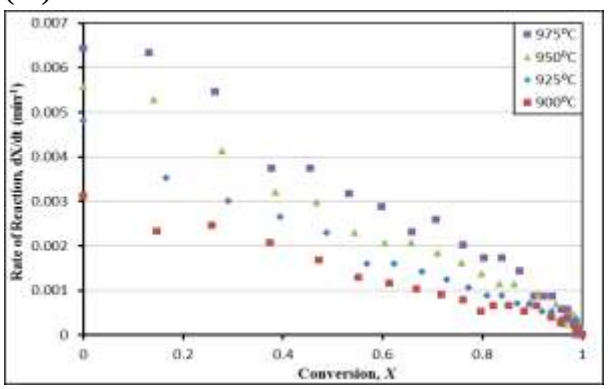

(v) GG50:WT50

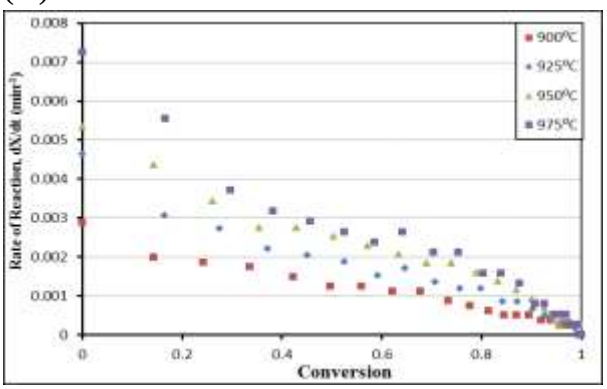

(vi) SF

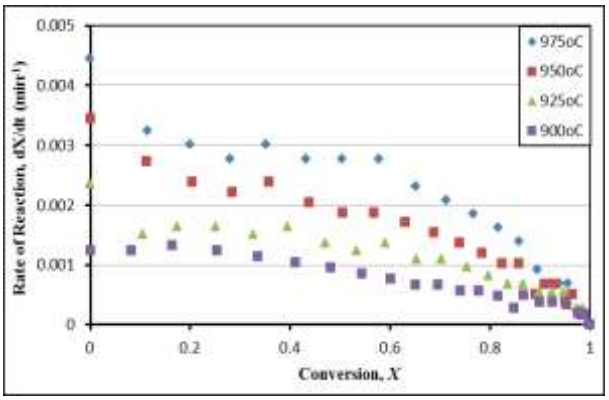

WT

Figure A.4: Reaction rate versus conversion plots

Appendix B: Effects of blending

SF/WT Blends

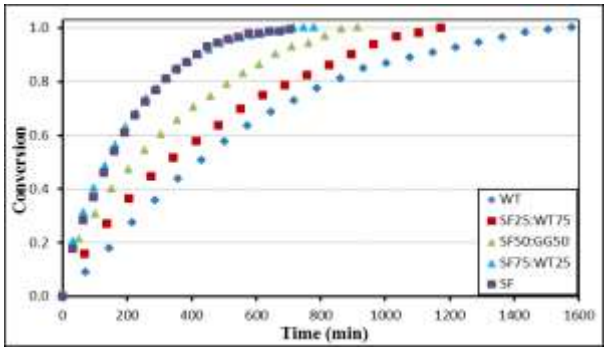

900ºC

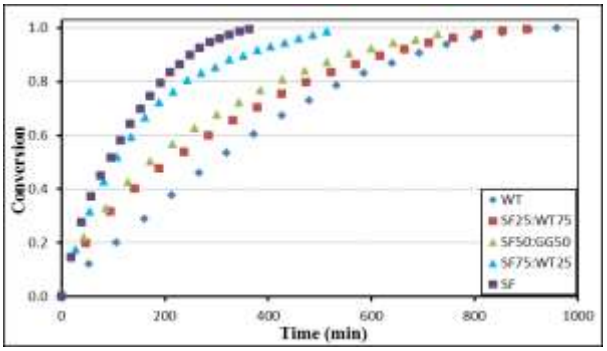

925ºC

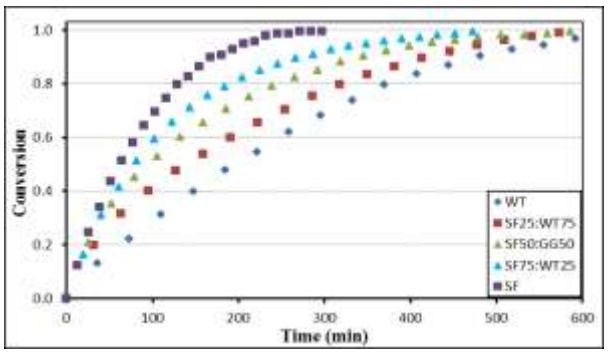

950ºC

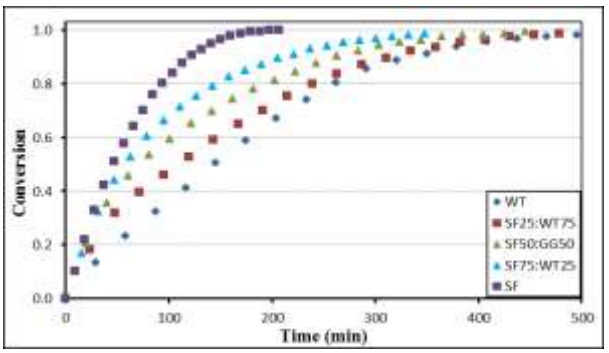

975º

Figure B.1: Effects of blending – SF:WT blends GG/WT Blends

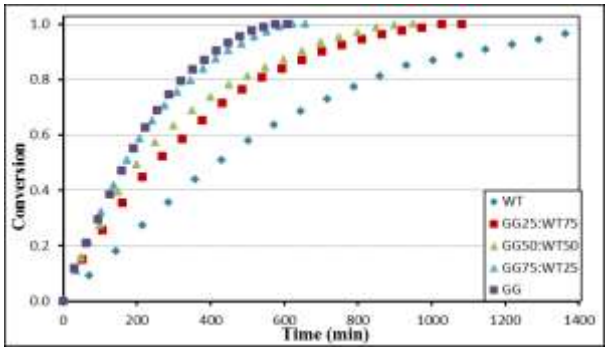

900ºC

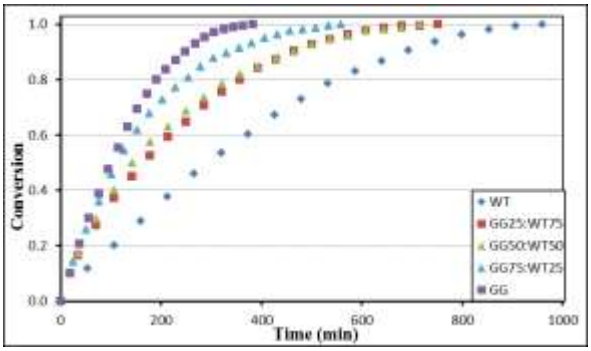

925ºC

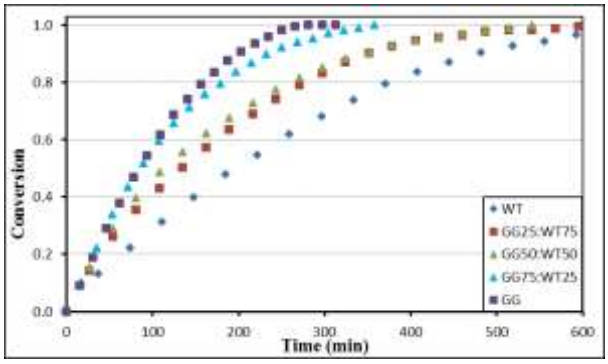

950ºC

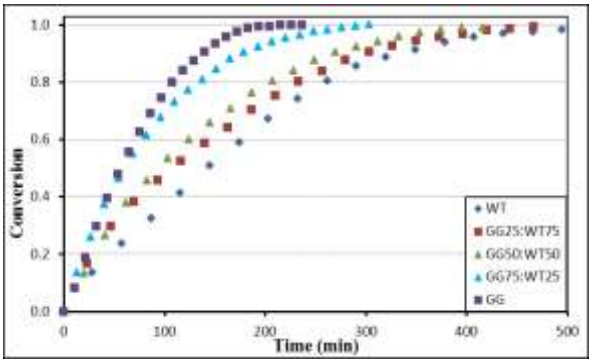

975ºC

Figure B.2: Effects of blending – GG/WT blends

Table B.1: Initial Reactivities for all the samples studied

Sample	Initial Reactivity X 10^3 (min^{-1})	Sample	Initial Reactivity X 10^3 (min^{-1})
900°C			
WT	1.59	WT	1.59
GG25:WT75	3.09	SF25:WT75	2.93
GG50:WT50	3.43	SF50:WT50	4.94
GG75:WT25	3.18	SF75:WT25	6.40
GG	3.76	SF	5.58
925°C			
WT	2.25	WT	4.75
GG25:WT75	4.55	SF25:WT75	4.08
GG50:WT50	4.99	SF50:WT50	5.42
GG75:WT25	5.66	SF75:WT25	6.54
GG	5.37	SF	7.39
950°C			
WT	3.53	WT	3.53
GG25:WT75	5.21	SF25:WT75	6.14
GG50:WT50	5.89	SF50:WT50	7.72
GG75:WT25	5.82	SF75:WT25	8.12
GG	6.15	SF	9.59
975°C			
WT	4.25	WT	4.25
GG25:WT75	6.91	SF25:WT75	7.47
GG50:WT50	6.33	SF50:WT50	9.43
GG75:WT25	9.82	SF75:WT25	10.9
GG	9.32	SF	11.7

Appendix C: Modelling

C.1: Kinetic parameters

Table C.1: Time factor, Initial reactivity and $t_{0.5}$ for the nine samples investigated

(i) Time factor, Initial reactivity and $t_{0.5}$ for three samples

WT				GG			GG75:WT25		
Temp.	t_f X 10^{-3} (min^{-1})	R X 10^{-3} (min^{-1})	$t_{0.5}$ (min)	t_f X 10^{-3} (min^{-1})	R X 10^{-3} (min^{-1})	$t_{0.5}$ (min)	t_f X 10^{-3} (min^{-1})	R X 10^{-3} (min^{-1})	$t_{0.5}$ (min)
900°C	1.05	1.59	418	3.03	3.76	170	3.66	3.18	169
925°C	1.59	2.25	296	5.1	5.37	100	4.89	5.66	113
950°C	1.72	3.53	195	6.33	6.15	85	6.98	5.82	84
975°C	3.16	4.25	143	9.26	9.32	56	9.02	9.82	60

(ii) Time factor, Initial reactivity and $t_{0.5}$ for six samples

GG50:WT50				**GG25:WT75**			**SF**		
Temp.	t_f X 10^{-3} (min^{-1})	R X 10^{-3} (min^{-1})	$t_{0.5}$ (min)	t_f X 10^{-3} (min^{-1})	R X 10^{-3} (min^{-1})	$t_{0.5}$ (min)	t_f X 10^{-3} (min^{-1})	R X 10^{-3} (min^{-1})	$t_{0.5}$ (min)
900°C	2.79	3.43	205	2.17	3.09	253	3.69	5.58	143
925°C	3.90	4.99	143	3.25	4.55	164	6.03	7.39	91
950°C	5.26	5.89	113	4.29	5.21	134	9.09	9.59	60
975°C	6.74	6.33	94	4.99	6.91	606	13.1	11.7	46
SF75:WT25				**SF50:WT50**			**SF25:WT75**		
Temp.	t_f X 10^{-3} (min^{-1})	R X 10^{-3} (min^{-1})	$t_{0.5}$ (min)	t_f X 10^{-3} (min^{-1})	R X 10^{-3} (min^{-1})	$t_{0.5}$ (min)	t_f X 10^{-3} (min^{-1})	R X 10^{-3} (min^{-1})	$t_{0.5}$ (min)
900°C	4.47	6.40	134	2.77	4.94	224	1.78	2.93	332
925°C	5.55	6.54	103	3.33	5.42	170	2.59	4.08	211
950°C	7.16	8.12	78	5.46	7.72	95	3.77	6.14	139
975°C	9.26	10.9	57	7.09	9.43	71	5.11	7.47	108

C.2: RPM fitting curves

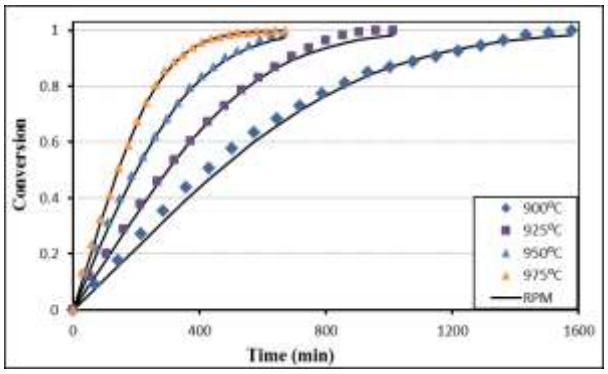

(i) WT

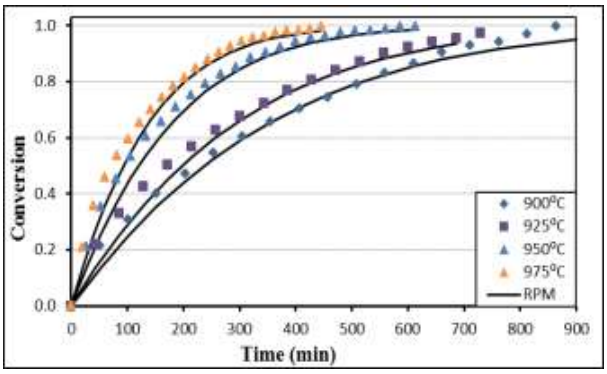

(ii) SF

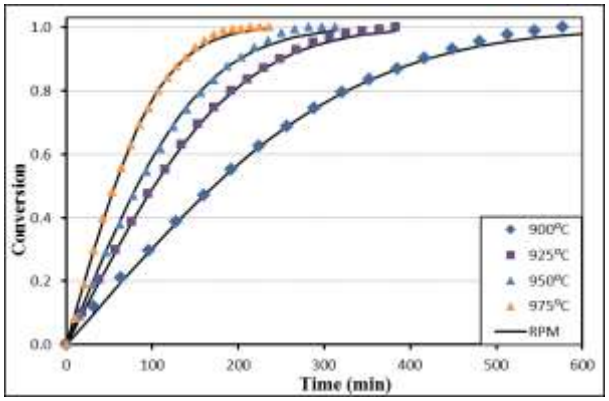

(iii) GG

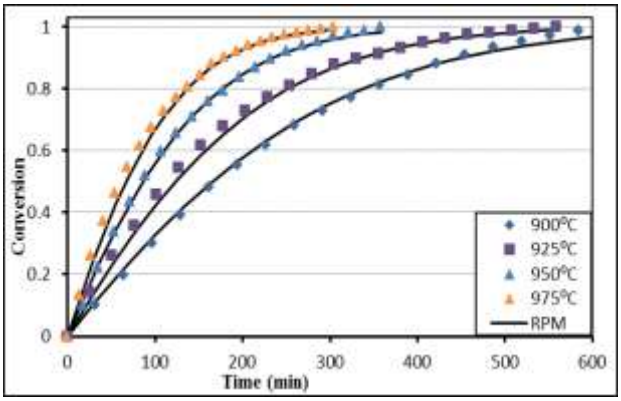

(iv) GG75:WT25

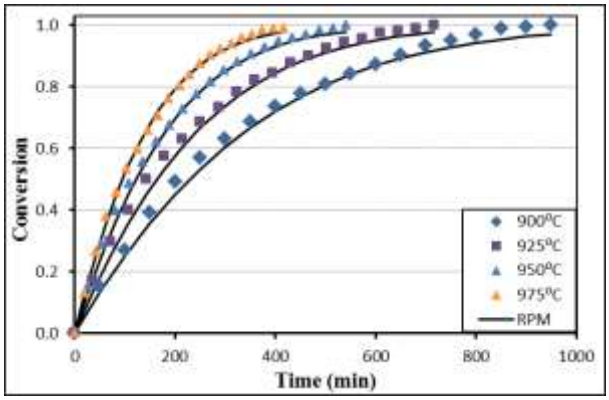

(v) GG50:WT50

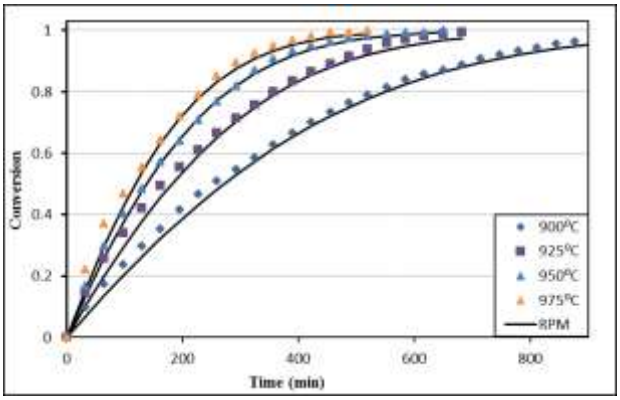

(vi) GG25:WT75

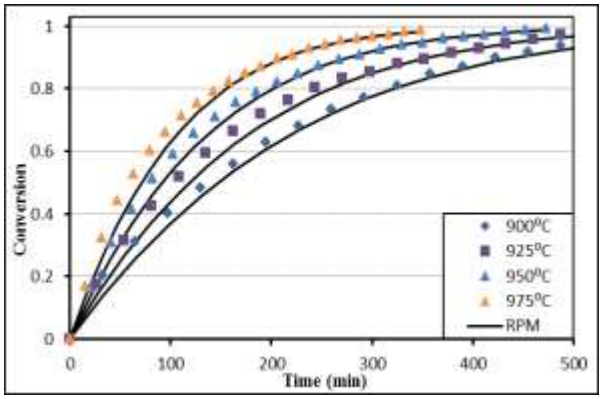

(vii) SF75:WT25

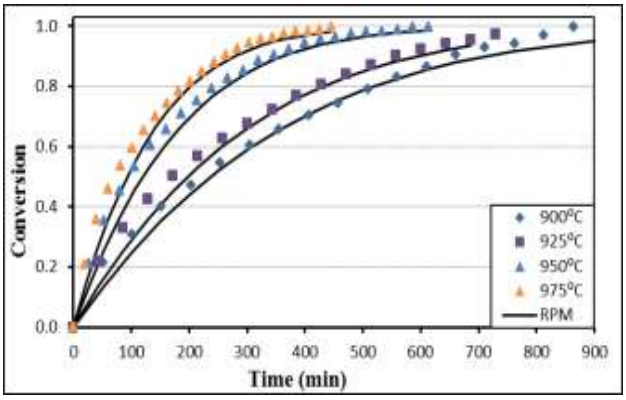

(viii) SF50:WT50

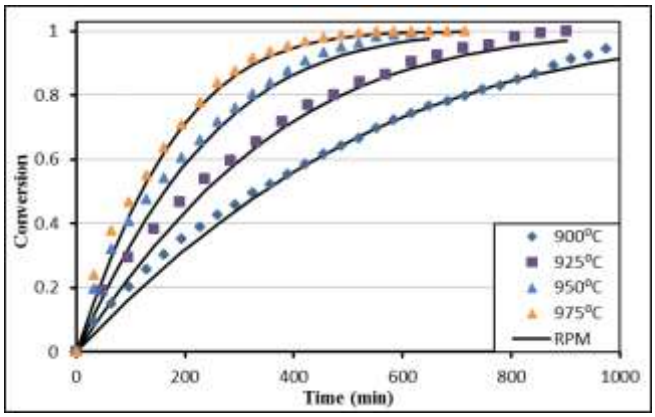

(ix) SF25:WT75

Figure C.1: Random pore model curve fitting for all samples studied.